

Division of Pharmaceutical Chemistry  
Faculty of Pharmacy  
University of Helsinki  
Finland

# **Protein Kinase C and Anaplastic Lymphoma Kinase Targeted Compounds**

Gustav Boije af Gennäs

ACADEMIC DISSERTATION

*To be presented, with the permission of the Faculty of Pharmacy of the University of Helsinki, for public criticism in Auditorium 1041, Viikki Biocenter 2 (Viikinkaari 5), on August 12<sup>th</sup>, 2011, at 12 noon.*

Helsinki 2011

**Supervised by:**

Professor Jari Yli-Kauhaluoma  
Division of Pharmaceutical Chemistry  
Faculty of Pharmacy  
University of Helsinki  
Finland

**Reviewed by:**

Professor Mats Larhed  
Department of Medicinal Chemistry  
Division of Organic Pharmaceutical Chemistry  
Uppsala University  
Sweden

Docent Tapio Nevalainen  
School of Pharmacy  
Faculty of Health Sciences  
The University of Eastern Finland  
Finland

**Opponent:**

Professor John Nielsen  
Department of Basic Sciences and Environment/  
Chemistry and Biochemistry  
Faculty of Life Sciences  
University of Copenhagen  
Denmark

© Gustav Boije af Gennäs 2011  
ISBN 978-952-10-7059-4 (paperback)  
ISBN 978-952-10-7060-0 (PDF)  
ISSN 1799-7372  
<http://ethesis.helsinki.fi>  
Helsinki University Print

Helsinki University Print  
Helsinki 2011

## Abstract

The protein kinases (PKs) belong to the largest single family of enzymes, phosphotransferases, which catalyze the phosphorylation of other enzymes and proteins and function primarily in signal transduction. Consequently, PKs regulate cell mechanisms such as growth, differentiation, and proliferation. Dysfunction of these cellular mechanisms may lead to cancer, a major predicament in health care. Even though there is a range of clinically available cancer-fighting drugs, increasing number of cancer cases and setbacks such as drug resistance, constantly keep cancer research active.

At the commencement of this study an isophthalic acid derivative had been suggested to bind to the regulatory domain of protein kinase C (PKC). In order to investigate the biological effects and structure-activity relationships (SARs) of this new chemical entity, a library of compounds was synthesized. The best compounds induced apoptosis in human leukemia HL-60 cells and were not cytotoxic in Swiss 3T3 fibroblasts. In addition, the best apoptosis inducers were neither cytotoxic nor mutagenic. Furthermore, results from binding affinity assays of PKC isoforms revealed the pharmacophores of these isophthalic acid derivatives. The best inhibition constants of the tested compounds were measured to 210 nM for PKC $\alpha$  and to 530 nM for PKC $\delta$ .

Among natural compounds targeting the regulatory domain of PKC, the target of bistramide A has been a matter of debate. It was initially found to activate PKC $\delta$ ; however, actin was recently reported as the main target. In order to clarify and to further study the biological effects of bistramide A, the total syntheses of the natural compound and two isomers were performed. Biological assays of the compounds revealed accumulation of 4n polyploid cells as the primary mode of action and the compounds showed similar overall antiproliferative activities. However, each compound showed a distinct distribution of antimetabolic effect presumably via actin binding, proapoptotic effect presumably via PKC $\delta$ , and pro-differentiation effect as evidenced by CD11b expression. Furthermore, it was shown that the antimetabolic and proapoptotic effects of bistramide A were not secondary effects of actin binding but independent effects.

The third aim in this study was to synthesize a library of a new class of urea-based type II inhibitors targeted at the kinase domain of anaplastic lymphoma kinase (ALK). The best compounds in this library showed IC<sub>50</sub> values as low as 390 nM for ALK while the initial low cellular activities were successfully increased even by more than 70 times for NPM-ALK-positive BaF3 cells. More importantly, selective antiproliferative activity on ALK-positive cell lines was achieved; while the best compound affected the BaF3 and SU-DHL-1 cells with IC<sub>50</sub> values of 0.5 and 0.8  $\mu$ M, respectively, they were less toxic to the NPM-ALK-negative human leukemic cells U937 (IC<sub>50</sub> = 3.2  $\mu$ M) and BaF3 parental cells (IC<sub>50</sub> = 5.4  $\mu$ M). Furthermore, SAR studies of the synthesized compounds revealed functional groups and positions of the scaffold, which enhanced the enzymatic and cellular activities.

## Acknowledgments

This study was a part of the 6<sup>th</sup> European Community Framework Programme “*Protein Kinases - Novel Drug Targets of Post Genomic Era*” (research project no. 503467) and was conducted during the years 2004 - 2011. The research was carried out in the Division of Pharmaceutical Chemistry, Faculty of Pharmacy, University of Helsinki. The author is highly grateful for the additional financial support granted by the Finnish Cultural Foundation, the Päivikki and Sakari Sohlberg Foundation, the Centre for Drug Research, the Chancellor’s Grant, and the Graduate School in Pharmaceutical Research.

My supervisor, Prof. Jari Yli-Kauhaluoma, Head of the Division of Pharmaceutical Chemistry, is the one who made this study possible. His ever enthusiastic personality and his constant availability to discuss research-related problems and possibilities made my time performing science under his supervision very pleasant. Even during times when there were only black clouds in the sky he was always there to encourage me to keep on trying. Thank you for teaching me science!

I also want to say a big thank you to all of the co-authors of the publications this thesis is based on. Research is performed in collaboration and not alone; without your contributions this study would never have been accomplished. In addition, I am grateful to Matti Wahlsten, Jouni Jokela, Miikka Olin and Tuuli Koivumäki for the analytical and technical help with the LC-MS runs. Furthermore, I want to express my gratitude to Jonas Hartman and Elina Ekoskoski for proofreading the text.

Without great workmates the days at work would not have been this enjoyable; therefore, I want to thank all the friends at the Div. of Pharm. Chem. and in particular Mikko, Raisa, Antti, Aleksi, Mohan, Irene, Andrew, Nenad, Leena, Paula, Martina, Kristian, Erik, Yuezhou, Sami, Ingo<sup>2</sup>, and Harri. In addition, the refreshing coffee breaks at “Ismon and Inkun kahvislonki” with Risto, Tapio, Moshe, Raimo, Anna, Gloria, Hongbo, Katariina, Kati, Laura, Leena, Linda, Marja, Markus, Mika, Mika-Matti, Miina, Ni(i)na<sup>2</sup>, Pekka, Piia, Päivi, Taina, Tiina<sup>2</sup>, Titti, and Teemu will always be in my mind!

Thanks to all of the M.Sc. students I have supervised and worked with: Mika, Niko, Tuire, Lasse, Marina, and Giovanni. In addition, the international visiting stars Ben and Pierluigi: I’m really happy you decided to spend time in our lab!

Last but not least, I wish to thank my family and friends: my father for always being interested in the last results of my research and my mother, for reminding me that there is also life outside of work, and both of you for teaching me the important things in life. There are no words to express my love and appreciation for you. And finally, Ammi, my love, thank you for your understanding and for not having too short a fuse. Without you this thesis would not have been at this stage.

Helsinki, June 2011  
Gustav Boije af Gennäs

# Contents

<b>Abstract</b>	<b>3</b>
<b>Acknowledgments</b>	<b>4</b>
<b>Contents</b>	<b>5</b>
<b>List of original publications</b>	<b>7</b>
<b>Abbreviations</b>	<b>8</b>
<b>1 Introduction</b>	<b>10</b>
<b>2 Review of the literature</b>	<b>12</b>
<b>2.1 Protein kinases and the phosphoryltransfer reaction</b>	<b>12</b>
<b>2.2 Protein kinase C</b>	<b>15</b>
<b>2.2.1 Structure, activation and regulation</b>	<b>17</b>
<b>2.2.2 The C1 domain of protein kinase C</b>	<b>20</b>
<b>2.2.3 Natural compounds targeting the C1 domain</b>	<b>23</b>
<b>2.2.4 Synthetic compounds targeting the C1 domain</b>	<b>31</b>
<b>2.3 Anaplastic lymphoma kinase</b>	<b>40</b>
<b>2.3.1 Structure, activation and regulation</b>	<b>41</b>
<b>2.3.2 The kinase domain of anaplastic lymphoma kinase</b>	<b>44</b>
<b>2.3.3 Synthetic compounds as anaplastic lymphoma kinase inhibitors</b>	<b>48</b>
<b>2.3.4 Natural compounds as anaplastic lymphoma kinase inhibitors</b>	<b>57</b>
<b>3 Aims of the study</b>	<b>59</b>
<b>4 Experimental</b>	<b>60</b>
<b>5 Results and discussion</b>	<b>61</b>
<b>5.1 Synthesis of isophthalic acid derivatives and SAR of the compounds (I and II)</b>	<b>61</b>
<b>5.2 Synthesis of bistramide A and its derivatives, and the biological outcome of the compounds (III)</b>	<b>72</b>

<b>5.3 Synthesis of urea-based anaplastic lymphoma kinase inhibitors and SAR of the compounds (IV)</b>	<b>78</b>
<b>6 Summary and conclusions</b>	<b>85</b>
<b>7 References</b>	<b>87</b>

## List of original publications

This thesis is based on the following publications:

- I** Galkin, A., Surakka, A., Boije af Gennäs, G., Ruotsalainen, T., Kreander, K., Tammela, P., Sivonen, K., Yli-Kauhahuoma, J., Vuorela, P. Hydrophobic Derivatives of 5-(Hydroxymethyl)isophthalic Acid that Selectively Induce Apoptosis in Leukemia Cells but not in Fibroblasts. *Drug Devel. Res.*, **2008**, **69** (4), 185-195.
- II** Boije af Gennäs, G., Talman, V., Aitio, O., Ekokoski, E., Finel, M., Tuominen, R.K., Yli-Kauhahuoma, J. Design, Synthesis and Biological Activity of Isophthalic Acid Derivatives Targeted to the C1 Domain of Protein Kinase C. *J. Med. Chem.*, **2009**, *52* (13), 3969-3981.
- III** Tomas, L., Boije af Gennäs, G., Hiebel, M.A., Gueyrard, D., Pelotier, B., Yli-Kauhahuoma, J., Piva, O., Goekjian, P.G. Total Synthesis of Bistramide A and Its 36-Z Isomers: Differential Effect on Cell Division, Differentiation, and Apoptosis. *Chem. –Eur. J.* (Submitted).
- IV** Boije af Gennäs, G., Mologni, L., Ahmed, S., Rajaratnam, M., Marin, O., Lindholm, N., Viltadi, M., Gambacorti-Passerini, C., Scapozza, L., Yli-Kauhahuoma, J. Design, Synthesis and Biological Activity of Urea Derivatives as Anaplastic Lymphoma Kinase Inhibitors. *ChemMedChem.* (Accepted).

The publications are referred to in the text by their roman numerals. The supporting information of original publications **II**, **III** and **IV** is not included in this thesis book. This material is available from the author or via the Internet at <http://pubs.acs.org> for original publication **II** (46 pages) and at <http://onlinelibrary.wiley.com/> for original publications **III** (78 pages) and **IV** (16 pages). The original publications **I**, **II** and **IV** are reproduced with the permission of the copyright holders. In addition, one unpublished manuscript (**III**) is included.

## Abbreviations

Abl	Abelson tyrosine kinase	MK	midkine
Ac	acetyl	NA/BaF3	BaF3 cells expressing the <u>NPM-ALK</u> fusion gene
AD	Alzheimer's disease	NFD-motif	Asn-Phe-Asp-motif
ADP	adenosine-5'-diphosphate	NPM	nucleophosmin
ALCL	anaplastic large cell lymphoma	NSCLC	non-small cell lung cancer
ALK	anaplastic lymphoma kinase	OD	oligomerization domain
A-loop	activation loop	PDBu	phorbol 12,13-dibutyrate
AMP-PNP	adenosine 5'-( $\beta,\gamma$ -imido)triphosphate	PK	protein kinase
ATP	adenosine-5'-triphosphate	PKA	protein kinase A
Bcr	breakpoint cluster region	PKC	protein kinase C
Bn	benzyl	PLC	phospholipase C
Boc	<i>tert</i> -butyloxycarbonyl	P-loop	phosphate binding loop
Bz	benzoyl	PMA	phorbol 12-myristate 13-acetate
DAG	1,2-diacylglycerol	PS	pseudosubstrate
DFG-motif	Asp-Phe-Gly-motif	Ptd-L-Ser	phosphatidyl-L-serine
DMF	<i>N,N</i> -dimethylformamide	PTN	pleiotrophin
DMSO	dimethyl sulfoxide	rt	room temperature
EC	Enzyme Commission	RTK	receptor tyrosine kinase
EML4	echinoderm microtubule-associated protein-like 4	SAR	structure-activity relationship
Fmoc	fluorenylmethyloxycarbonyl	SCID	severe combined immunodeficiency
G-rich	glycine-rich	Scr	sarcoma
h	human	TADDOL	(4 <i>R</i> ,5 <i>R</i> )-2,2-dimethyl- $\alpha,\alpha,\alpha',\alpha'$ -tetraphenyldioxolane-4,5-dimethanol
HIV	human immunodeficiency virus	TBS	<i>tert</i> -butyldimethylsilyl
HL	human leukemia	THF	tetrahydrofuran
HRD-motif	His-Arg-Asp-motif	TIPS	triisopropylsilyl
Hsp	heat-shock protein	TM	transmembrane
IGF-1R	insulin-like growth factor-1 receptor	TPM3	tropomyosin $\alpha$ -3
IR	insulin receptor	VAIK-motif	Val-Ala-Ile-Lys-motif
IRK	insulin receptor kinase	VAVK-motif	Val-Ala-Val-Lys-motif
LDL	low-density lipoprotein	WT	wild type
m	mouse	Å	ångström
MAM	meprin-A5 protein-receptor protein tyrosine phosphatase $\mu$		



Amino acid	3-Letter symbol	1-Letter symbol	Amino acid	3-Letter symbol	1-Letter symbol
Alanine	Ala	A	Methionine	Met	M
Arginine	Arg	R	Phenylalanine	Phe	F
Asparagine	Asn	N	Proline	Pro	P
Aspartic acid	Asp	D	Pyrrolysine	Pyl	O
Cysteine	Cys	C	Selenocysteine	Sec	U
Glutamic acid	Glu	E	Serine	Ser	S
Glutamine	Gln	Q	Threonine	Thr	T
Glycine	Gly	G	Tryptophan	Trp	W
Histidine	His	H	Tyrosine	Tyr	Y
Isoleucine	Ile	I	Valine	Val	V
Leucine	Leu	L			

### Compound and inhibitor constants and parameters

$EC_{50}$	the concentration of an compound which causes 50% of a maximal effect
$IC_{50}$	the concentration of an inhibitor which causes 50% inhibition
$IG_{50}$	the concentration of an inhibitor which causes 50% growth inhibition
$K_i$	inhibitor dissociation constant
$K_d$	dissociation constant

# 1 Introduction

The PKs account for about 1.7% of the proteins encoded by the human genome, and thus belong to the largest single family of enzymes.<sup>1</sup> With its over 500 members, the main role of PKs is signal transduction and therefore they regulate the growth, differentiation, proliferation and various cell mechanisms.<sup>2</sup> However, when dysfunction of these cellular mechanisms occurs, they subsequently may cause diseases such as cancer.<sup>2</sup> With an estimation by the Finnish Cancer Registry of a quarter more cancer cases in Finland in year 2020,<sup>3</sup> and by the American Cancer Society of over 1,500,000 new cancer diagnoses in USA alone for the year 2010,<sup>4</sup> finding highly specific therapeutic anti-cancer drugs is an important challenge for health care the world around.

Therapies for diseases such as cancer may include the inhibition of growth-related kinases.<sup>2</sup> Probably one of the most studied PKs is the PKC (EC 2.7.11.13) family. When PKC was found in 1977,<sup>5,6</sup> it had not been linked to signal transduction. However, shortly after this, the first isoform of PKC was shown to be calcium-activated and phospholipid-dependent,<sup>7</sup> diacylglycerol-induced,<sup>8</sup> and coupled to the activation of G-protein-coupled receptors,<sup>9</sup> thus linked to signal transduction. Since then, PKC research has only accelerated. At the moment, PKC has been suggested as a potent therapeutic target not only in cancer,<sup>10,11</sup> but also in neurological diseases;<sup>12</sup> especially Alzheimer's disease (AD),<sup>13-15</sup> immunological diseases,<sup>16,17</sup> and cardiovascular diseases.<sup>18-20</sup>

Targeting the kinase domain of PKC has yielded two isoform selective PKC $\beta$  inhibitors so far: ruboxistaurin (LY333531)<sup>21</sup> and enzastaurin (LY317615),<sup>22</sup> however, these inhibitors inhibit also other kinases.<sup>23,24</sup> The main stumbling block has been the highly conserved ATP-binding pocket of PKC, however, targeting the regulatory domain could more easily provide PKC selective compounds. Consequently, one part of this thesis deals with known natural and synthetic compounds targeted to bind the regulatory domain of PKC as well as the development of novel compounds.

A relatively new PK target is ALK (EC 2.7.10.1). In 1988, a chromosomal translocation in anaplastic large cell lymphomas (ALCLs) was described by several groups,<sup>25,26</sup> and in 1994 the fusion product of the chromosomal translocation was identified.<sup>27,28</sup> Since then, several other fusion products of ALK have been discovered.<sup>29</sup> The function of the wild type (WT) ALK is still poorly known. This receptor tyrosine kinase (RTK) has been shown to have a part in the development of the central and peripheral nervous system<sup>30</sup> as well as be involved in neuronal cell differentiation and regeneration, synapse formation and muscle cell migration.<sup>31</sup> In contrast, fusion products of ALK have constitutive kinase activity and are highly oncogenic.<sup>32</sup> Recently the dual kinase inhibitor crizotinib was shown to inhibit fusion products of ALK and is now in clinical trials (phase I-III) for the treatment of lung cancer.<sup>33</sup> However, there is a constant need for new inhibitors in ALK-positive tumors since crizotinib resistant cell lines have already been obtained.<sup>34</sup>

Inhibitors targeting only the ATP-binding pocket of the kinase domain are prone to tumor resistance and are more difficult to make specific. Preparing inhibitors that also target residues

outside of the site,<sup>35</sup> or exclusively outside the pocket,<sup>36</sup> would increase specificity among kinases. In addition, inhibitors that target the inactive conformation of the kinase further increase specificity.<sup>36,37</sup> Therefore, the second part of this thesis deals with the development of novel, as well as known natural and synthetic, kinase domain-targeted ALK inhibitors.

## 2 Review of the literature

### 2.1 Protein kinases and the phosphoryltransfer reaction

The PKs, also called phosphotransferases, are enzymes that catalyze the phosphorylation of proteins, such as enzymes.<sup>38</sup> The superfamily of PKs can be divided into several classes according to which amino acids are phosphorylated on the target proteins; serine/threonine kinases (EC 2.7.11.1), tyrosine kinases (EC 2.7.10.1 and 2.7.10.2) and dual-specificity kinases (EC 2.7.12.1).<sup>39</sup> The latter group phosphorylates all the three above-mentioned amino acids. In addition, a fourth and more rare group of kinases is that which phosphorylates histidines (EC 2.7.13.3). In addition to phosphorylation specificity of the above-mentioned amino acids, specificity among substrates containing those amino acids can also be obtained.<sup>40</sup> In these cases, the adjacent amino acids infer the specificity of these substrates.

In the phosphoryltransfer reaction, a PK binds adenosine-5'-triphosphate (ATP, **1**), the target protein moves to the kinase-ATP complex, and the PK transfers the  $\gamma$ -phosphate group of ATP to the hydroxy group of the target protein (Figure 1).<sup>39</sup> The order in which the PK binds ATP and

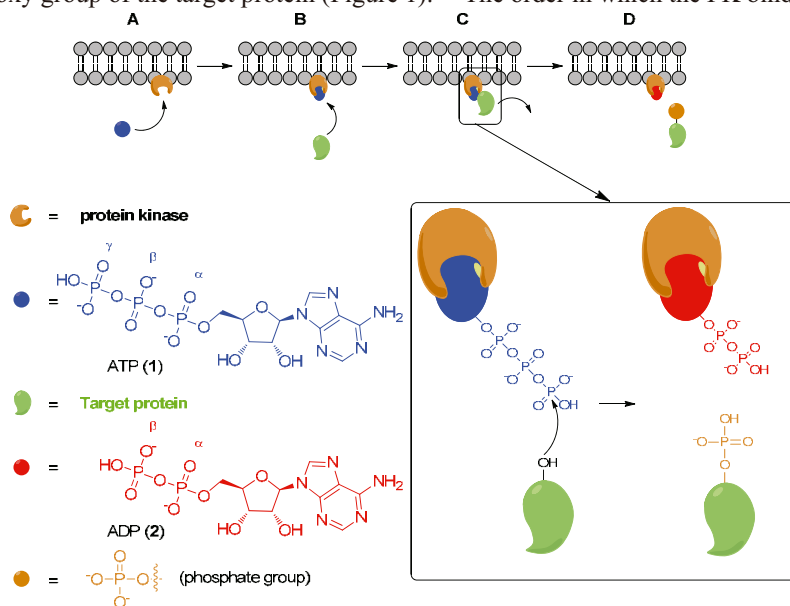


**Figure 1** Phosphorylation of target proteins by protein kinases; **A)** a protein kinase binds ATP, **B)** a target protein binds to the protein kinase-ATP complex, **C)** the protein kinase transfers a phosphate group from ATP to the target protein and the phosphorylated target protein leaves the complex, **D)** a protein kinase-ADP complex and a phosphorylated target protein as products. Adenosine-5'-triphosphate (ATP, **1**), adenosine-5'-diphosphate (ADP, **2**).

the target protein is not always identical, the opposite order can also be the case. The same is true for the order of the release of the phosphorylated product and adenosine-5'-diphosphate (ADP, 2); which dissociates first from the PK can vary from kinase to kinase. The phosphorylation of a target enzyme usually leads to its conformational change, consequently activating or deactivating the target enzyme. Other effects caused by phosphorylation of the target proteins are subcellular relocation and association with other proteins.<sup>1, 41</sup>

The phosphoryltransfer reaction takes place in the highly conserved kinase domain of PKs. The reaction involves a cascade of interactions between the substrate, ATP and the PK (Figure 2).<sup>39, 42</sup> For example, in the catalytic site of protein kinase A (PKA, EC 2.7.11.11), the Asp166 carboxylate is thought to act as a catalytic base to the serine hydroxy of the substrate (residue numbering corresponds to that of PKA).<sup>43</sup> Alternatively, the Asp166 is suggested to act as an orientating residue, as such the aspartate would orientate the hydroxy group of the substrate towards the  $\gamma$ -phosphate of ATP.<sup>44</sup> In contrast, the latest quantum mechanical/molecular

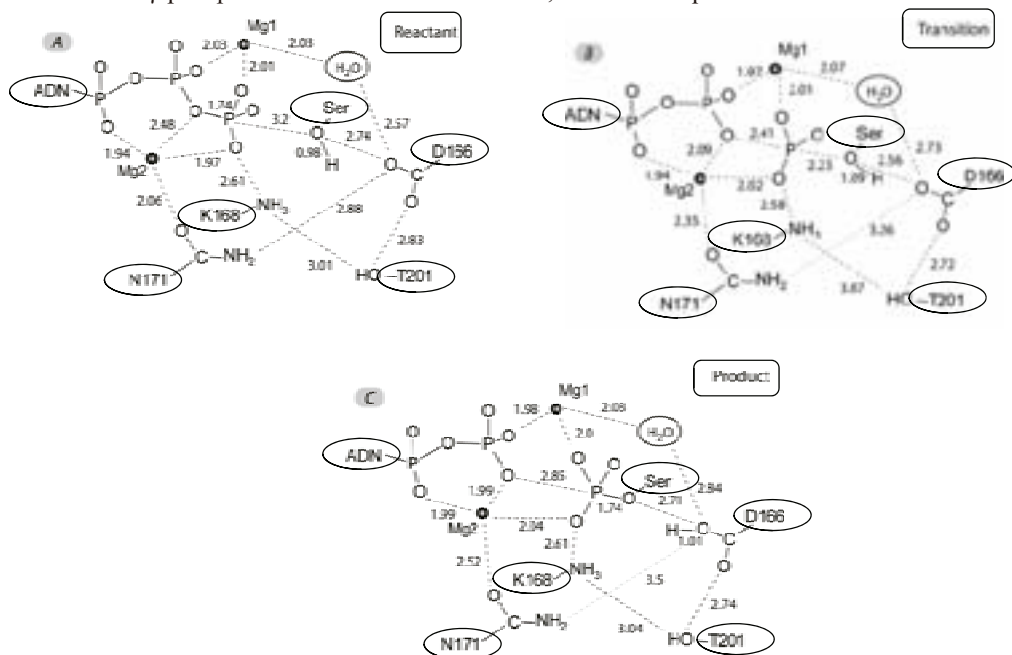


**Figure 2** The distances between the residues, substrate protein, ATP/ADP and water molecules in a phosphoryltransfer reaction of protein kinase A (PKA).<sup>42</sup> The structures represent the **A)** reactant, **B)** the transition state and **C)** the product. The numbers indicate the optimized bond lengths in ångströms (Å) and were obtained from quantum mechanical/molecular mechanics simulations. Adenosine (ADN); Asn171 (N171); Asp166 (D166); Lys168 (K168) and Thr201 (T201). Adapted with permission from ref. 42. Copyright 2011 American Chemical Society.

mechanics simulations suggest that Asp166 functions as a hydrogen bond acceptor late in the reaction process (Figure 2C).<sup>42</sup> Other residues which are in close proximity to the phosphoryltransfer site are Asn171, Lys168 and Thr201 (Figure 2 and Figure 3).

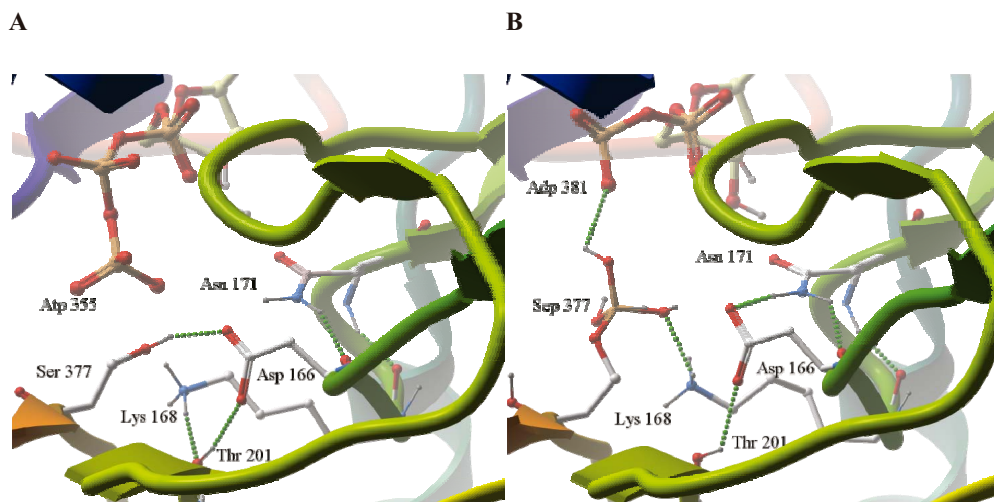


**Figure 3** *The catalytic site of the crystal structure of PKA in complex with a peptide inhibitor and ATP or ADP.*<sup>43,45</sup> **A** *The hydroxy group of the serine residue (Ser377) of the unphosphorylated peptide and ATP (Atp355). Ser377, ATP and the residues which are thought to be involved in the phosphoryltransfer reaction are represented in ball and stick representation and colored by atom type, hydrogen bonds are denoted as green spheres. The figure was created by deleting ADP (Adp381) from the crystal structure of PKA (PDB-code: 1JBP)<sup>43</sup> and adding ATP (Atp355) from an other crystal structure of PKA (PDB-code: 1ATP)<sup>45</sup> to 1JBP. **B** *The phosphorylated hydroxy group of the serine residue (Sep377) in the substrate peptide and ADP (Adp381). Represented as in A). The figure was created by adding ADP (Adp381) from 1JBP<sup>43</sup> to the crystal structure of 1JLU.<sup>45</sup> The figures were created using ICM-Browser (version 3.7-2a, MolSoft L.L.C.).**

In addition to these residues, several other amino acids help to coordinate ATP in the binding site by forming hydrogen bonds to it (Figure 4). First, the adenine ring of ATP is hydrogen-bonded to the hinge region residues Glu121 and Val123 as well as to residue Thr183 (numbering as for PKA).<sup>45</sup> The ribose moiety of ATP is hydrogen-bonded to amino acids Glu127 and Glu170 and the  $\alpha$ -,  $\beta$ - and  $\gamma$ -phosphates of ATP are bonded by the P-loop residues Ser53, Phe54 and Gly55 as well as residues Lys72 and Lys168. Furthermore, the  $Mg^{2+}$  ions are coordinated with the help of residues Asn171 and Asp184 as well as with the help of the  $\alpha$ -,  $\beta$ - and  $\gamma$ -phosphate groups (in Figure 4 the  $Mg^{2+}$  ions are replaced with  $Mn^{2+}$  ions).

In the next chapters, the PKC and ALK enzymes will be discussed in more detail (Chapters 2.2 and 2.3, respectively).

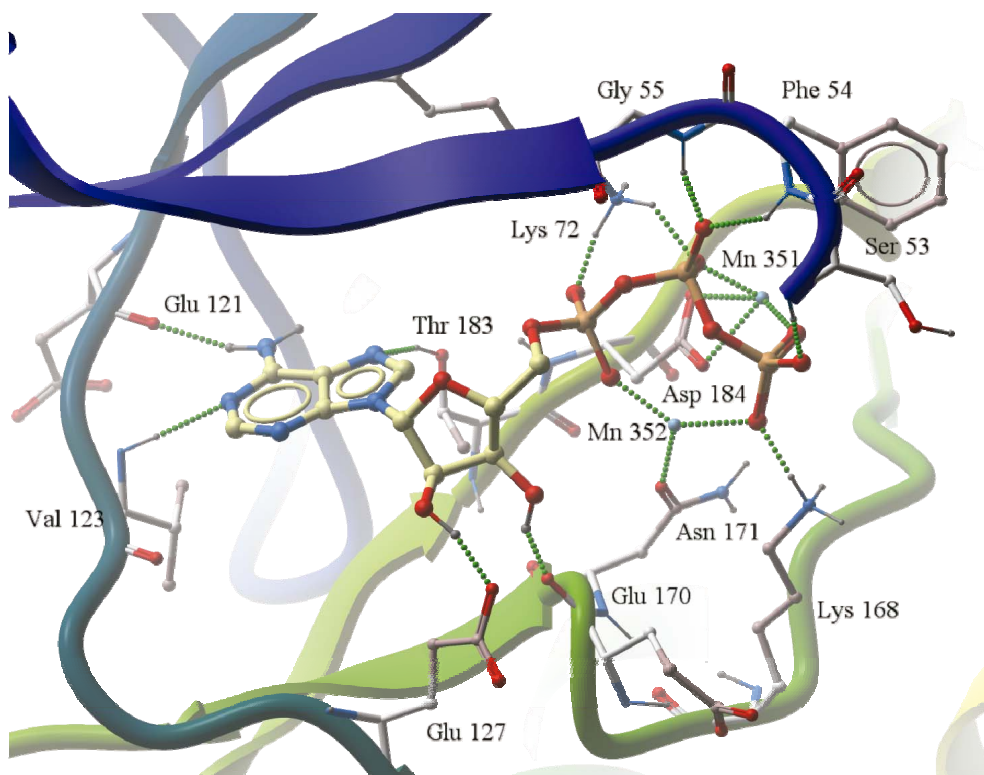


**Figure 4** *ATP is coordinated in the catalytic site of PKA by a nest of hydrogen bonds (PDB-code: 1ATP).<sup>45</sup> ATP and residues forming hydrogen bonds (green spheres) to ATP are presented in ball and sticks representation and colored by atom type. The  $Mn^{2+}$  ions (Mn352 and Mn351) are shown as grey dots. For the sake of clarity, a part of the P-loop (see Chapter 2.3.2.) was deleted. The figure was created using ICM-Browser (version 3.7-2a, MolSoft L.L.C.).*

## 2.2 Protein kinase C

The PKC isoenzymes are involved in intracellular signal transduction cascades and in cellular events such as proliferation, differentiation and apoptosis.<sup>9,46</sup> PKCs belong to the larger subclass of PKs termed the adenine-guanine-cytosine (AGC) kinases and are serine/threonine kinases.<sup>41</sup> The PKC family is divided into three categories according to the structure of the regulatory domain and cofactor requirements, and consists of at least ten mammalian isoenzymes. According to these requirements, the PKCs are grouped into **classical** or **conventional** PKCs

(cPKCs, subtypes  $\alpha$ ,  $\beta$ I and II, and  $\gamma$ ), the **novel** PKCs (nPKCs, subtypes  $\delta$ ,  $\epsilon$ ,  $\eta$  and  $\theta$ ) and the **atypical** PKCs (aPKCs, subtypes  $\zeta$ ,  $\tau/\lambda$ ) (Table 1).<sup>41</sup> All PKCs are dependent on anionic phospholipids for activation, with phosphatidyl-L-serine (Ptd-L-Ser, **3**) being the most important.<sup>47</sup> In addition, cPKCs require both  $\text{Ca}^{2+}$  and 1,2-diacylglycerol (DAG, **4**) for activation, whereas nPKCs require only DAG (**4**). The third group, the aPKCs, requires neither DAG (**4**) nor  $\text{Ca}^{2+}$  for activation.

DAG (**4**), a central intracellular second messenger, selectively interacts with proteins containing a C1 domain. The production of DAG (**4**) and  $\text{Ca}^{2+}$  is a result of a signal transduction cascade, which starts from the activation of G protein-coupled receptors and receptor-tyrosine kinases.<sup>48,49</sup> When activated, these in turn activate phospholipase C (PLC, EC 3.1.4.11), which hydrolyzes the phospholipid phosphatidylinositol bisphosphate (PIP<sub>2</sub>, found in membranes) to give inositol 1,4,5-triphosphate (IP<sub>3</sub>) and DAG (**4**).<sup>50</sup> DAG (**4**) stays bound to the cell membrane but IP<sub>3</sub> migrates to the endoplasmic reticulum, where  $\text{Ca}^{2+}$  is consequently released into the cytosol and activates PKC.

Phorbol esters (**5**) are products obtained from croton oil, which is derived from the seeds of *Croton tiglium* L.<sup>51</sup> The phorbol esters (**5**) were shown to bind similarly as DAG (**4**) to the C1 domain of PKC, however, many of the phorbol esters are tumor promoting.<sup>52-54</sup>

**Table 1.** Cofactors needed to activate the different isoforms of PKC.<sup>a</sup>

Isoform	Cofactors		
	Ptd-L-Ser ( <b>3</b> )	DAG ( <b>4</b> )	$\text{Ca}^{2+}$
cPKC ( $\alpha$ , $\beta$ I+II, $\gamma$ )	+	+	+
nPKC ( $\delta$ , $\epsilon$ , $\eta$ , $\theta$ )	+	+	-
aPKC ( $\zeta$ , $\tau/\lambda$ )	+	-	-

<sup>a</sup> Ptd-L-Ser (phosphatidyl-L-serine), 1,2-diacylglycerol (DAG), classical/conventional PKC (cPKC), novel PKC (nPKC), atypical PKC (aPKC), needed (+), not needed (-).

The PKCs are non-receptor kinases, which in the inactive conformation can be found in the cytoplasm of cells.<sup>41</sup> Once the enzyme is activated, it localizes to various membranes,<sup>55,56</sup> such as the plasma membrane, the perinuclear membrane<sup>57</sup> and the membrane of the Golgi apparatus.<sup>58</sup> In fact, the isoform-specific effects on cells are a result of the different subcellular localizations of the isoforms of PKC.<sup>11,59</sup> The effects of PKC on apoptosis and proliferation form the basis for targeting PKC. PKC has been correlated to a number of conditions, including cancer,<sup>10,11</sup> neurological diseases;<sup>12</sup> especially AD,<sup>13-15</sup> immunological diseases,<sup>16,17</sup> and cardiovascular diseases.<sup>18-20</sup>

It is important to choose the right isoform of PKC when validating the therapeutic target enzyme, since the different isoforms of PKCs show specific biological effects.<sup>60</sup> Inhibition or activation of the target isoform also has to be taken into consideration as the different isoforms can produce opposite outcomes. For example, activation of PKC $\epsilon$  before ischemia protects the heart by mimicking preconditioning, whereas inhibition of PKC $\delta$  during reperfusion protects the



heart from reperfusion-induced damage.<sup>61</sup> Hence, isozyme-selective PKC therapeutics are greatly needed.

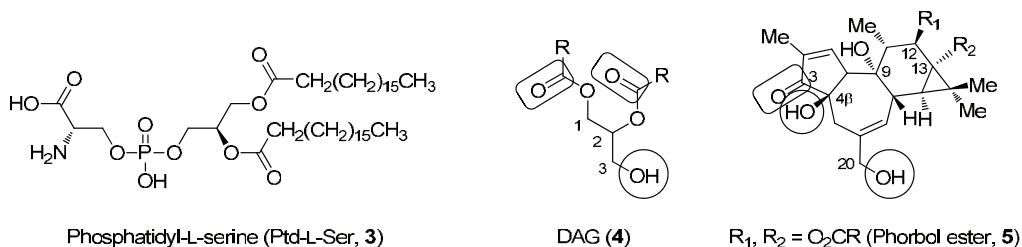


**Figure 5** The structures of phosphatidyl-L-serine (Ptd-L-Ser, **3**), 1,2-diacylglycerol (DAG, **4**) and phorbol esters (**5**). Functional groups that interact with the C1 domain are highlighted.

## 2.2.1 Structure, activation and regulation

### Structure

The PKCs consist of a highly conserved C-terminal catalytic domain and a less conserved N-terminal regulatory domain (Figure 6).<sup>62</sup> The catalytic domain contains the kinase part, where the ATP-binding site can be found. This site is highly conserved among PKs; the kinase domain of ALK will be discussed in more detail in Chapter 2.3.2.

The Ca<sup>2+</sup>-binding C2 domain and the DAG/phorbol ester-binding C1 domain can be found in the regulatory part of cPKCs (Figure 6). Furthermore, the C1 domain consists of a tandem repeat

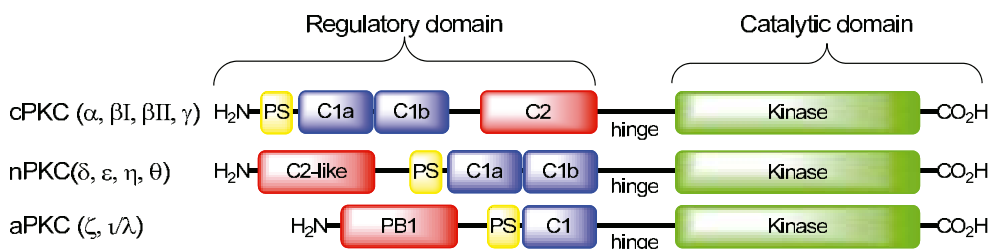


**Figure 6** Structures and domains of protein kinase C isoforms. PS = pseudosubstrate, PB1 = Phox and Bem 1.

sequence of about 50 residues, which is termed C1a and C1b. Similar to the cPKCs, the nPKCs also contain the tandem C1 domains but the positions are switched in the linear sequence compared to the cPKCs (Figure 6). As mentioned earlier, the C2 domain of nPKCs does not bind to  $\text{Ca}^{2+}$ ; hence it is called a C2-like domain. The aPKCs do not have a  $\text{Ca}^{2+}$ -binding C2 domain but instead a protein-protein interaction PB1 (Phox and Bem 1) domain. In addition, the aPKCs have an atypical C1-domain, because it is a single copy of the C1 domain and it does not bind DAG (4) or phorbol esters (5). Furthermore, all of the PKC isoforms have an autoinhibitory pseudosubstrate domain.

The C1 domain will be discussed in more detail in Chapter 2.2.2.

### *Priming phosphorylations of PKC*

Unphosphorylated PKCs can be found in the cytoplasm/detergent-insoluble fraction of cells and require two (aPKCs) or three (cPKCs and nPKCs) phosphorylations to fully mature (priming phosphorylations).<sup>63, 64</sup> The first modification is an autophosphorylation or a phosphoinositide-dependent kinase 1 (PDK-1)-catalyzed phosphorylation of a threonine found in the activation loop (A-loop), a highly conserved motif of the catalytic domain. The phosphate group produces a negative charge in the peptide-binding surface of the domain and subsequently, stabilizes the active conformation. Next, a threonine/serine is phosphorylated at the conserved turn motif. The turn motif can be found at the C-terminal end of the catalytic domain and is usually flanked by prolines. The incorporated negative charge further stabilizes the PKCs and is crucial for catalytic activity.<sup>64</sup> Once the turn motif of the mature PKC is phosphorylated, selective dephosphorylation(s) of another phosphate group(s) does (do) not result in any loss of activity. Hence, a phosphate group at the turn motif of a mature PKC is all that is needed for catalytic activity. The third modification is an autophosphorylation (for cPKCs) of a threonine/serine residue 19 residues C-terminal to the turn motif.<sup>65</sup> This conserved FXXFS/TF/Y motif is flanked by hydrophobic residues and is therefore also called the hydrophobic motif. Among the nPKCs, this motif can also be transphosphorylated.<sup>66</sup> In contrast to the cPKC and nPKC isoforms, aPKCs do not have the corresponding threonine/serine residue at the hydrophobic motif. However, this residue is replaced by a glutamic acid residue and consequently, the aPKCs contain the needed negative charge in the hydrophobic moiety. In addition to these phosphorylations, other serine/threonine residues of the enzyme can also be phosphorylated.<sup>41</sup>

### *Activation and regulation of PKC*

PKCs are allosterically regulated by their pseudosubstrate.<sup>67, 68</sup> In the inactive conformation, the pseudosubstrate is bound to the catalytic domain and inhibits enzyme activity (Figure 7A). In addition, the C1b domain is in close proximity to the catalytic domain, clamping the highly conserved NFD-motif (see Chapter 2.2.2.) off the ATP-binding site resulting in a low activity state.<sup>69</sup> The activation cascade starts when the C2 domain binds Ptd-L-Ser (all isoforms) and  $\text{Ca}^{2+}$  (only cPKCs). This causes the C2 domain to translocate to the cell membrane (Figure 7B).

Next, the C1a domain (of cPKCs and nPKCs) binds to DAG (4)/phorbol ester (5), causing it to translocate to the membrane. As a result, the enzyme undergoes conformational changes, causing the pseudosubstrate to move out from the ATP-binding site (Figure 7C).<sup>41</sup> However, the enzyme is not yet fully activated since the C1b domain is still located at the ATP-binding site.<sup>69</sup> Only after the C1b domain has bound to DAG (4)/phorbol ester (5) and translocated to the membrane, causing the interactions between the C1b and kinase domain to be lost, will the enzyme subsequently be activated (Figure 7D). The conformational change of the enzyme reveals the hinge region between the catalytic domain and the C2 domain. The hinge region becomes proteolytically labile, and if it is cleaved a constitutively active kinase domain is formed.<sup>6</sup>

DAG (4)/phorbol esters (5) and  $\text{Ca}^{2+}$  do not affect the activation or the regulation of aPKCs.<sup>41</sup> In contrast, the regulation is affected by phospholipids, PDK-1, the PB1 domain and other proteins.

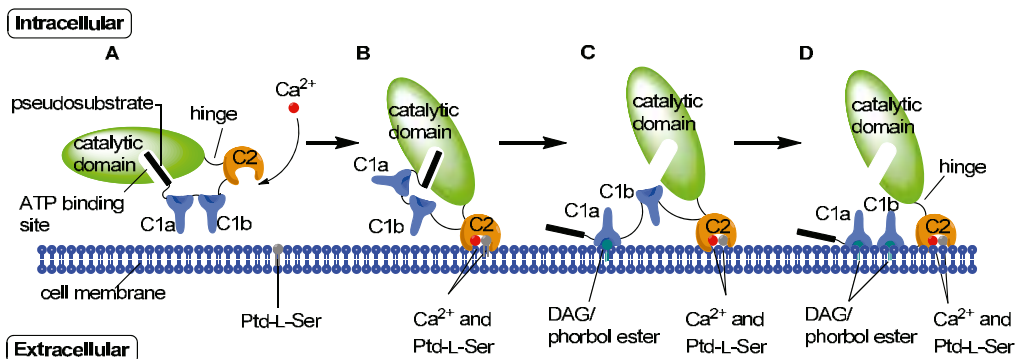


**Figure 7** Activation of cPKCs. **A)** In the inactive conformation, the pseudosubstrate is bound to the catalytic site of the kinase domain. **B)** The C2 domain binds  $\text{Ca}^{2+}$  and phosphatidyl-L-serine (Ptd-L-Ser, 3) and the domain localizes to the cell membrane. **C)** The C1a domain binds diacylglycerol (DAG, 4)/phorbol ester (5) at the cell membrane and a conformational change has moved the pseudosubstrate off the catalytic site. The C1b domain is still in front of the ATP-binding site, producing a low activity state of the catalytic site. **D)** The active conformation where the C1b domain is not anymore at the front of the catalytic domain but binds DAG (4)/phorbol ester (5) at the membrane.

Once the PKCs are phosphorylated and subsequently activated, they become highly sensitive to dephosphorylation; membrane-bound PKC is two orders of magnitude more sensitive to dephosphorylation than is PKC found in the cytoplasm.<sup>70</sup> In addition, dephosphorylation and down-regulation of PKC also takes place if cells are activated by phorbol esters (5) for an extended time, leading to proteolysis in the detergent-insoluble fraction of cells.<sup>71</sup> Other regulation methods include caveolin-dependent targeting to endosomes,<sup>72</sup> ubiquitin-mediated proteolysis,<sup>73, 74</sup> and binding of the heat-shock protein 70 (Hsp70).<sup>75</sup>

## 2.2.2 The C1 domain of protein kinase C

The regulatory part of cPKCs and nPKCs contains two DAG-sensitive C1 domains named C1a and C1b, respectively.<sup>62</sup> The C1a and C1b domains do not have equal roles in the isoenzymes; e.g. the C1b domain of PKC $\delta$  binds phorbol 12-myristate 13-acetate (PMA, **6**) with higher affinity than the C1a domain,<sup>76</sup> in contrast to PKC $\alpha$ , where both the C1a and C1b domains equally respond to PMA (**6**) and target the enzyme to the membranes.<sup>77</sup> Furthermore, in the case of PKC $\delta$ , the binding affinity for DAG (**4**) is the opposite: the C1a domain binds DAG (**4**) with higher affinity than the C1b domain.<sup>78</sup> In contrast, the C1 domains of cPKCs (e.g. PKC $\alpha$ ) have an affinity for DAG (**4**) which is two orders of magnitude lower than the C1 domains of nPKCs (e.g. PKC $\delta$ ),<sup>79</sup> which can be explained<sup>80</sup> by a single residue only found in the C1b domain of the cPKCs: Tyr123 (PKC $\beta$ II numbering).<sup>69</sup> In all other C1 domains this residue is tryptophan. In contrast, the aPKCs contain a single C1 domain which is not able to bind DAG (**4**) /phorbol esters (**5**).

Until very recently (January 2011),<sup>69</sup> the only crystal structure available of a DAG (**4**)/phorbol ester (**5**)-binding C1 domain of PKC was that of a C1b domain of PKC $\delta$  complexed with phorbol 13-*O*-acetate (**7**, PDB ID: 1PTR, Figure 8a).<sup>81</sup> Other C1 domain structures available are obtained from NMR methods (PDB ID: 2ENN, 2ENZ, 2ELI, 2E73, 1TBN and 1TBO).<sup>82, 83</sup> The crystal structure reveals an approximately 50 residues long sequence that contains two zinc finger structures where each zinc atom is coordinated by three cysteines and a histidine residue. The “bottom” third of the domain contains negatively charged amino acids and the “central” part of the domain is hydrophilic. The binding site of DAG (**4**) and phorbol esters (**5**) can be found in the hydrophobic “top” third of the domain, where a deep, narrow and polar groove can be found between two  $\beta$ -sheets (Figure 8b). The C1 domain-DAG (**4**)/-phorbol ester (**5**) complex is thought to be partly buried in the membrane bilayer,<sup>81, 84</sup> hence the positively charged amino acids in the central part of the domain could interact with anionic membrane phospholipids and the negatively charged amino acids in the bottom of the domain could face the cytoplasm. Furthermore, to overcome an enthalpy penalty caused by interactions between the polar groove of the binding site and the bilayer, the ligands are thought to act as caps on the top part of the domain to produce a continuous hydrophobic surface and thus masking the polar groove.<sup>81</sup>

The crystal structure of the C1b domain complexed with phorbol 13-*O*-acetate (**7**) reveals pivotal hydrogen bonds between the ligand and the binding site (Figure 8 and Figure 9).<sup>81</sup> The carbonyls of Leu121 and Thr113 (residue numbering corresponds to that of PKC $\beta$ II)<sup>69</sup> at the bottom of the groove act as hydrogen bond acceptors for the C20 hydroxy of **7**. In addition, the amide hydrogen of Thr113 acts as a hydrogen bond donor for the C20 hydroxy of **7**. Furthermore, the carbonyl of Gly124 is hydrogen-bonded to the C4 hydroxy of **7**, and the C3 carbonyl is also hydrogen-bonded to the amide proton of the same residue (Gly124). Among the 12,13-*O*-diesters of phorbols, the C13 carbonyl group is essential for high-affinity binding while the C12 carbonyl group is not.<sup>85-87</sup> This fact is illustrated by the inhibitor dissociation constant ( $K_i$ ) values of the monoesters 12-*O*-decanoate (**8**) and 13-*O*-decanoate (**9**); ca. 380 nM and 10

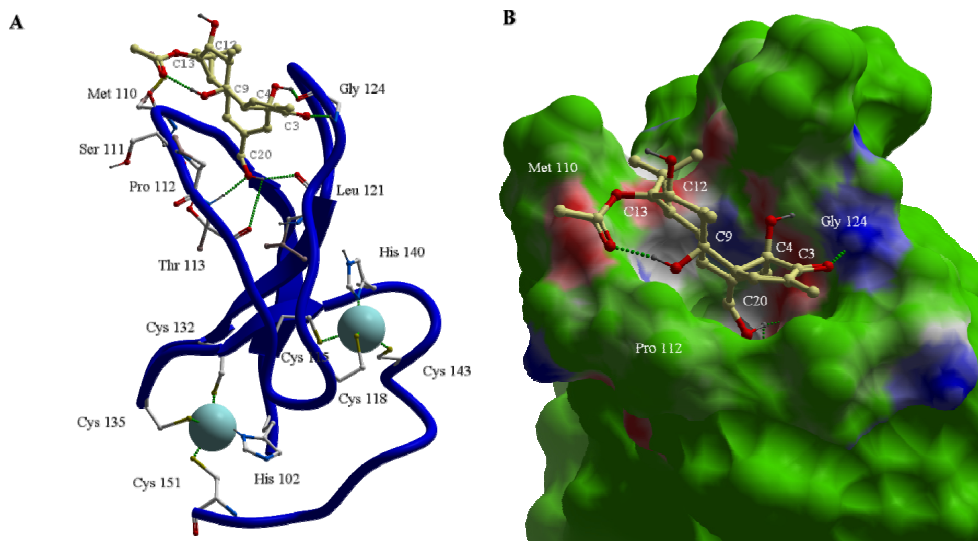


**Figure 8** The crystal structure of the PKC $\delta$  C1b domain complexed with phorbol 13-O-acetate (7, 2.2 Å resolution, PDB ID: 1PTR).<sup>81</sup> Residue numbering corresponds to that of PKC $\beta$ II (PDB ID: 3PFQ).<sup>69</sup> **A)** Side view of the structure. The pivotal polar functional groups of the phorbol ester involved in C1 domain recognition include the hydroxy groups in the carbon atoms C4 and C20 and the carbonyl group on C3. The carbonyls of Gly124, Leu121 and Thr113 are hydrogen bond acceptors (green spheres), and the amide protons of Gly124 and Thr113 are hydrogen bond donors (green spheres). The Cys and His residues coordinating the two zinc atoms (grey) are also shown. The phorbol ester and the residues are presented in ball and stick representation and colored by atom type. **B)** Top view of the binding pocket of the crystal structure. The surface is colored as follows: oxygen atoms (red), nitrogen atoms (blue), carbon atoms (green), hydrophobic groups (grey) and rest of the C1b surface is colored green. The figures were created using ICM-Browser (version 3.7-2a, MolSoft L.L.C.).

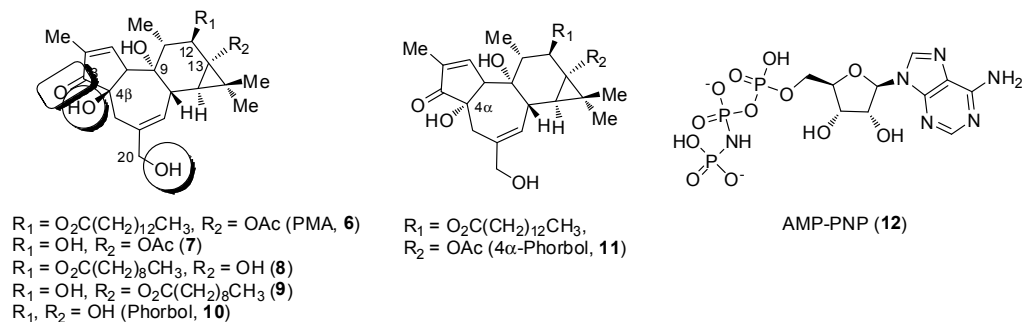


**Figure 9** Structures of phorbols 6-11. Functional groups that interact with the C1 domain are highlighted.

nM (for PKC $\delta$ ), respectively. Phorbol (**10**), with no acyl groups at C12 and C13, shows a  $K_i$  value of only 10 nM.<sup>88</sup> Even though the crystal structure does not confirm any interactions between the C13 carbonyl and the domain, it is hypothesized that the C13 carbonyl could be bridged via a water molecule to Met110,<sup>89</sup> hydrogen-bonded to Ser111 (of PKC $\gamma$ ),<sup>90</sup> to the bilayer and/or to the C9 hydroxy of **7**.<sup>82,90</sup> Furthermore, no interaction between the C9 hydroxy and the protein can be observed in the crystal structure, but it has been hypothesized that the C9 hydroxy is also involved in interactions with the bilayer.<sup>90</sup> To accomplish PKC activity, the absolute configuration of the hydroxy-bearing carbon atom C4 in phorbol esters has to be *R*, the respective *S*-configuration (e.g., compound **11**) provides an inactive compound.<sup>91</sup> In contrast, these 4 $\alpha$ -epimers (**11**) have been found to interact with the cation channel Transient Receptor Potential Vanilloid (TRPV4).<sup>92,93</sup> However, the C4 hydroxy is not essential to provide high binding to PKC.<sup>94</sup>

The C3 hydroxy of DAG (**4**, Figure 5) shows the same interactions with Leu121 and Thr113 as phorbol 13-*O*-acetate (**7**). Furthermore, the carbonyl group of the acyl moiety of DAG (**4**) at C1 has the same interaction with the protein as the C3 carbonyl of phorbol 13-*O*-acetate (**7**).

The recently published crystal structure of PKC is that of the full-length  $\beta$ II isoform complexed with adenosine 5'-( $\beta,\gamma$ -imido)triphosphate (AMP-PNP (**12**), PDB ID: 3PFQ).<sup>69</sup> Even though the crystal structure displays a modest resolution (4.0 Å), it reveals previously unknown interactions between the C1b domain and the catalytic domain, that produce a low activity state of the catalytic site (Figure 10). The kinase active site is open for substrate but, because the C1b domain clamps to the kinase domain, the conserved NFD-motif with the ATP-binding side chain of Phe629<sup>95</sup> is moved away from the binding site, resulting in the low activity state.<sup>69</sup> Upon membrane binding, the interactions between the C1b and kinase domains are lost and subsequently, the NFD-motif with the Phe629 can move back to the higher activity ATP-binding conformation. Indeed, Leonard et al. suggested that the NFD helix regulation of PKC is an alternative for the perhaps inoperative  $\alpha$ C helix mechanism of the PKCs.<sup>69</sup>

In addition to above-mentioned allosteric regulation by the NFD-motif and the C1b domain, the crystal structure reveals additional interactions between the kinase domain and the C1b domain (Figure 10b).<sup>69</sup> Residues 619-623 fill the DAG-binding site of the C1b domain and mimic DAG/phorbol ester binding. The C1b domain Gly124, which is hydrogen-bonded to the C3 carbonyl and the C4 hydroxy of phorbol esters (Figure 8), forms hydrogen bonds with the carbonyl of Pro619 and the amide proton of Ala621. Furthermore, the carbonyl of Ser110 forms a hydrogen bond with Gly623. In addition to these polar interactions, the C1b domain forms several hydrophobic interactions with the kinase domain, especially the C1b membrane penetrating side chains of residues Leu125 and Ile126 are in close contact to Phe629 of the NFD-motif.<sup>69</sup>

In addition to the crystal structures of the PKC $\delta$  and - $\beta$ II C1b domains, another crystal structure of a C1 domain has been reported (PDB ID: 1XA6).<sup>96</sup> The C1 domain part of the uncomplexed  $\beta$ 2-chimaerin crystal structure shows high similarities with those of the C1b domains of PKC $\beta$ II<sup>69</sup> and PKC $\delta$ .<sup>81</sup> Similarly as in the crystal structure of the full-length PKC $\beta$ II,<sup>69</sup> the N-terminal residues 27-34 of  $\beta$ 2-chimaerin form a helix that covers the binding groove of the C1 domain.<sup>96</sup> In addition, residue Gln32 forms a hydrogen bond with Gly235 in

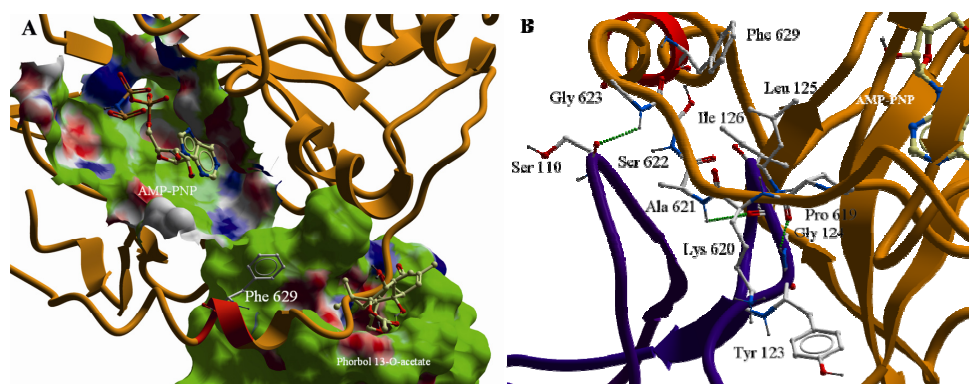


**Figure 10** *A)* The crystal structure of the C1b domain of PKC $\delta$  complexed with phorbol 13-O-acetate (7, PDB ID: 1PTR)<sup>81</sup> superimposed on the crystal structure of the full-length PKC $\beta$ II complexed with adenosine 5'-( $\beta,\gamma$ -imido)triphosphate (AMP-PNP (12), 4.0 Å resolution, PDB ID: 3PFQ).<sup>69</sup> The binding pockets of the C1b domain and the ATP-binding site are presented as surfaces and are colored as follows: oxygen atoms (red), nitrogen atoms (blue), carbon atoms (green), hydrophobic groups (grey) and rest of the C1b surface is colored green. Phorbol 13-O-acetate (7), AMP-PNP (12) and residues are presented in ball and stick representation and colored by atom type. The conserved NFD-motif is colored red and rest of the kinase domain is colored orange. *B)* Side view of the PKC $\beta$ II C1b domain (colored blue), otherwise colored as in A. Hydrogen bonds are represented as green spheres. The figures were created using ICM-Browser (version 3.7-2a, MolSoft L.L.C.).

the “top” of the binding groove (Gly235 corresponds to Gly124 and Gly253 of PKC $\beta$ II and PKC $\delta$ , respectively, see Figure 8 and Figure 10). Other proteins that contain a DAG-responsive C1 domain are the protein kinase D (PKD), the guanyl nucleotide-releasing proteins (RasGRPs), the Unc-13 scaffolding proteins, myotonic dystrophy kinase-related Cdc42-binding kinases (MRCK) and the DAG kinases  $\beta$  and  $\gamma$ .<sup>97,98</sup> Since the number of C1 domain-containing proteins is considerably smaller than the number of kinases<sup>1</sup> and the catalytic domain and, in particular, the ATP-binding site of PKs is highly conserved,<sup>99</sup> the C1 domain provides an attractive target for designing selective PKC modulators.<sup>60,100</sup>

### 2.2.3 Natural compounds targeting the C1 domain

In addition to phorbol esters (5), several natural compounds target the C1 domain of PKC.<sup>100</sup> Among these ligands, most bind to the C1 domain with similar interactions as the phorbol esters; however, there are some exceptions. The total syntheses of natural ligands are usually laborious; therefore, the pharmacophores of the natural ligands have been used to design simplified compounds, these will be presented in the next chapter (Chapter 2.2.4.). In this chapter some of the most important natural compounds targeting the C1 domain are presented.

## Prostratins

Prostratin (**13**) was initially isolated from the extracts of *Homalanthus nutans* G. Forst.; Guill. and used in traditional Samoan herbal medicine for treatment of hepatitis.<sup>101</sup> Prostratin (**13**) and 12-deoxyphorbol 13-phenylacetate (DPP, **14**) have the phorbol ester skeleton but lack the C12 hydroxy/acyl group found in phorbols (Figure 9 and Figure 11).<sup>102, 103</sup> This small difference in the chemical structure makes these derivatives non-tumor promoters, unlike most of the phorbol esters.<sup>104</sup> Prostratin shows a  $K_i$  value of 12.5 nM for PKC.<sup>101</sup> In addition, prostratin derivatives have been suggested to be effective in HIV therapy by a PKC-dependent mechanism.<sup>105-108</sup> A five-step synthesis of prostratin and its derivatives starting from readily available phorbol (**10**) was recently published, thus facilitating the preparation of these complex structures (for synthetic compounds, see Chapter 2.2.4.).<sup>102</sup> Prostratin shows the same interactions with the C1 domain as the phorbol esters (*vide supra*).

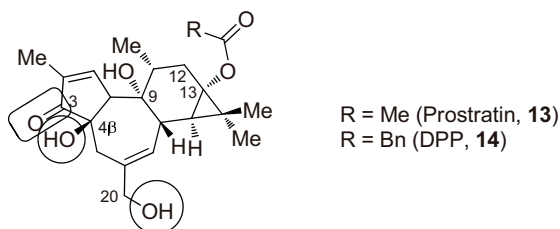


**Figure 11** Structures of prostratin (**13**) and 12-deoxyphorbol 13-phenylacetate (DPP, **14**). Functional groups that interact with the C1 domain are highlighted.

## Ingenols

The ingenols (**15** and **16**) are structurally closely related to phorbol esters (**5**) and can be extracted from the sap of *Euphorbia peplus* L.<sup>109</sup> Ingenols have been used in traditional medicine to treat skin diseases like warts, corns and skin cancers as well as asthma and migraine.<sup>110, 111</sup> Indeed, PEP005 (**16**) has shown promising results in the treatment of skin tumors.<sup>111</sup>

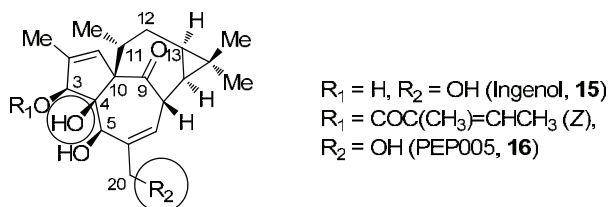


**Figure 12** Structures of ingenols (**15** and **16**). Functional groups that interact with the C1 domain are highlighted.



When compared to the seven-membered ring of the tumor-promoting phorbol esters (**5**), ingenols (**15** and **16**) have an additional hydroxy group at C5 (Figure 9 and Figure 12). In addition, in ingenols (**15** and **16**) the C9 hydroxy of the phorbols is in an oxidation state of a carbonyl. Furthermore, the six-membered ring of the phorbols corresponds to the new seven-membered ring in the ingenols, where no ester groups at C12 or C13 can be found. The C3 carbonyl in the five-membered ring of phorbols is replaced with an acyl or hydroxy group in ingenols. These differences in the structures of the corresponding ingenols make them more hydrophilic than the phorbol esters; for example, the  $\text{clog}P$  values of PEP005 (**16**) and PMA (**6**) are 3.89 and 6.65, respectively.<sup>112</sup>

Ingenol (**15**) binds more tightly than phorbol (**10**) to PKC ( $K_i$  values of 30  $\mu\text{M}$  and 10 nM, respectively).<sup>88, 113</sup> PEP005 (**16**),<sup>114</sup> with an (*Z*)-2-methylbut-2-enoyl group at C3, shows  $K_i$  values of 0.1-0.4 nM, depending on the PKC isoform studied.<sup>112</sup> Despite the lack of specificity among isoforms, PEP005 (**16**) activates PKC $\delta$  more potently than PKC $\alpha$  in vitro. While PMA (**6**) induces the translocation of PKC $\delta$  to the plasma membrane, PEP005 (**16**) induces an initial translocation of the enzyme from the cytosol to the nuclear and perinuclear membranes.<sup>112, 115, 116</sup>

### Bryostatins

The bryostatins (e.g. **17** and **18**) were first isolated from the marine bryozoan *Bugula neritina* L.;<sup>117</sup> however, the symbiotic bacteria are thought to be the actual sources of the compounds.<sup>118</sup> There are at least 20 naturally occurring bryostatins that bind to the regulatory domain of PKC with high affinity.<sup>119</sup> Bryostatin 1 (**17**), the most extensively examined bryostatatin, and bryostatin 2 (**18**), show  $K_i$  values of 1.35 and 5.9 nM, respectively, for PKC $\alpha$ .<sup>120</sup> Bryostatins have proceeded to clinical trials as potential treatment for different cancers, AD, and also acting as activators of effector cells of the immune system.<sup>33, 100</sup> The highly complex structures of the

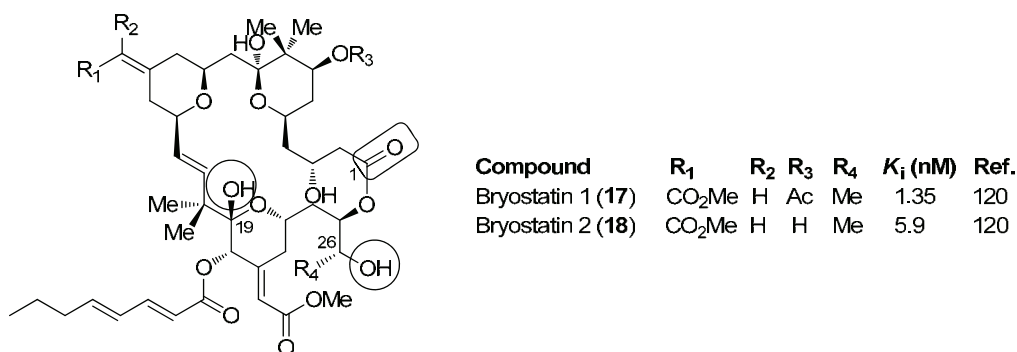


**Figure 13** Structures of representative examples of bryostatins (**17** and **18**). Functional groups that interact with the C1 domain are highlighted. The  $K_i$  (nM) values are also shown.

bryostatins make the total synthesis laborious; generally over 40 linear synthesis steps are required.<sup>119, 121, 122</sup> However, simplified derivatives of the bryostatins have been synthesized (see Chapter 2.2.4.).

The bryostatins bind to the regulatory domain in the same way as phorbol esters (**5**). Functional groups which are involved in forming hydrogen bonds with the C1 domain are the carbonyl of C1 and the hydroxy of C19 and C26 (Figure 13). Bryostatin 1 (**17**) competes for binding with DAG and phorbol esters. However, specific to bryostatin 1 (**17**) is that the phorbol ester antagonism, at least for leukemia cell differentiation, is non-competitive<sup>123</sup> and it shows biphasic concentration-dependent effects in many biological responses.<sup>100</sup> Furthermore, bryostatin 1 (**17**) functions as an activator and induces translocation of PKC $\delta$  almost exclusively to the nuclear membrane.<sup>56</sup>

### *Aplysiatoxins*

The marine spiroketals aplysiatoxin (**19a**) and debromoaplysiatoxin (**19b**, Figure 14) can be isolated from the sea hare *Stylocheilus longicauda* Quoy & Gaimard.<sup>124</sup> These structurally complex spiroketals compete with [20-<sup>3</sup>H]phorbol 12,13-dibutyrate ([<sup>3</sup>H]PDBu) for binding to its receptors<sup>125</sup> but are tumor-promoters.<sup>126</sup> Interestingly, compound **19a** was shown to inhibit [<sup>3</sup>H]PDBu binding in cloned rat embryo fibroblast (CREF) cells more strongly than compound **19b** (IC<sub>50</sub> values of 14 and 94 nM, respectively); however, the bromine in the phenol ring caused also higher tumor-promoting activity.<sup>125</sup> The measured  $K_i$  values for **19a** and **19b** are 3.0 nM<sup>127</sup> and 20 nM,<sup>128</sup> respectively, for PKC $\delta$ .

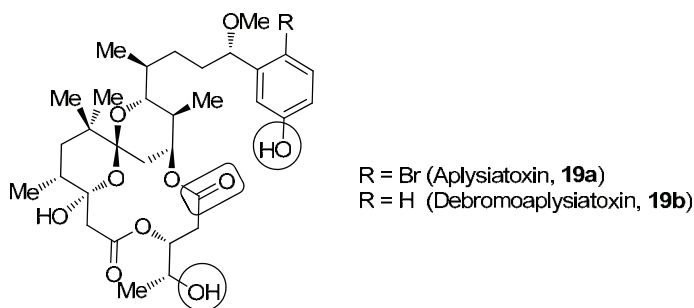


**Figure 14** Structures of aplysiatoxins (**19a** and **19b**). Functional groups that interact with the C1 domain are highlighted.

### *Indolactams*

Among the indolactams, the teleocidin family of indole alkaloids was first isolated from *Streptomyces mediocidicus* Labeda; Wellington et al.<sup>129</sup> These teleocidins are tumor promoters<sup>130</sup> and bind to the C1 domain.<sup>131</sup> The structurally simplest indolactam is (-)-

indolactam V (**20**), which is considered to be the minimum-sized structure exhibiting tumor-promoter activity.<sup>132</sup> Indolactam V (**20**) and teleocidin B-4 (**21**) show  $K_i$  values of 80 and 0.4 nM, respectively, for PKC $\delta$ .<sup>133</sup> The discovery of the indolactams has led to the development of synthetic indo- and benzolactam derivatives, these will be discussed in more detail in Chapter 2.2.4.

The indolactams bind to the C1b domain of PKC in a similar way as the phorbol esters (**5**).<sup>134,135</sup> The primary hydroxy groups of indolactams form hydrogen bonds to Thr113 and Leu121 in the groove of the PKC $\delta$  C1b domain (Figure 15, residue numbering corresponds that of PKC $\beta$ II, see Figure 8). In addition, the lactam N-hydrogen is hydrogen-bonded to Leu121 and the C11 carbonyl group acts as a hydrogen bond acceptor for Gly124. Furthermore, the indole rings of indolactams are thought to have CH/ $\pi$  interactions with Pro112 of PKC $\delta$ .<sup>136</sup>

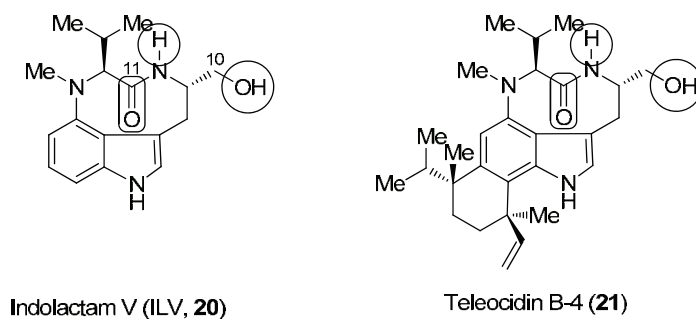


**Figure 15** Structures of indolactam (**20**) and teleocidin B-4 (**21**). Functional groups that interact with the C1 domain are highlighted.

### Anthracyclines

Anthracyclines, such as doxorubicin (DOX, **22**) and daunorubicin (daunomycin (**23**), Figure 16), are chemotherapeutic agents that are obtained from *Streptomyces peuceletii* Grein et al. and *S. coeruleorubidus* Preobrazhenskaya; Pridham et al.<sup>137,138</sup> Doxorubicin (**22**) has been used in the clinic for more than 30 years and remains one of the most widely used cancer chemotherapeutics.<sup>139</sup> However, tumor cells are able to develop resistance to doxorubicin (**22**). Fortunately, synthetic derivatives have been developed to overcome this setback (see Chapter 2.2.4.).

Doxorubicin (**22**) does not effectively bind PKC (< 20% inhibition of [<sup>3</sup>H]PDBu at 20  $\mu$ M) and localizes in the nucleus.<sup>139</sup> The anthracyclines exert their antitumor effects mainly via interference with a DNA-topoisomerase II interaction during DNA replication.<sup>140</sup> Doxorubicin (**22**) intercalates into DNA with rings B and C between the adjacent base pairs of DNA and the aminoglycoside moiety located in the minor groove of DNA.<sup>138</sup> This stabilizes the DNA-topoisomerase complex, and the DNA replication and cell division are halted. However, when the 3'-amino group of the daunosamine aminoglycoside is substituted with, for example, a benzyl group, and more importantly, the C14 hydroxy group of **22** is acylated, the new derivative

binds DNA only weakly and PKC activity can be obtained instead.<sup>139</sup> The synthetic anthracyclines are further discussed in Chapter 2.2.4.

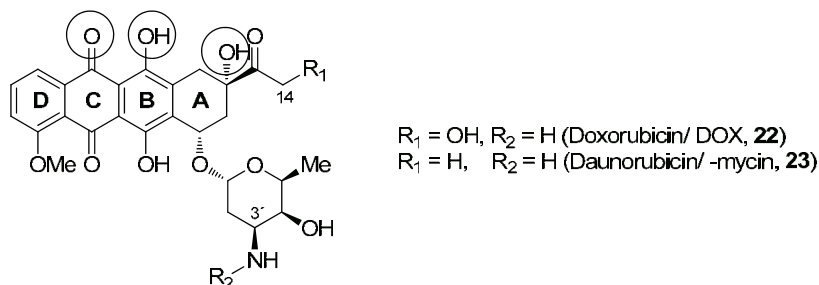
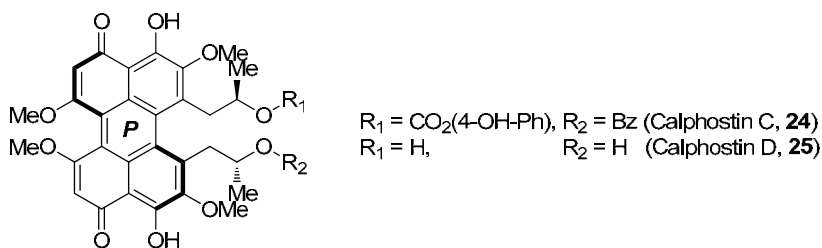


**Figure 16** Structures of anthracyclines (**22** and **23**). Functional groups that interact with the C1 domain are highlighted.

### Calphostins

The calphostins (e.g. **24** and **25**) are polycyclic aromatic perylenequinones and potent PKC-selective inhibitors isolated from the fungus *Cladosporium cladosporioides* Fresenius; de Vries.<sup>141, 142</sup> Of the calphostins, the best binding affinity to PKC can be obtained by calphostin C (**24**). It selectively binds the C1 regulatory domain of PKC, showing an  $\text{IC}_{50}$  value of 50 nM for rat brain PKC isoenzymes, when the  $\text{IC}_{50}$  values for example PKA and polyphosphate kinase (PPK) are greater than 100  $\mu\text{M}$ .<sup>141, 143</sup> Interestingly, the inhibitory effects of calphostin C (**24**) include both the inhibition of phosphotransferase activity and the inhibition of phorbol ester binding to the C1 domain.<sup>141, 144</sup> The activities of the calphostins are light-induced, making them candidates for photodynamic therapeutics.<sup>145-147</sup>



No molecular modeling results of calphostin C (**24**) docked to the C1 domain can be found in literature. On the other hand, one could assume that the calphostins bind to the C1 domain in a similar way as the structurally related anthracyclines (*vide supra*). The total syntheses of natural compounds are usually laborious and this is also the case with the calphostins; the present total

synthesis of calphostin C (**24**) requires 12 steps.<sup>148, 149</sup> Derivatives of calphostins have been synthesized, see Chapter 2.2.4.

Although calphostin C (**24**) has been reported to show proapoptotic effects in numerous cancer cell lines<sup>150-152</sup> and it has been suggested as a candidate for photodynamic cancer therapy,<sup>147, 153</sup> there are few or no reports describing the effects of calphostin C (**24**) on in vivo models of cancer.

### *Iridals and SJ23B*

The iridal type triterpenoids can be obtained from sword lilies (e.g. *Iris tectorum* Maxim. and *I. germanica* L.) and bind to the C1 domains and activate PKC.<sup>154, 155</sup> Two iridals (**26** and **27**, Figure 17) were shown to bind to PKC $\alpha$  with  $K_i$  values of 84 and 76 nM, respectively, and with slightly better binding affinities ( $K_i$  values of 42 and 16 nM, respectively) for Ras guanyl-releasing protein 3 (RasGRP3).<sup>156</sup> The iridals have shown anti-tumor activity in several cell lines and in some cases to be less affected by multi-drug resistance expressing cell lines than doxorubicin (**22**) or paclitaxel.<sup>157</sup> Recently, the first total synthesis of an iridal (**28**) was performed, requiring over 20 steps.<sup>158</sup>

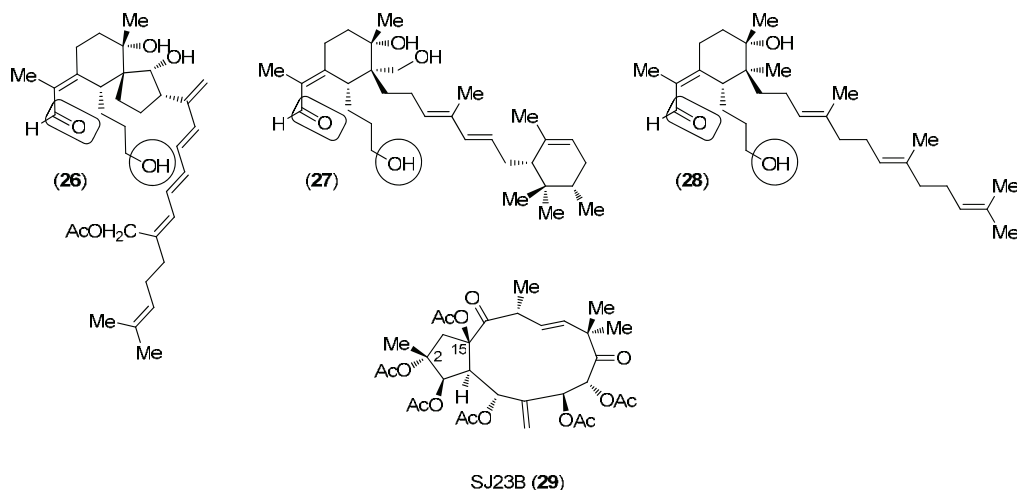


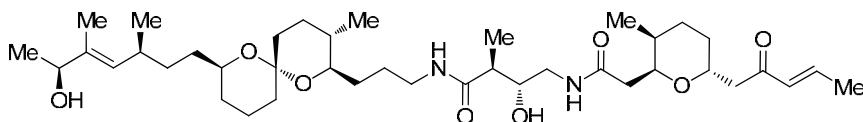
**Figure 17** Structures of iridals (**26-28**) and SJ23B (**29**). Functional groups that interact with the C1 domain are highlighted.

A jatropane diterpene SJ23B (**29**, Figure 17) isolated from *Euphorbia semiperfoliata* Viv.<sup>159</sup> has shown in vitro potential PKC $\alpha$ -mediated antiviral effects on HIV-1 infection and activation of latent HIV-1 gene expression, being 10-fold more potent than prostratin (**13**).<sup>160</sup> Furthermore, it is not toxic and it does not induce cell transformation, suggesting that it lacks tumor-promoting

activity. So far, no PKC-binding data has been provided. Studies with other jatrophone diterpenes revealed the importance of the acetoxy groups at C2 and C15 for activity in HIV-1 models.<sup>160</sup>

### Bistramide A

Bistramide A (bistratene A, **30**) is a bioactive cyclic polyether initially isolated from the marine ascidian *Lissoclinum bistratum* Sluiter in 1988 by Verbist et al.<sup>161</sup> Six years later four additional members of the family were isolated.<sup>162</sup> This class of compounds shows important cyto-<sup>163</sup> and neurotoxicity,<sup>164-166</sup> for example IC<sub>50</sub> values of bistramide A (**30**) for the human-derived A549 lung and MCF-7 breast adenocarcinoma cells were between 1.0 and 2.9 nM.<sup>167</sup> Bistramide A (**30**) has been shown to have a short half-life in cell culture medium; only 2.8 hours.<sup>167</sup> The bistramides also show antiparasitic<sup>168,169</sup> and immunomodulatory activities,<sup>163</sup> and they play a complex role in cell cycle regulation, differentiation, and apoptosis, thus have emerged as a potential anti-inflammatory and anti-tumor agents.<sup>162</sup>



**30**

Bistramide A (**30**) was initially found to activate PKC $\delta$  in human leukemia (HL)-60 and MM96E cells.<sup>163,170,171</sup> More recently, covalent modification of actin and disruption of filamentous actin were reported as the major mode of action for bistramide A (**30**) in various cancer cell lines.<sup>172</sup> The  $K_i$  value of bistramide A (**30**) for PKC $\delta$  was found to be only 28  $\mu$ M. In contrast, the dissociation constant ( $K_d$ ) value of bistramide A (**30**) for actin was determined to be 6.8 nM. Hence, there has been little consensus on the activation of PKC $\delta$ : bistramide A (**30**) does not activate PKC $\delta$  in vitro, nor does it compete with phorbol esters in binding to the C1 domain.<sup>167,172,173</sup> However, while bistramide A (**30**) failed to translocate green fluorescent protein (GFP)-PKC $\delta$  in rat basophilic leukemia (RBL) cells,<sup>172</sup> immunostaining and fractionation studies showed migration of PKC $\delta$  to the perinuclear region rather than the nuclear or plasma membrane.<sup>170</sup> Furthermore, only specific substrates of PKC $\delta$  were phosphorylated, suggesting an atypical mode of activation.<sup>174</sup>

In 2004, Kozmin et al. performed the first total synthesis of bistramide A (**30**).<sup>175</sup> Since then, the research groups of Crimmins,<sup>176</sup> Panek,<sup>177,178</sup> and Yadav<sup>179</sup> have synthesized bistramide A (**30**) with a longest linear sequence of 18 steps. The crystal structure of actin complexed with bistramide A (**30**) was published in 2006 (PDB ID: 2FXU).<sup>180</sup> The crystal structure helped researchers to develop simplified analogs of bistramide A (**30**) and to perform SAR studies.<sup>173,181</sup> Bistramide C is another member of the bistramide family, which has been synthesized.<sup>182,183</sup>

### *Summary of the natural compounds targeting the C1 domain*

Several natural compounds show very potent binding to the C1 domain of PKC (e.g. bryostatin 1 (**17**) and PEP005 (**16**)), however, the resulting biological outcomes of the ligands are more important than only the inhibitor dissociation constant. For example, while the indolactam teleocidin B-4 (**21**) shows impressive binding of PKC $\delta$  ( $K_i$  of 0.4 nM), it is also a tumor-promoter.<sup>130</sup> In contrast, although prostratin (**13**) is a non-tumor promoting PKC ligand, it exhibits possible cytotoxic properties.<sup>108</sup> Furthermore, bryostatin 1 (**17**) shows impressive antineoplastic properties but it has not shown to be efficient enough as a single agent in clinical trials.<sup>184, 185</sup> One promising natural compound is PEP005 (**16**), which has shown to be potent in topical treatment of actinic keratosis and will probably reach the market in the near future.<sup>111, 186, 187</sup>

Even though C1-domain-binding compounds can be obtained from natural sources, the isolated yields of the compounds are usually very low. In addition, the compounds show often highly complex structures and hence, the total syntheses of the compounds are often laborious. Nevertheless, the studies of the natural compounds have yielded valuable pharmacophores, which have been used to develop simplified analogs of the natural compounds.

### **2.2.4 Synthetic compounds targeting the C1 domain**

Natural compounds targeting the C1 domain can generally be obtained in small quantities from natural sources. Even though biotechnological methods have been used in some cases to produce larger quantities of active compounds, synthetically prepared compounds could enhance the effectiveness of the production and the development of improved derivatives. However, since natural compounds often show complex structures, the total syntheses are generally laborious. In fact, many synthetic compounds targeting the C1 domain are semisynthetic, that is, a natural compound has been used as a starting material for the derivatives. In addition, the pharmacophores of the natural compounds have been used to develop derivatives with simplified structures. Rational design has also been used in preparing totally unique C1-targeting compounds. In this chapter, some of the most important synthetic compounds targeting the C1 domain are presented.

#### *Prostratin analogs*

The complex structure of prostratin (**13**, Figure 11) has been one of the reasons why prostratin based compounds of this non-tumor-promoting ligand have not been developed. However, Wender et al. recently published a five-step synthesis of prostratin (**13**), DPP (**14**) and the 13-*O*-ether analogs **31** and **32** starting from readily available phorbol (**10**) (Figure 9 and Figure 18).<sup>102</sup> Examples of prostratin analogs synthesized since then are **33-35** and these were shown to bind to

a mixture of PKC isoforms, e.g. the  $K_i$  value of analog **33** was 1.6 nM.<sup>188</sup> The analogs **33-35** also showed activity against the human leukemia cell line K562,  $EC_{50}$  values ranging between 0.02-0.03 nM. In addition, compounds **33-35** induced the expression of HIV in cells with latent viral expression.

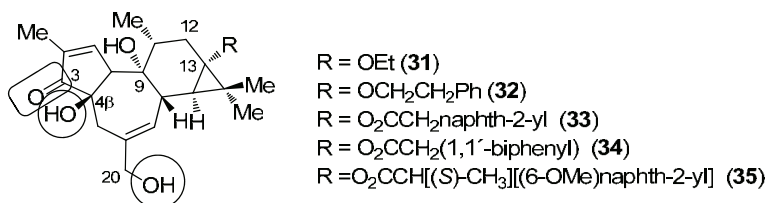


**Figure 18** Structures of prostratin analogs (**31-35**). Functional groups that are thought to interact with the C1 domain are highlighted.

### Ingenol derivatives

The 3-*O*-tetradecanoyl (**36**)<sup>189</sup> and 3-*O*-benzoyl (**37**)<sup>190</sup> derivatives of ingenol are semisynthetic compounds which have been prepared starting from ingenol (**15**) (Figure 12 and Figure 19). The derivative **37** shows a  $K_i$  value of 0.14 nM for PKC $\alpha$ .<sup>190</sup> The  $K_i$  value for **36** is 7 nM but the value cannot be compared to the  $K_i$  value of **37** since it was measured in vitro by release of [<sup>3</sup>H]phorbol 12,13-dipropionate bound specifically to mouse epidermal particulate fraction.<sup>191</sup> However, **36** and **37** were found to be tumor-promoting. Interestingly, a dibenzoate derivative (**38**,  $K_i = 240$  nM for PKC $\alpha$ )<sup>190</sup> was found to induce apoptosis in Jurkat cells, however, not via PKC-mediated activation, but via caspase-3 activation.<sup>192</sup> The fact that induction of apoptosis is not via PKC is not surprising, since **38** cannot form the same interactions with the groove in the binding site of the C1 domain as is seen for **36** because of its C20 benzoate group. Another diester (PEP008, **39**) has showed permanent growth arrest in solid tumor (melanoma, breast, and colon) cell lines.<sup>193</sup>

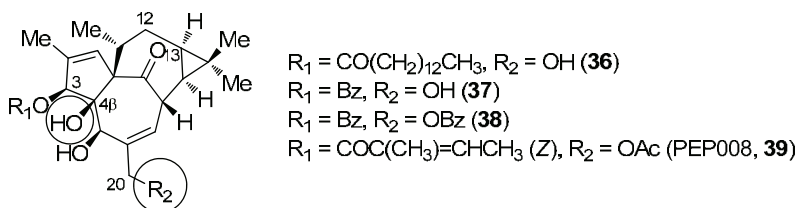


**Figure 19** Structures of synthetic ingenol derivatives (**36-39**). Functional groups that are thought to interact with the C1 domain are highlighted.



## Bryostatin analogs

The naturally occurring bryostatins show high affinity for the C1 domain of PKC,<sup>119</sup> however, the total syntheses of these highly complex macrocyclics require generally over 40 linear steps.<sup>119, 121, 122</sup> In addition, results from clinical trials of bryostatins as single agents<sup>184, 185</sup> or in combination therapy with established cancer drugs<sup>194-201</sup> have been rather disappointing. Therefore, research groups have put on an effort into reducing the required steps for total synthesis as well as developing analogs of bryostatins.<sup>119</sup> The Wender group developed a synthesis route for simplified derivatives (**40-44**) of bryostatin 1 (**17**) with a significantly reduced number of reaction steps.<sup>202, 203</sup> Removal of the methyl substituent at C26 of compound **40** ( $K_i$  value of 3.4 nM for rat brain PKC isoenzymes)<sup>204</sup> gave compound **41**,<sup>120</sup> which showed higher affinity ( $K_i$  value of 0.25 nM for rat brain PKC isoenzymes), as predicted by the pharmacophore of phorbol esters (Figure 9). Interestingly, the addition of an acetoxy substituent to C7, similar to bryostatin 1 (**17**), reduced the  $K_i$  value to 13 nM (compound **42**), and the addition of a hydroxy group to C7 (analog **43** and **44**) reduced the binding affinity even further by three to four orders of magnitude. On the other hand, bryostatin 2 (**18**), with a hydroxy group at C7, shows only a slight reduction in binding affinity compared to bryostatin 1 (**17**, see Chapter 2.2.3.).<sup>120</sup> Alternatively, compound **45** (see Figure 13;  $R_1 = H$ ,  $R_2 = H$ ,  $R_3 = Ac$ ,  $R_4 = Me$ ), which has a C7 acetoxy group as bryostatin 1 (**17**) and analog **42**, but lacks the C30 methoxy carbonyl group found in bryostatin 1 (**17**), exhibited a reduced  $K_i$  value of 0.52 nM for PKC $\alpha$  but is also a functional antagonist of PMA (**6**).<sup>205</sup> It has been speculated that these differences in binding affinities are due to the C8 *gem*-dimethyl groups found in the natural bryostatins (e.g. bryostatin 1 (**17**)), which are able to shield a polar C7 substituent. Furthermore, the C3 hydroxy group of bryostatins is pivotal for high binding affinity.<sup>204</sup> For further SAR information, see reviews in ref. 100 and 119.

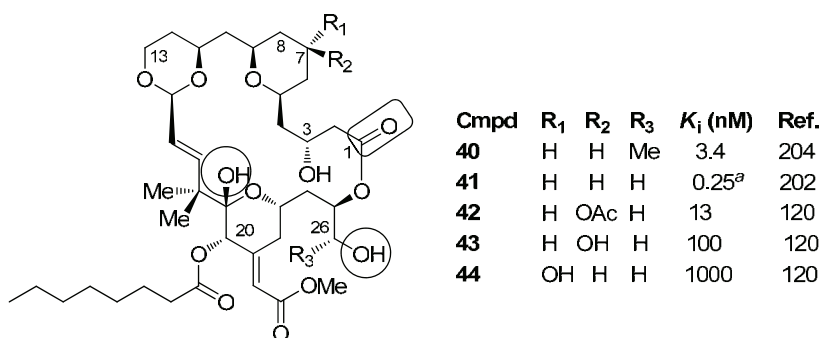


**Figure 20** Structures of synthetic bryostatin analogs (**40-44**). Functional groups that are thought to interact with the C1 domain are highlighted. The  $K_i$  values are also shown. <sup>a</sup> Wender et al. also reported a  $K_i$  value of 3.1 nM for the same derivative.<sup>206</sup>

### *Aplysiatoxin analogs*

The natural aplysiatoxins **19a** and **19b** bind to PKC with high affinity but are tumor-promoting compounds.<sup>125</sup> Recently, Nakagawa et al. speculated that the bromine present in the natural aplysiatoxin **19a**, as well as the hydrophobicity of the compound, produces the tumor-promoting activity.<sup>127</sup> Indeed, Nakagawa et al. synthesized a structurally simpler aplysiatoxin analog (**46**) with bryostatin-like activity, which showed a  $K_i$  value of 15 nM to PKC $\delta$  (the  $K_i$  value of **19a** is 3.0 nM).<sup>127</sup> Removal of the phenolic hydroxy group from **19a** gave compound **47**, which showed an even more reduced binding affinity ( $K_i$  of 400 nM for PKC $\delta$ ), suggesting that the geminal dimethyl group and/or the phenolic hydroxy group of analog **46** specifically interact with PKC $\delta$ . Furthermore, compound **46** functions as a PKC activator but does not induce translocation of the enzyme only to the plasma membrane but also to the nuclear membrane,<sup>127</sup> which could be an indication of a non-tumor-promoting modulator.<sup>56</sup> The synthesis of analog **46** requires 22 steps.<sup>127</sup>

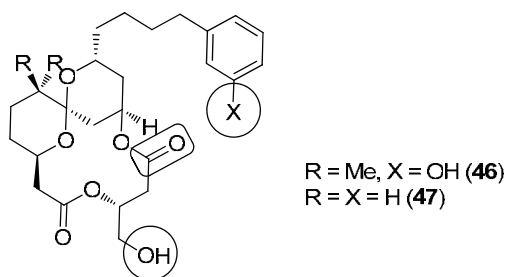


**Figure 21** Structures of synthetic aplysiatoxin analogs (**46** and **47**). Functional groups that are thought to interact with the C1 domain are highlighted.

### *Indo- and benzolactams*

The natural indolactams **20** and **21** are tumor-promoting compounds but bind with high affinity to PKC (e.g. **20** shows a  $K_i$  of 80 nM for PKC $\delta$ , cf. 2.2.3.).<sup>133</sup> Endo et al. introduced the benzolactams as a result from research into the active structure of teleocidin (**21**).<sup>207</sup> Benzolactam **48** showed a decreased binding affinity towards PKC $\delta$  ( $K_i$  of 1700 nM), however, compound **49**, with a lipophilic side chain at C9, showed an improved  $K_i$  value of 1.8 nM (PKC $\delta$ ). In addition to the above-mentioned compounds, several research groups have prepared synthetic benzo- (e.g. **48-55**) and indolactams (e.g. **56-57**) and have revealed important SARs (see, e.g. ref. 100, 133, and 208-210). Many of these compounds show improved selectivity profiles compared to the natural indolactam family of compounds.<sup>100, 135, 208, 211-214</sup> The benzolactam derivatives have been studied for their antiproliferative effects on cancer cells,<sup>133, 207, 211, 215</sup> and their neuroprotective effects in cell-based models of AD.<sup>216</sup> The indolactam **20**

and several benzolactam derivatives (e.g. **49**) have been reported to inhibit the proliferation of HL-60 leukemia cells.<sup>133, 207, 215</sup>

The benzolactams bind to the regulatory domain of PKC (Figure 8) with the same interactions as the indolactams (see Chapter 2.2.3.) but do not have CH/ $\pi$  interactions with Pro112 of PKC $\delta$  (Figure 15 and Figure 22, residue numbering corresponds to PKC $\beta$ II).

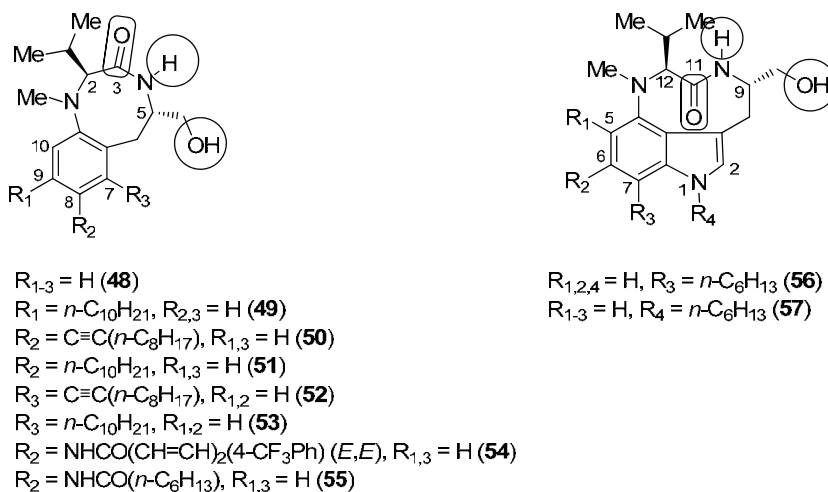


**Figure 22** Structures of synthetic benzo- (**48-55**) and indolactams (**56** and **57**). Functional groups that are thought to interact with the C1 domain are highlighted.

### Anthracyclines

To overcome doxorubicin (**22**) resistance and to reduce doxorubicin-induced cardiotoxicity, a novel semisynthetic anthracycline derivative AD 198 (**58**) was prepared.<sup>217</sup> It only weakly binds to DNA and has little inhibitory activity on topoisomerase II, suggesting that it has a different mechanism of action than conventional anthracyclines.<sup>140</sup> AD 198 (**58**) activates PKC<sup>218</sup> by targeting the C1 domain<sup>219</sup> but shows a modest  $K_i$  value of 2.5  $\mu\text{M}$  for PKC $\delta$ .<sup>219</sup> However, AD 198 (**58**) is effective in vitro against several cancer cell lines<sup>220-223</sup> and its anti-tumor activity is superior to doxorubicin (**22**).<sup>224</sup>

By using the crystal structure of the PKC $\delta$  C1b domain,<sup>81</sup> three theoretical binding models were proposed in which AD 198 (**58**) binds to the C1 domain.<sup>219</sup> In these models, AD 198 (**58**) binds in the groove of the C1b domain but less deeply than phorbol esters (**5**) and with different interactions (Figure 24A). In one of the binding models of AD 198 (**58**), Ser111 (residue numbering corresponds to that of the crystal structure of full-length PKC $\beta$ II)<sup>69</sup> and Gln128 bind to the C9 hydroxy and Gly124 binds to the C12 carbonyl and C11 hydroxy, which is also

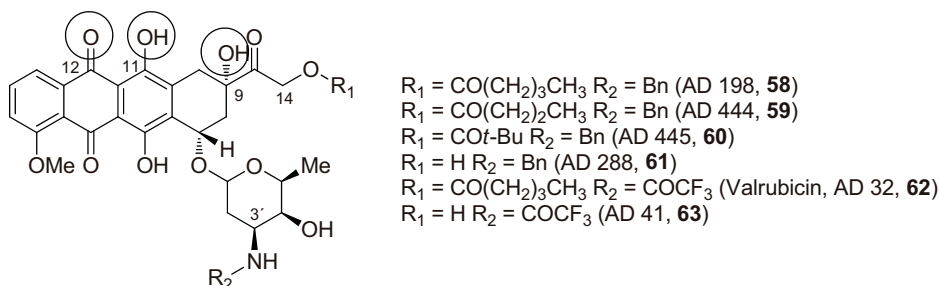


**Figure 23** Structures of synthetic anthracyclines (**58-63**). Functional groups that are thought to interact with the C1 domain are highlighted.

hydrogen-bonded to Leu121 (Figure 23 and Figure 24B). The C14 valerate and C3' N-benzyl group were thought to play a similar role to the acyl groups of phorbol esters (**5**) in binding to C1 domains (Figure 8), and the positively charged amino group was suggested to be at least partially responsible for the translocation to the nuclear membrane. Furthermore, the valerate group of AD 198 (**58**) increases the lipophilicity compared to doxorubicin (**22**) and induces AD 198 (**58**) to localize in the perinuclear region.<sup>225</sup>

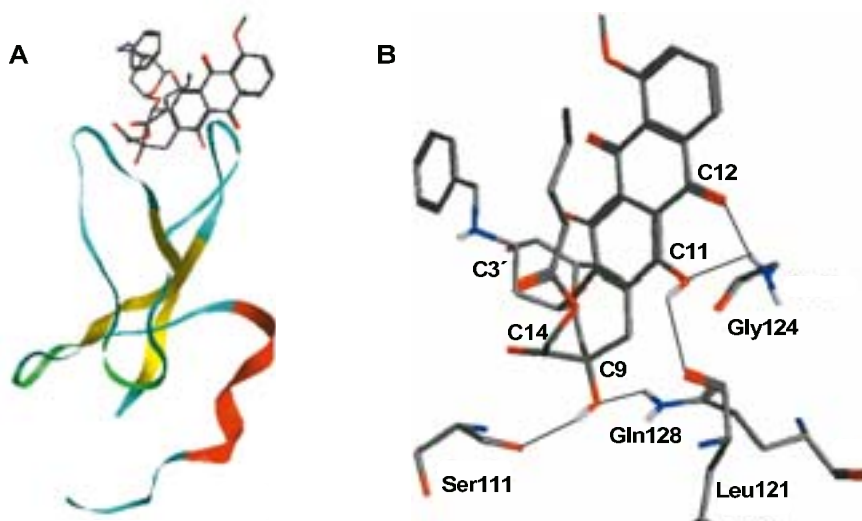


**Figure 24** One of the suggested binding models of AD 198 (**58**) to the C1 domain.<sup>219</sup> **A)** AD 198 (**58**) docked to the C1b domain of PKC $\delta$ . **B)** A binding model of AD 198 (**58**) in the C1b domain of PKC $\delta$  showing hydrogen bonds to the residues (black lines). Residue numbering corresponds to that of the crystal structure of full-length PKC $\beta$ II.<sup>69</sup> AD 198 (**58**) and the residues are presented in stick representation and are colored by atom type. Adapted with permission from ref. 219. Copyright 2011 American Chemical Society.

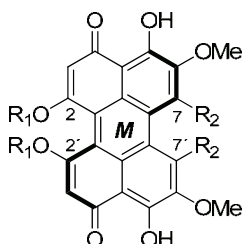
Among different C14 acyl-substituted derivatives synthesized, compounds containing 4-5 carbons (e.g., AD 198 (**58**), AD 444 (**59**) and AD 445 (**60**)) were found to be the most promising.<sup>139</sup> Interestingly, doxorubicin (**22**) and AD 288 (**61**), the principal metabolite of AD198 (**58**), are both incapable of inhibiting PKC activity or competing for [<sup>3</sup>H]PDBu binding.<sup>139</sup>

Another semisynthetic anthracycline derivative, valrubicin (AD 32, **62**),<sup>221</sup> has similar PKC-inhibitory properties to AD 198 (**58**),<sup>226</sup> and the mechanism of action of its valerate-free metabolite AD 41 (**63**) can be compared to that of AD 288 (**61**) and doxorubicin (**22**).<sup>225</sup> Valrubicin (**62**) was reported to be safe in a phase I trial with advanced gynecological malignancies<sup>227</sup> and has thereafter been approved in the US for topical treatment of bladder cancer.<sup>140</sup>

### Calphostin analogs

Morgan and co-workers used *ent*-pleichrome (**64**, an atropisomer of calphostin D (**25**)) and the crystal structure of the PKC $\delta$  C1b domain<sup>81</sup> to design new perylenequinone derivatives.<sup>228</sup> The docking studies showed an unfilled hydrophobic pocket in the protein, where the C2,C2'-methoxy groups were pointing; thus, the corresponding bisisopropyl and bis-*n*-propyl derivatives (compounds **65** and **66**, respectively) were synthesized. Both compounds showed increased binding affinities to rat brain PKC isoenzymes compared to **64** (IC<sub>50</sub> values of 0.8, 1.5 and 3.5  $\mu$ M, respectively), however, higher values than for the natural calphostin C (**24**, IC<sub>50</sub> = 0.05  $\mu$ M). Among the natural calphostins, higher binding affinities can be obtained with more hydrophobic groups at C7 and C7'.<sup>143</sup> Substitution of the 2-hydroxypropyl groups at C7 and C7' (R<sub>2</sub> in **64**) with *n*-propyl groups resulted in better binding.<sup>228</sup> The obtained IC<sub>50</sub> value of derivative **67** was 0.4  $\mu$ M. Furthermore, 16- to 28-fold higher binding affinities could be obtained with the *M*-atropisomers compared to the *P*-atropisomers.

No binding interaction data can be found in the literature. On the other hand, one could assume that the calphostins bind to the C1 domain in a similar way as the structurally related anthracyclines (*vide supra*).



R<sub>1</sub> = Me, R<sub>2</sub> = (2*R*-OH)propyl (*ent*-Pleichrome, **64**)  
 R<sub>1</sub> = isopropyl, R<sub>2</sub> = (2*R*-OH)propyl (**65**)  
 R<sub>1</sub> = *n*-propyl, R<sub>2</sub> = (2*R*-OH)propyl (**66**)  
 R<sub>1</sub> = Me, R<sub>2</sub> = *n*-propyl (**67**)

### DAG-lactones

The Blumberg and Marquez groups used endogenous DAG (**4**) as a starting point in the design of DAG-lactones (e.g. **68-71**).<sup>60, 229</sup> Their plan was to design conformationally constrained  $\gamma$ -

lactones to overcome the entropic penalty caused by the flexible structure of DAG (**4**) upon binding to the C1 domain.<sup>60, 229</sup> To improve the interactions with the conserved hydrophobic amino acids in the space between the two  $\beta$ -sheets of the C1 domain (Figure 8), the acyl and alkylidene groups were substituted with various lipophilic side chains (Figure 25).<sup>230</sup> Subsequently, the potency of the DAG-lactones was increased to  $K_i$  values as low as 1.45 nM (enantiomer (2*R*)-**68**, PKC $\alpha$ ).<sup>231</sup> Synthesis of the optically pure (2*R*)-DAG-lactones (the active enantiomers)<sup>229, 231</sup> requires 11 linear steps, significantly fewer than the number of synthesis steps required for many of the natural compounds (see Chapter 2.2.3.).<sup>231</sup>

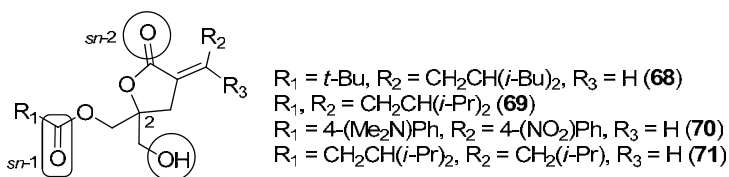


**Figure 25** Structures of synthetic DAG-lactones (**68-71**). Functional groups that are thought to interact with the C1 domain are highlighted.

Molecular modeling studies performed on the DAG-lactones reveal two competing binding modes to the C1 domain (Figure 26).<sup>89, 230</sup> In the “*sn-1*” mode, the acyl group carbonyl of lactone **69** is hydrogen-bonded to Gly253 of the C1 domain, and the alkylidene group is pointing towards the lipid membranes (residue numbers correspond to that of the C1b domain of PKC $\delta$ , see Figure 26). The hydroxy group is hydrogen-bonded, as the C20 hydroxy group of phorbol esters (**5**), to Thr242 and Leu251. In the “*sn-2*” mode, the lactone carbonyl is hydrogen-bonded to Gly253 and the alkyl chain of the acyl group is pointing towards the lipid membranes. Again, the hydroxy group is hydrogen-bonded to Thr242 and Leu251.

Several DAG-lactones show some PKC isoenzyme selective binding;<sup>232, 233</sup> however, differences in binding do not necessarily translate into differences in the potency to induce biological effects.<sup>59</sup> Nevertheless, a striking binding selectivity of compound **70** between the individual C1 domains of the PKC isoforms was observed: the  $K_i$  values of the isolated C1a and C1b domains of PKC $\delta$  were 2780 and 1.78 nM, respectively, and the  $K_i$  values of the C1a and C1b domains of PKC $\alpha$  were 610 and > 10000 nM, respectively.<sup>233</sup> On the other hand, DAG-lactone **70** showed only modest selectivity between the whole isoforms. For SAR studies of DAG-lactones, please see ref. 100 and 229.

Several DAG-lactones have shown antiproliferative and proapoptotic activity, e.g. **68**<sup>234</sup> and (2*R*)-**68**<sup>235</sup> exhibited proapoptotic activities in lymph node carcinoma of the prostate (LNCaP) cells. The DAG-lactones **68** and **71** have also shown to be active in HIV-1 eradication in *ex vivo* culture experiments.<sup>236</sup>

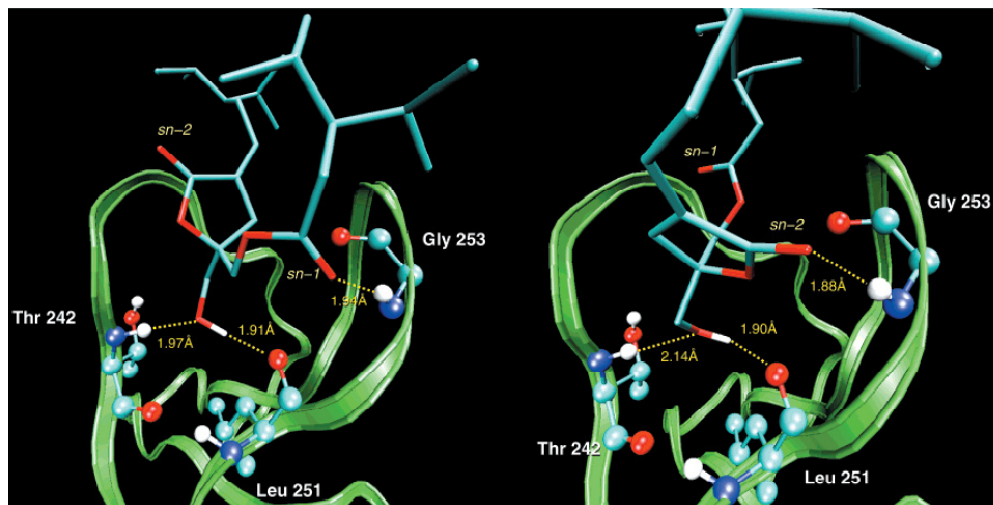


**Figure 26** The binding modes of DAG-lactone **69** to the C1b domain of PKC $\delta$ : “sn-1” (left) and “sn-2” (right).<sup>230</sup> Residue numbering corresponds to that of the crystal structure of the C1b domain of PKC $\delta$ ,<sup>81</sup> the corresponding PKC $\beta$ II residue numbers are (in parenthesis): Gly253 (Gly124), Leu251 (Leu121) and Thr242 (Thr113). DAG-lactone **69** is presented in stick representation, the residues in ball and stick representation, and are colored by atom type. Hydrogen bonds are shown with yellow dotted lines and the respective distances showed in ångströms (Å). Reprinted with permission from ref. 230. Copyright 2011 American Chemical Society.

### Summary of the synthetic compounds targeting the C1 domain

The complex chemical structures and the lack of availability of compounds targeting the C1 domain of PKC from sensitive ecosystems such as oceans and seas have been driving forces in the development of structurally simplified analogs of the natural compounds. Indeed, a recently published five-step synthesis of prostratin (**13**) and its analogs opens a new opportunity in the development of improved prostratin analogs with reduced toxic properties.<sup>102, 188</sup>

Extensive research has also been performed in simplifying the chemical structure of the natural bryostatins.<sup>100</sup> By using the pharmacophores of phorbol esters, newly designed compounds showed increased binding affinities while the required reaction steps of the synthesis route were significantly reduced.<sup>202, 203</sup> Indeed, synthetic analogs of bryostatin may provide the answer to overcome the inefficacy issues faced in clinical trials of bryostatin 1 (**17**).<sup>184, 185</sup> The aplysiatoxin analogs are other macrocyclic lactones that are products from structure simplification of the natural counterparts and show indications of non-tumor-promoting modulators.<sup>56, 127</sup>

The indo- and benzolactams have also provided evidence to be potential future drug candidates against cancer and AD.<sup>133, 207, 211, 215, 216</sup> However, more in vivo studies are needed to validate these compounds.

Another class of interesting C1 domain-targeted compounds is the DAG-lactones. Research into these structurally constrained DAG analogs has not only provided high binding compounds<sup>231</sup> but also important information of the correlation between ligand structure and the biological response of PKC.<sup>59</sup> On the other hand, more in vivo tests of these DAG-lactones are needed to validate them as potent drug candidates.

## 2.3 Anaplastic lymphoma kinase

ALK is a RTK, which is comprised of an extracellular ligand-binding domain, a putative transmembrane domain and a cytoplasmic tyrosine kinase domain (Figure 27).<sup>31</sup> Among the RTKs, the extracellular domain of ALK is most similar to that of leukocyte tyrosine kinase (LTK),<sup>28</sup> which is a member of the superfamily of insulin receptors (IRs).

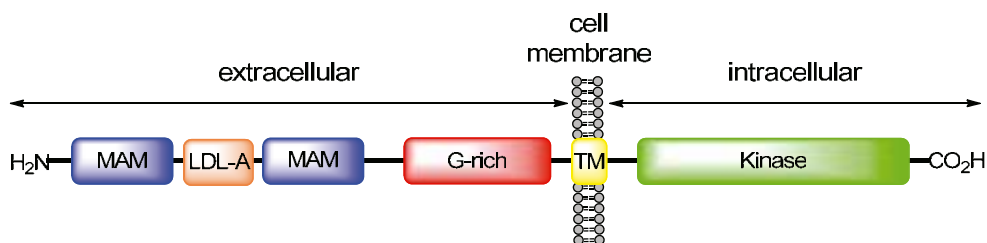


**Figure 27** The structure of anaplastic lymphoma kinase. MAM (meprin-A5 protein-receptor protein tyrosine phosphatase  $\mu$ ), LDL-A (low-density lipoprotein class A), G-rich (glycine-rich) and TM (transmembrane domain).

The natural ligand of ALK is still to be found, hence, ALK is an orphan receptor. The growth factors pleiotrophin (PTN)<sup>237</sup> and midkine (MK)<sup>238</sup> have been suggested as natural ALK ligands, however, there is a high level of debate about this.<sup>31, 239, 240</sup> ALK is also a dependence receptor,<sup>241</sup> that is, ALK can exert opposite cellular effects depending on the absence or presence of a ligand.<sup>239, 242</sup> In the absence of a ligand, the kinase is inactive and ALK is enhancing apoptosis. However, in the presence of a ligand the kinase is active and apoptosis is decreased; this is also true in the constitutively activated fusion products of ALK (*vide infra*). When ALK is unligated, the cleavage of ALK by caspases exposes an intracellular and proapoptotic juxta-membrane domain of ALK, which facilitates apoptosis.<sup>243</sup> Ligands used to demonstrate these phenomena were agonist anti-ALK antibodies.<sup>244</sup>

Although the function of the full-length ALK receptor is still poorly known, it has been shown that ALK plays an important role in the development of the central and peripheral nervous system.<sup>30</sup> ALK expression is restricted to rare scattered neural cells<sup>245</sup> and recent data suggest that ALK is involved in neuronal cell differentiation and regeneration, synapse formation and muscle cell migration.<sup>31</sup> Despite ALK having a role in development and expression patterns,



ALK-deficient mice appear normal and display no visible tissue abnormalities.<sup>246</sup> However, ALK can be aberrantly activated as a result of a (2;5)(p23;q35) chromosomal translocation in ALCLs.<sup>247, 248</sup> In most cases, the translocation causes the fusion of the intracellular catalytic domain of ALK to the oligomerization domain (OD) of nucleophosmin (NPM, *vide infra*). The resulting NPM-ALK fusion product has constitutive kinase activity and is highly oncogenic.<sup>32</sup> Several additional fusion partners that have dimerization domains have also been described.<sup>31, 249</sup> Oncogenic mutants or fusion variants of ALK have also been identified in neuroblastomas, inflammatory myofibroblastic tumors and diffuse large B-cell lymphoma.<sup>31</sup> Furthermore, the echinoderm microtubule-associated protein-like 4 (EML4)-ALK fusion gene was recently discovered to be expressed in a subset of non-small cell lung cancers (NSCLCs), breast and colorectal cancers.<sup>250, 251</sup>

Sixty to eighty percent of ALCLs are ALK-positive; and seventy to eighty percent of ALK-positive ALCLs express the NPM-ALK fusion protein.<sup>252</sup> Children and young adults are more likely to be affected by these tumors and with a slight male predominance, accounting for approximately 20-40% of non-Hodgkin lymphomas (NHL) in children and < 5% of all cases.<sup>253, 254</sup>

### 2.3.1 Structure, activation and regulation

#### *Structure – the wild type enzyme*

The domain organization of ALK is conserved throughout evolution, with the kinase domains showing the highest similarities between species.<sup>240</sup> Mouse (m) and human (h) ALK show 87% overall homology at the protein level, and within the kinase domain these differ at only four amino acids. Compared to mALK, hALK contains one extra tyrosine residue, Tyr1604, which has been implicated in tumor progression.<sup>243</sup>

Among RTKs, ligand-binding to the extracellular domain induces activation of the kinase on the cytoplasmic side, which initiates the intracellular signaling.<sup>255</sup> Also the hALK consists of an extracellular ligand-binding domain, a putative transmembrane (TM) domain and a cytoplasmic kinase domain (Figure 27).<sup>30, 31</sup> In the extracellular domain there is an N-terminal signal peptide, two meprin-A5 protein-receptor protein tyrosine phosphatase  $\mu$  (MAM) domains, one low-density lipoprotein class A (LDL-A) domain and a glycine-rich (G-rich) region.<sup>240</sup> Within ALK, the LDL-A domain has an unknown function. However, in the low-density lipoprotein (LDL) receptor, this domain is involved in binding to LDL,<sup>256, 257</sup> suggesting a potential role in ligand-binding for this domain of ALK. The importance of the MAM domains for ALK function is also unclear. Interestingly, ALK is the only RTK known to date that have MAM domains.<sup>258</sup> MAM domains comprise about 160 amino acids that are present in transmembrane proteins such as the meprins and receptor protein-tyrosine phosphatases, where they are thought to function in cell-cell interactions.<sup>259, 260</sup> The importance of the MAM domain in *Drosophila* ALK (dALK) was showed by a point mutation of a highly conserved aspartic residue; an arginine residue at that

position gave an inactive dALK.<sup>261</sup> The third extracellular domain, the G-rich region, also seems to have a functional significance in ALK.<sup>261</sup> Again, point mutations that convert a single glycine residue within the G-rich region into an acidic amino acid showed inactive dALK mutants.

The TM domain connects the extracellular domain with the kinase intracellular domain (Figure 27).<sup>30, 262</sup> This putative TM domain consists generally of 28 hydrophobic amino acids, consistent with a membrane-spanning segment. In addition, the TM domain is flanked on its cytoplasmic side by basic amino acid residues typical of the junction between transmembrane and cytoplasmic domains.

The intracellular region contains the kinase domain. The kinase domain will be discussed in more detail in Chapter 2.3.2. At the C-terminus of ALK, the phosphotyrosine-dependent binding site for the substrate protein Scr (sarcoma) homology 2 domain-containing (SHC) can be found.<sup>263, 264</sup> In addition, an interaction site for the phosphotyrosine-dependent binding of PLC- $\gamma$  can also be found in the intracellular region of ALK.<sup>243, 264</sup> PLC- $\gamma$  is involved in the generation of DAG and IP<sub>3</sub>, which are involved in the activation of PKC (see Chapter 2.2.1).

### Structure – the fusion proteins

As a result of the (2;5)(p23;q35) chromosomal translocation, ALK can be unexpectedly activated.<sup>247, 248</sup> In most cases, the translocation causes the fusion of the intracellular catalytic domain of ALK to the OD of NPM (Figure 28), but several additional fusion partners that have dimerization domains have also been described.<sup>31, 249</sup> For example, the EML4-ALK fusion gene was recently discovered.<sup>250, 251</sup>

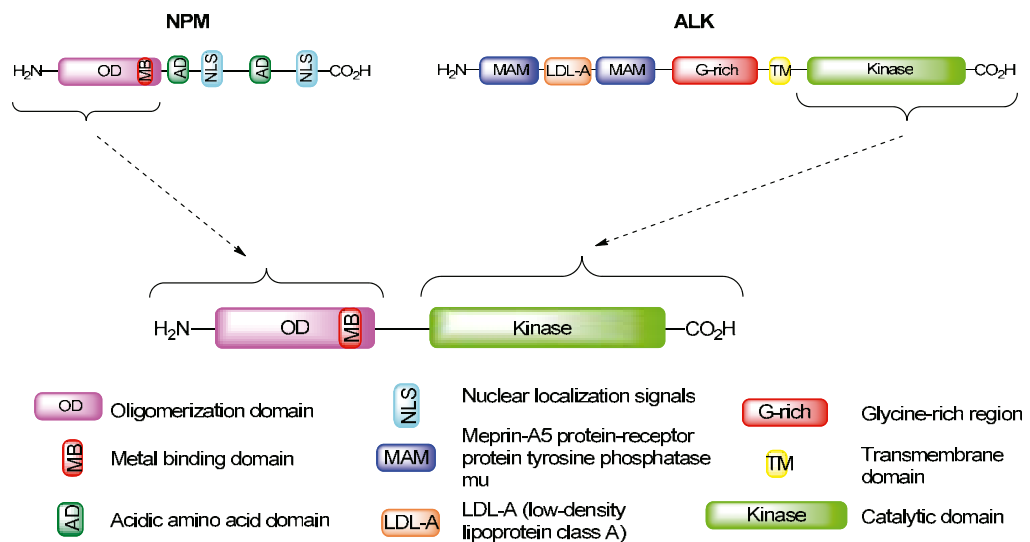


**Figure 28** Structures of nucleophosmin (NPM), anaplastic lymphoma kinase (ALK) and the NPM-ALK fusion product.

The NPM-ALK fusion product does not have the TM domain and the extracellular domains of ALK (Figure 28), and the fusion product of NPM-ALK is cytosolic or nuclear.<sup>265, 266</sup> However, it is the fusion partner and not the kinase part of ALK in the homo- or heterodimers of the fusion products which determines the distribution of the fusion products (Figure 29). For example, in the case of the heterodimer of the NPM-ALK fusion product, NPM contains the nuclear localization signals but these cannot be found in the homodimer of the fusion product. Hence, the heterodimer is distributed in the nucleus and the homodimer is distributed in the cytosol. In contrast, both the hetero- and homodimers of the fusion products of tropomyosin  $\alpha$ -3 (TPM3) and ALK are distributed in the cytosol since TPM3 does not contain a nuclear localization signal.

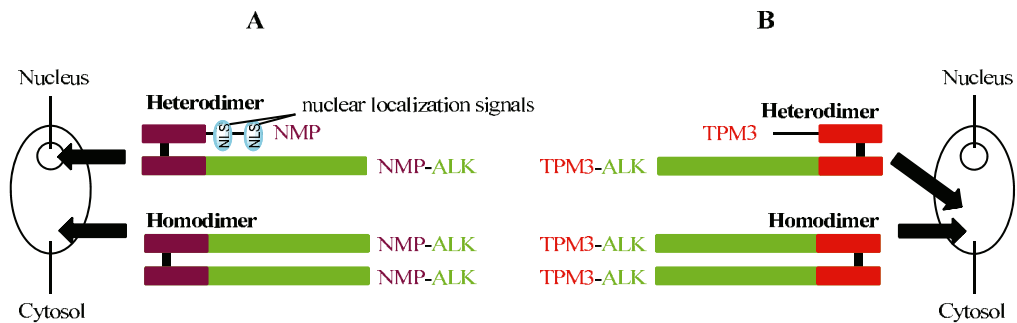


**Figure 29** Distribution of hetero- and homodimers of fusion products of ALK in the cells. **A)** NPM-ALK and **B)** TPM3-ALK. ALK (anaplastic lymphoma kinase); NLS (nuclear localization signals); NPM (nucleophosmin); TPM3 (tropomyosin  $\alpha$ -3).

### Activation

The full length WT ALK expression decreases rapidly after birth and is maintained at low levels in adults.<sup>240</sup> However, dimerization of the NPM-ALK fusion product stimulates the autophosphorylation of the ALK catalytic domain<sup>267, 268</sup> and, subsequently, phosphorylation of other tyrosine residues in NPM-ALK resulting in activation.<sup>269</sup> Alternatively, it has been suggested that autophosphorylation of ALK can occur when the receptor protein tyrosine phosphatase Z1 (PTPRZ1) is inactivated.<sup>270</sup>

Within the activation loop (A-loop) of the kinase domain (see Chapter 2.3.2.), ALK contains a triple tyrosine ( $\underline{Y}^{1278}\text{xxx}\underline{Y}^{1283}$ ; Y = tyrosine; x = variable amino acid) motif like the insulin receptor kinase (IRK) subfamily.<sup>271</sup> Phosphorylation of the first tyrosine residue (Tyr1278) of this YxxxYY motif is predominant in the autoactivation of the ALK kinase domain. The amino acid triplet xxx, which follows immediately Tyr1278, is “RAS” in ALK ( $\underline{Y}^{1278}\underline{\text{RAS}}\underline{\text{Y}}^{1283}$ ) and appears to determine in part the phosphorylation of Tyr1278 in the A-loop. This respectively amino acid triplet of IRK is “RTK”.<sup>269, 271</sup>

Binding of a ligand to the extracellular domain of RTKs induces activation of the kinase on the cytoplasmic side leading to intracellular signaling and, subsequently, the activated RTKs phosphorylate themselves and cytoplasmic substrates.<sup>255</sup> The endogenous ligand(s) for hALK is

a subject of debate.<sup>31, 240</sup> The mammalian ALK is not able to respond to the dALK ligand Jelly belly (the JEB ligand),<sup>272</sup> however, PTN<sup>237</sup> and MK<sup>238</sup> are suggested to be possible binders of hALK. Recently, ALK was reported to be activated by endogenous zinc.<sup>273</sup>

### *Regulation*

As earlier mentioned, ALK expression is normally restricted to only specific regions in the body and is normally down-regulated in the adult, resulting in very low levels of expression.<sup>30, 245, 262</sup> hALK exists as a full length 220 kDa protein and a shorter 140 kDa protein, which is only found in the brain and in some transfected cells.<sup>30</sup> The shorter protein is thought to result from a cleavage of the extracellular domain of hALK.<sup>239</sup> No function of this shorter protein has been reported and therefore, it may be generated as part of down-regulation or degradation processes within the cell.<sup>240</sup> The cleavage of the full length protein was recently reported to be prevented by an as yet unidentified factor secreted by Schwann cells.<sup>274</sup>

The Hsp chaperones are proteins that have a critical role in the folding and maturation of several PKs and interact with the kinase domain region of tyrosine kinases to stabilize these proteins.<sup>275-277</sup> Among Hsps, the Hsp90 chaperone was shown to interact with NPM-ALK and destabilization of this Hsp90/NPM-ALK complex induced Hsp70/NPM-ALK complex formation.<sup>278</sup> Since the Hsp70 is known to be involved in protein degradation,<sup>279</sup> the Hsps show an important role in regulating NPM-ALK stability and function.

### **2.3.2 The kinase domain of anaplastic lymphoma kinase**

The key function of the kinase domain of PKs is to catalyze the reaction between ATP and generally a hydroxy group of a serine, threonine or tyrosine (see Chapter 2.1; Figure 1). Until recently, only a homology model of the kinase domain of ALK could be found in literature.<sup>280</sup> However, crystal structures of the kinase domain of ALK complexed with various inhibitors (e.g. PHA-E429 (**72**), NVP-TAE684 (**73**), and staurosporine (**74**)) were recently published (see Figure 30 for the crystal structure of NVP-TAE684 (**73**) complexed with ALK).<sup>281, 282</sup> The ALK structures reported there displayed features that are characteristic of both an inactive and active PK (*vide infra*). It is generally accepted that a high level of similarity exists for the active PK structures, while there are significant differences for the inactive structures.<sup>283, 284</sup>

The intracellular catalytic domain consists of an N- and C-terminal lobe with an ATP-binding site situated in a deep cleft between the domains, which is highly conserved among the PKs (Figure 30A and B).<sup>285</sup> Also the 254-amino acid catalytic domain of ALK contains the conserved motifs found in PKs and possesses paired tyrosine residues (ALK amino acids 1282 and 1283) characteristic of the major autophosphorylation site of the IR subfamily.<sup>262</sup> The key regions of the ATP-binding site include the hydrophobic purine-binding cavity, the hinge

segment, the gatekeeper residue, the VAIK-motif, the phosphate binding (P)-loop, the activating (A)-loop, the catalytic loop and the regulatory  $\alpha$ -helix (Figure 30C).

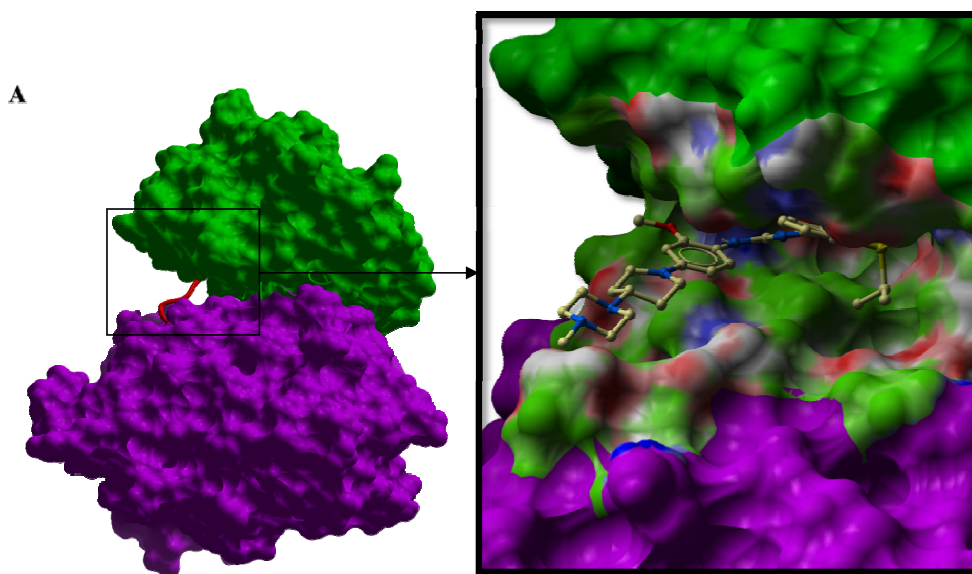
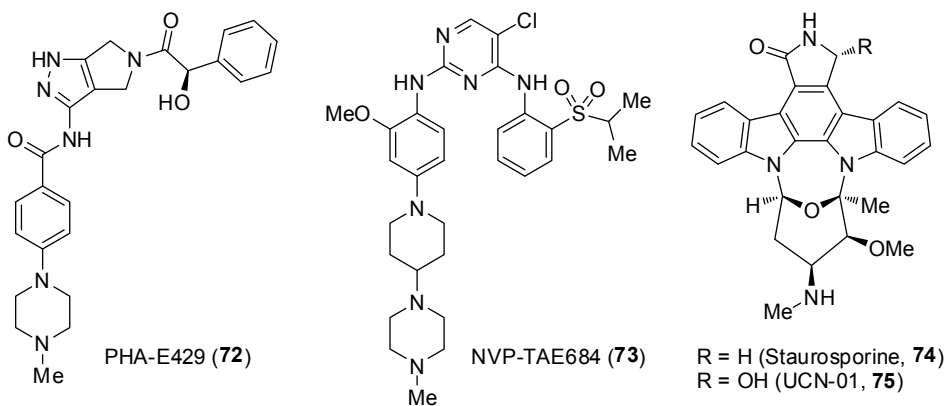


**Figure 30** The crystal structure of ALK complexed with NVP-TAE684 (73) (2.5 Å resolution, PDB-code: 2XB7).<sup>281</sup> **A**) The N-terminal lobe is colored **green**, the C-terminal lobe is **violet** and the hinge segment is **red**. NVP-TAE684 (73) is removed. **B**) NVP-TAE684 (73, ball and sticks, colored by atom type) bound to the active site of the kinase domain. The hinge segment was deleted for the sake of clarity. The binding pocket is colored as follows: oxygen atoms (**red**), nitrogen atoms (**blue**), carbon atoms (**green**), hydrophobic groups (**grey**) and rest of the protein as in A).

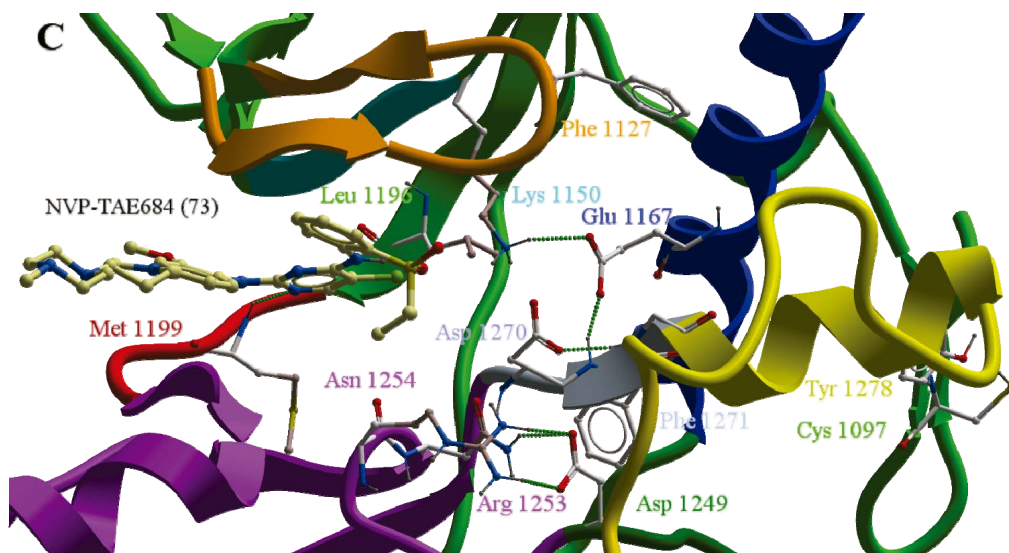


**Figure 30** C) The crystal structure of ALK complexed with NVP-TAE684 (73) (2.5 Å resolution, PDB-code: 2XB7).<sup>281</sup> Interactions between some of the pivotal amino acids and NVP-TAE684 (73) in the ATP-binding site. The residues and NVP-TAE684 (73) are presented in ball and stick representations and colored by atom type. The hydrogen bonds are represented as **green** spheres. The N-terminal lobe is colored **green**; the C-terminal lobe **violet**; the hinge segment **red**; the P-loop **orange**; the VAIK-motif **light blue**; the  $\alpha$ C-helix **blue**; the DFG-motif **grey**; the A-loop **yellow** and the HRD-motif **dark green**. A part of the A-loop (residues 1275-1288) of the ALK crystal structure 3LCT<sup>282</sup> has been added to 2XB7. The figures were created using ICM-Browser (version 3.7-2a, MolSoft L.L.C.).

### The hinge segment

As for other PKs, the hinge segment of the kinase domain of ALK connects the N- and C-terminal kinase domains (shown as red in Figure 30A and C). The main function of the hinge segment is to orientate the adenine group of ATP in the active site and that is why the segment is highly conserved among PKs. Furthermore, the acidic hinge residue found in the kinase domain of ALK, which usually interacts with the ribose group of ATP, is aspartate (Asp1203).<sup>281</sup>

### The gatekeeper

Immediately N-terminal to the hinge segment is the gatekeeper residue (Figure 30C). This residue controls the size of the ATP-binding site and is usually a bulky amino acid, thus never a glycine or an alanine.<sup>286</sup> The gatekeeper residue is an important factor in designing kinase inhibitors targeting the active site, since it determines, partly at least, the binding and specificity of the inhibitor.<sup>280</sup> In ALK, the gatekeeper residue is a leucine (Leu1196).<sup>281</sup> In many cases, drug resistant tumors are due to a mutation of the gatekeeper residue.<sup>35, 280, 287</sup>

### *The VAIK-motif*

The VAIK-motif contains a highly conserved lysine (Lys1150) which interacts with the  $\alpha$ - and  $\beta$ -phosphates of ATP thus anchoring and orientating it (shown as light blue in Figure 30C, see also Figure 4 in Chapter 2.1; Lys72 of PKA corresponds to Lys1150 of ALK).<sup>45</sup> In ALK, the VAIK-motif has a second Val residue (Val1149; Val<sup>1147</sup>-Ala<sup>1148</sup>-Val<sup>1149</sup>-Lys<sup>1150</sup>; “VAVK” in ALK) instead of the Ile residue usually found in PKs.<sup>281</sup>

### *The P-loop*

The P-loop is a glycine-rich loop and forms the ‘ceiling’ of the active site (shown as orange in Figure 30C). The glycine residues allow the loop to be highly flexible in the absence of ATP and for that reason, they also help small inhibitors to enter the active site.<sup>284</sup> When ATP is present, the P-loop forms very close interactions with the phosphates of ATP, thus coordinating the phosphates in the active site. In addition, at the tip of the P-loop, the conserved phenylalanine (Phe1127 in ALK) functions as a hydrophobic cap of the active site.

### *The A-loop*

Another loop found in PKs is the A-loop, where the Y<sup>1278</sup>xxxYY<sup>1283</sup> motif can be found. The A-loop translocates as a function of kinase phosphorylation (shown as yellow in Figure 30C). A large number of kinases are activated by phosphorylation of the A-loop which is typically disordered in its inactive state and assumes a stable structure suitable for substrate binding in its phosphorylated active state.<sup>285, 288</sup> Hence, in the inactive, unphosphorylated state of the kinase, the A-loop is situated in front of the ATP-binding pocket and blocks the entry of ATP. However, when the three tyrosines (Tyr1278, Tyr1282 and Tyr1283) are phosphorylated, a conformational change moves the A-loop away from the active site and allows ATP to move freely into the binding pocket. Subsequently, the highly conserved Asp<sup>1270</sup>-Phe<sup>1271</sup>-Gly<sup>1272</sup> (DFG)-motif (shown as grey in Figure 30C), situated at the N-terminal side of the A-loop, also undergoes a rearrangement and the Asp1270 residue will point towards the catalytic site. This conformation is also called the active DFG-Asp-in conformation, whereas the inactive conformation has the Asp1270 pointing out from the catalytic site and is called the inactive DFG-Asp-out conformation. In the active DFG-Asp-in conformation, the Asp1270 forms polar interactions with the three phosphate groups of ATP, directly or via Mg<sup>2+</sup> ions (see Figure 4 in Chapter 2.1; Asp184 of PKA corresponds to Asp1270 of ALK).<sup>289</sup> In addition, the Phe1271 forms hydrophobic interactions with the  $\alpha$ C helix (shown as blue in Figure 30C, *vide infra*) and the His<sup>1247</sup>-Arg<sup>1248</sup>-Asp<sup>1249</sup> (HRD)-motif (shown as dark green in Figure 30C, *vide infra*). In contrast, the Gly1272 of the DFG-motif has an unknown function. The overall conformational change from DFG-Asp-out to DFG-Asp-in exposes a large additional cavity adjacent to the ATP-binding site, which has been exploited by suitably designed inhibitors.<sup>290</sup>

### *The HRD-motif of the catalytic loop*

The function of the highly conserved catalytic HRD-motif (shown as dark green in Figure 30C) is to orientate the phosphate acceptor hydroxy group of the peptide substrate and to support the conformation of the A-loop/DFG-motif.<sup>289</sup> More specific, the His1247 binds to the Asp1270 and Phe1271 of the DFG-motif, the Arg1248 functions as a link between the catalytic HRD-motif, the phosphorylation site and the magnesium-binding-loop (consisting of the DFG-motif, Met1273, and Ala1274), and the Asp1249 functions as the orientating residue for the hydroxy group of the substrate peptide. In addition, Asp1249 has been suggested to act as a base in the catalytic event.<sup>43</sup>

### *The regulatory $\alpha$ C-helix*

The  $\alpha$ C-helix (shown as blue in Figure 30C) can be found in the N-terminal lobe of the kinase domain. The main function of the  $\alpha$ C-helix is to stabilize the inactive and active conformations of the kinase domain by forming interactions with the VAIK- (VAVK in ALK) and DFG-motifs.<sup>284</sup> In the crystal structure of ALK complexed with NVP-TAE684 (**73**),<sup>285</sup> Glu1167 of the  $\alpha$ C-helix forms a conserved hydrogen bond with the conserved Lys1150 found in the VAIK-motif, a feature that is generally representative of an active kinase.<sup>281</sup> However, the kinase is inactive on the basis of its degree of lobe closure and the incorrect positioning of the  $\alpha$ C-helix. Thus, the authors suggested a drastically different autoinhibition mechanism of ALK that uses intramolecular interactions between the N-terminal  $\beta$ -sheet and the DFG-helix to lock the structure in an inactive conformation (Figure 30C).<sup>281</sup>

## **2.3.3 Synthetic compounds as anaplastic lymphoma kinase inhibitors**

In general, ATP-competitive kinase inhibitors can be divided into two types, depending on whether they take advantage of the hydrophobic pocket that results from the conformational change of the DFG-motif in kinase activation.<sup>281,291</sup> Type I inhibitors are the more common and recognize the active DFG-in conformation but achieve specificity only by utilizing structural divergence in the highly conserved ATP-binding pocket.<sup>290</sup> An example of a type I inhibitor is the ATP-competitive inhibitor crizotinib (PF-02341066, **76**, Figure 31).<sup>292</sup> In contrast, type II inhibitors (e.g. imatinib (Gleevec, **77**),<sup>293</sup> doramapimod (BIRB-796, **78**),<sup>294</sup> and sorafenib (Nexavar, **79**)<sup>295</sup>), recognize the inactive DFG-out conformation<sup>36, 37</sup> resulting from the reorganization of the N-terminal portion of the A-loop that exposes a large additional hydrophobic cavity.<sup>281,290,296</sup> This cavity is located outside the ATP-binding pocket where less conserved PK residues can be found. Therefore, because the type II inhibitors do not only target the ATP-binding site, they are thought to show increased specificity.<sup>293,297</sup> In addition, because the DFG-out conformation of PKs is generally less conserved than the DFG-in conformation,<sup>298</sup> binding to the inactive DFG-out conformation would further increase specificity among



kinases.<sup>35, 299</sup> Type II inhibitors have also been shown to be superior in drug resistant mutants of PKs where even second generation kinase inhibitors have failed to show activity.<sup>300</sup> It is worth mentioning the irreversible type II inhibitors, a subtype of type II inhibitors.<sup>287</sup> For example, neratinib (HKI-272, **80**) inhibits the kinase by forming a covalent bond with the kinase at the catalytic site, preventing ATP to bind.<sup>301</sup>

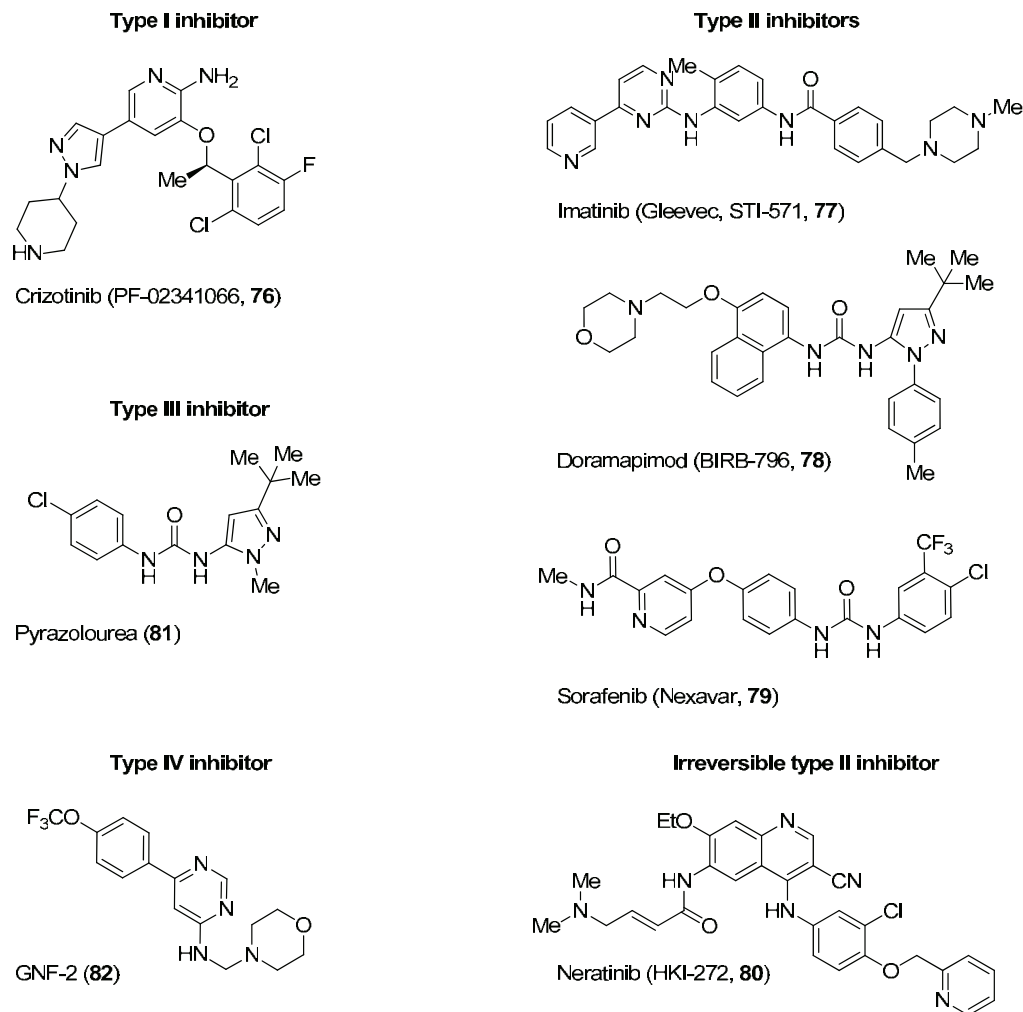


**Figure 31** Type I (**76**), II (**77-79**), III (**81**) and IV (**82**) kinase inhibitors as well as an irreversible type II kinase inhibitor (**80**).

In addition to type I and II inhibitors, type III inhibitors are those, which completely bind outside but adjacent the ATP-binding pocket and therefore show inhibition via a non-ATP competitive mechanism.<sup>36</sup> As an example of a type III inhibitor is the pyrazolourea **81**. Type IV inhibitors are those, which bind the kinase domain but not adjacent the ATP-binding pocket or the hinge region and therefore inhibit via an allosterically non-ATP competitive mechanism.<sup>36, 302</sup> The small molecule GNF-2 (**82**) is an example of a type IV inhibitor.<sup>302</sup>

There is no totally selective inhibitor of ALK available in the clinic at the moment. Recently, however, a growing interest in ALK has led to an increased number of publications of new drug candidates. Some of the most interesting compounds are presented next.

#### *Crizotinib (PF-02341066)*

In a screen of a panel of more than 120 PKs, Pfizer's crizotinib (PF-02341066, **76**) was found to inhibit NPM-ALK-catalyzed phosphorylation in human Karpas 299 ALCL cell line with an IC<sub>50</sub> value of 24 nM<sup>292</sup> and an IC<sub>50</sub> value of 74 nM for BaF3 cell lines expressing the fusion product EML4-ALK.<sup>34</sup> On the other hand, crizotinib (**76**) also inhibited the RTK c-Met in human tumor cell lines with an IC<sub>50</sub> value of 11 nM ( $K_i = 4$  nM) but with the exception of these two kinases, it was found to be selective among the panel of the kinases tested. In a study of the sensitivity of 500 solid tumor-derived human cell lines to 14 selective kinase inhibitors, crizotinib (**76**) was found to be selective for oncogenic ALK and c-Met containing tumors.<sup>303</sup> Crizotinib (**76**) is currently in clinical trials (phase I-III) for the treatment of lung cancer.<sup>33</sup>

#### *2,4-Diaminopyrimidine-based inhibitors*

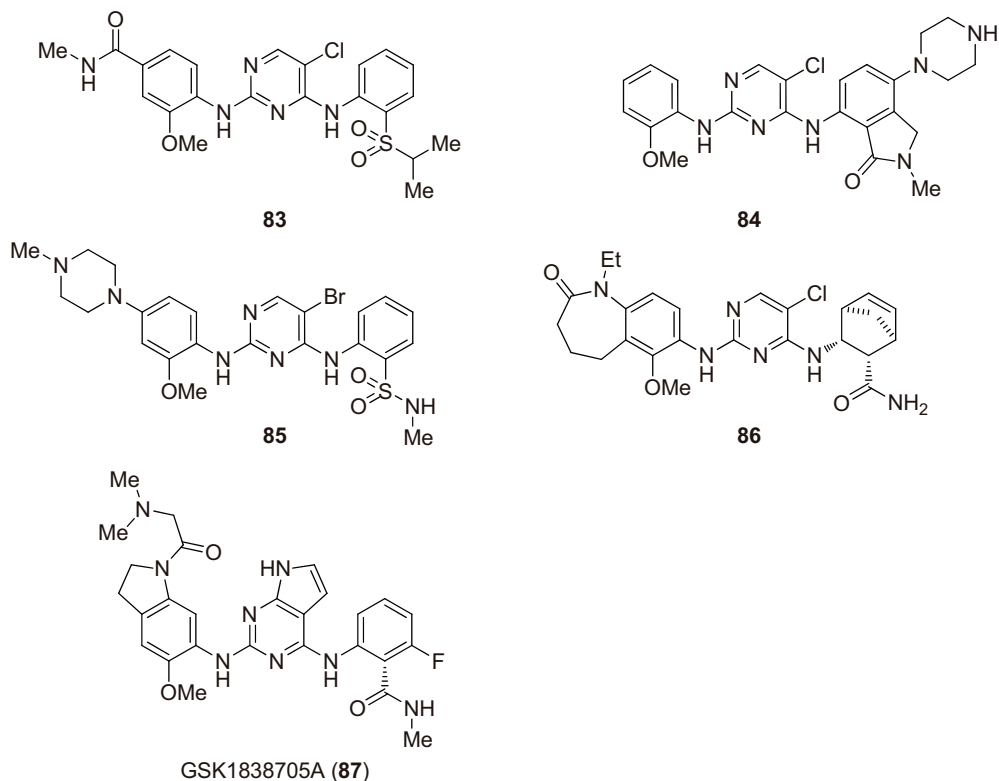
NVP-TAE684 (**73**), an inhibitor from Novartis, was identified in a cellular screen of a kinase-directed small-molecule library to search for compounds that were selectively cytotoxic to BaF3 NPM-ALK, but not to nontransformed parental BaF3 cells.<sup>299</sup> NVP-TAE684 (**73**) inhibited the proliferation of BaF3 NPM-ALK cells with an IC<sub>50</sub> value of 3 nM (IC<sub>50</sub> value of > 1 μM for parental BaF3 cells). NVP-TAE684 (**73**) inhibited the human Karpas 299 ALCL cell line but with an IC<sub>50</sub> value of 3 nM, improved on crizotinib (**76**). Furthermore, among a panel of 35 BaF3 cells transformed with various tyrosine kinases constitutively activated by fusion to the TEL oncogene, NVP-TAE684 (**73**) showed from 100 to 1000 times higher IC<sub>50</sub> values for non-ALK kinases.<sup>299</sup> It was speculated that the specificity was a result of the bulkier hinge region residue at the 1198 position of the non-ALK kinases (e.g. Phe or Tyr compared to Lys found in ALK). In addition, NVP-TAE684 (**73**) was found to be superior over crizotinib (**76**) in the SU-DHL-1 and Karpas 299 lymphoma cell lines in a study where over 600 cancer cell lines were screened for sensitivity to an ALK selective inhibitor.<sup>304</sup> In another study of the sensitivity of 500 solid tumor-derived human cell lines to 14 selective kinase inhibitors, NVP-TAE684 (**73**) was found to be selective for oncogenic ALK containing tumors.<sup>303</sup>

Novartis has also patented other 2,4-diaminopyrimidines with structures similar to NVP-TAE684 (**73**), including compounds **83** and **84**.<sup>305</sup> The IC<sub>50</sub> values of these compounds vary between 0.01 and 1 μM, however, no further preclinical information has been published. Compound **85**,<sup>306</sup> with a bromine instead of a chlorine in the 2,4-diaminopyrimidine ring,

inhibited EML4-ALK with an  $IC_{50}$  of 1 nM<sup>307</sup> and showed impressive results in the EML4-ALK transgenic mouse model.<sup>308</sup> Oral daily doses of 10 mg/kg resulted in tumor disappearance in the treated animals compared to large tumor masses in the lungs of control animals.

Cephalon has also published 2,4-diaminopyrimidines targeted to ALK.<sup>309</sup> Compound **86** is orally bioavailable and completely inhibits NPM-ALK tyrosine phosphorylation in ALCL tumors subcutaneously implanted in severe combined immunodeficiency (SCID) mice at an oral dose of 55 mg/kg. Inhibitor **86** was also effective against EML4-ALK tyrosine phosphorylation and induced cytotoxicity in EML4-ALK-positive NSCLC cell lines as well as in the NB-1 neuroblastoma cell line bearing ALK amplification.<sup>29</sup>

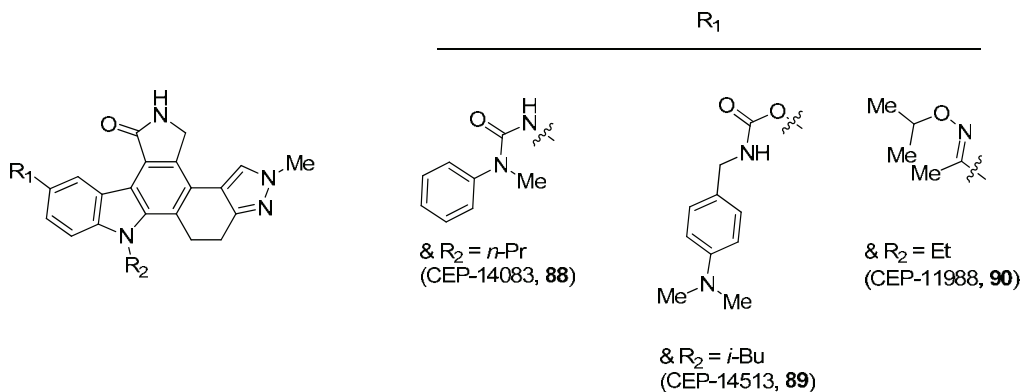
Pfizer's contribution to this class of ALK inhibitors is GSK1838705A (**87**), which has a [2,3-*d*] fused pyrrolyl in the 2,4-diaminopyrimidine core instead of the chlorine or bromine found in compounds **83-86**.<sup>310</sup> GSK1838705A (**87**) shows good pharmacokinetic properties, an excellent oral bioavailability (98%),<sup>311</sup> and an excellent  $IC_{50}$  value of ALK (0.5 nM).<sup>310</sup> However, it also inhibits the insulin-like growth factor-1 receptor (IGF-1R) and IRK with low nanomolar activity ( $IC_{50}$  values of 1.6 and 2 nM, respectively). GSK1838705A (**87**) showed weak or no inhibition in a panel of 43 other serine/threonine and tyrosine kinases ( $IC_{50}$  values of > 1  $\mu$ M). In addition, when GSK1838705A (**87**) was tested at a concentration of 0.3  $\mu$ M in a panel of 224 PKs it



inhibited only seven additional kinases > 50%.<sup>310</sup> GSK1838705A (**87**) was also shown to inhibit the proliferation of different tumor cell lines, such as the ALCL tumors L-82, SU-DHL-1 and Karpas 299 (IC<sub>50</sub> values of 24, 31 and 52 nM, respectively) with a dose-dependent down-modulation of NPM-ALK.<sup>310</sup> Furthermore, GSK1838705A (**87**) inhibited phosphorylation of EML4-ALK in the NSCLC cell line NCI-H2228 with an IC<sub>50</sub> value of 31 nM and the proliferation of these cells (IC<sub>50</sub> value of 191 nM).<sup>310</sup> Treatment of SCID mice bearing Karpas 299 tumors with GSK1838705A (**87**) resulted in complete tumor regression at a well-tolerated dose of 60 mg/kg once daily.<sup>310</sup>

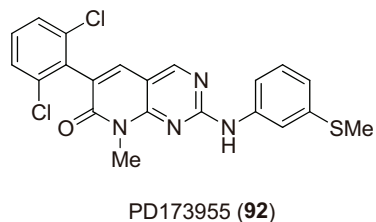
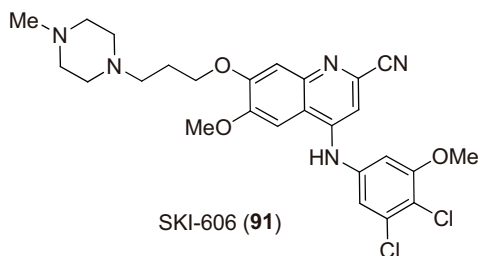
### *Pyrrolocarbazoles*

The staurosporine (**74**) analogs CEP-14083 (**88**)<sup>312</sup> and CEP-14513 (**89**)<sup>312</sup> were found to inhibit ALK with IC<sub>50</sub> values of 2 and 3 nM, respectively.<sup>313</sup> In addition, both CEP-14083 (**88**) and CEP-14513 (**89**) showed cellular IC<sub>50</sub> values of 10-30 nM for NPM-ALK phosphorylation in ALCL cells. Furthermore, CEP-14083 (**88**) was shown to induce growth arrest and cell death in neuroblastoma cells overexpressing WT or mutated ALK when tested at 60 nM, indicating a potential therapeutic strategy for neuroblastoma patients.<sup>314</sup> Interestingly, the pyrrolocarbazole CEP-11988 (**90**) did not show any inhibitory activity (IC<sub>50</sub> value > 20 μM).<sup>312</sup>



### *SKI-606*

Initially designed as a dual kinase inhibitor of the c-Src (sarcoma tyrosine kinase) and c-Abl (Abelson tyrosine kinase) kinases,<sup>315</sup> SKI-606 (**91**) was shown to inhibit the L256T mutant NPM-ALK (numbering of the NPM-ALK fusion gene) with an IC<sub>50</sub> value of 150 nM.<sup>280</sup> However, SKI-606 (**91**) did not inhibit the WT ALK, which was explained by the larger gatekeeper residue (threonine vs. leucine) in the kinase domain of the WT ALK. Docking experiments of SKI-606 (**91**) to homology models of ALK in an intermediate or active conformation of both the mutant and the WT, confirmed the experimental results. In contrast, imatinib (**77**), inhibited neither the L256T mutant nor the WT ALK.

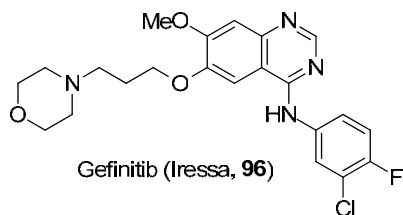
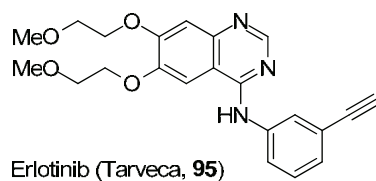
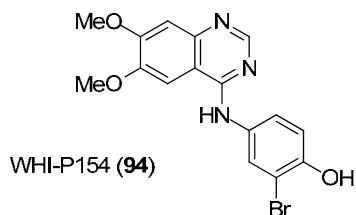
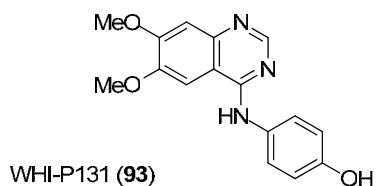


### PD173955

The Src<sup>316</sup> and breakpoint cluster region (Bcr)-Abl<sup>317</sup> kinase inhibitor PD173955 (**92**) has also been shown to inhibit the L256T mutant NPM-ALK but with an IC<sub>50</sub> of only 2.5 μM.<sup>280</sup> As for SKI-606 (**91**), PD173955 (**92**) did not inhibit the WT ALK.

### Quinazoline-based inhibitors

The quinazoline-based inhibitors WHI-P131 (**93**) and WHI-P154 (**94**) inhibit NPM-ALK enzymatic activity with modest IC<sub>50</sub> values in in vitro kinase and cell proliferation assays (10 and 5 μM, respectively).<sup>318</sup> These inhibitors are structurally closely related to the epidermal growth factor receptor (EGFR) tyrosine kinase inhibitors erlotinib (Tarveca, **95**)<sup>319</sup> and gefitinib (Iressa, **96**),<sup>320</sup> which are used as drugs against NSCLC, pancreatic cancer and several other types of cancers. Erlotinib (**95**) has also been studied in a clinical trial (phase II) for patients showing the EML4-ALK translocation.<sup>33</sup> However, EML4-ALK-positive cells have been shown to be resistant to erlotinib (**95**) and gefitinib (**96**).<sup>321</sup>

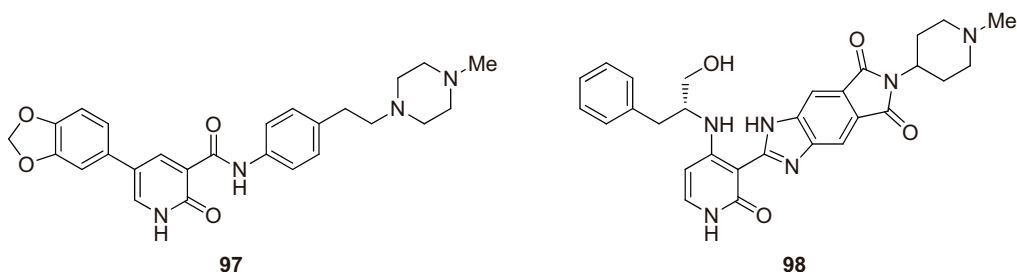


### Pyridone-based compounds

Co-operation between ChemBridge Research Laboratories and St Jude Children's Research Hospital resulted in a discovery of pyridone-based inhibitors of ALK.<sup>322, 323</sup> After lead optimization rounds, the best inhibitor (**97**) showed an IC<sub>50</sub> value of 0.4 μM for ALK. Pyridone **97** showed selective inhibition of ALK compared to the tyrosine kinases IRK, IGF-1R, fms-like tyrosine kinase receptor-3 (Flt3), Src and Abl (10-fold, 18-fold, > 10-fold, > 50-fold and > 50-fold, respectively), however, even though compound **97** showed activity in cell-based antiproliferative assays (NA/BaF3, BaF3, Karpas 299, K562 and Jurkat), it did not show selectivity among them.

Another ChemBridge–St Jude compound that displays ALK-inhibitory activity is the pyridone **98**, showing an IC<sub>50</sub> value of “less” than 0.5 μM.<sup>324</sup> However, pyridone **98** is non-selective among the IR superfamily (e.g. IR and IGF-1R) and also in cell-based antiproliferative assays.<sup>266</sup>

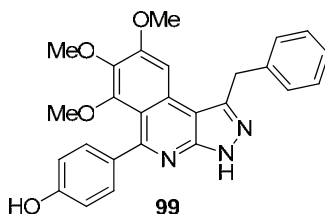
Recently, the same co-operation between ChemBridge–St Jude has yielded a third generation ATP competitive and ALK inhibiting pyridone-based compound (CRL151104A), however, no structural information has been published.<sup>266, 324</sup> CRL151104A shows an ALK IC<sub>50</sub> value of 10 nM when measured at 100 μM ATP and showed little or no inhibition of ten structurally diverse serine/threonine kinases (when tested at a 50 nM concentration). CRL151104A also showed a dose-dependent growth inhibition of the Kelly (F1174L), SH-SY5Y (F1174L) and CHLA-90 (F1245V) neuroblastoma cell lines, with IC<sub>50</sub> values of 610, 500 and 370 nM, respectively. In addition, cellular cytotoxicity assays of NPM–ALK-dependent human ALCL cell lines (Karpas 299, SU-DHL-1, JB6, SUP-M2, UConnL2) demonstrated potent inhibition (IC<sub>50</sub> values < 100 nM); by contrast, the lowest IC<sub>50</sub> value observed for 12 non-ALK-dependent cell lines was approximately 2.5 μM, indicating a minimum 25-fold differential cytotoxicity.<sup>266</sup> Furthermore, neuroblastomas with aberrant forms of ALK harboring activating point mutations, such as R1275Q, are sensitive to this ALK inhibitor, making CRL151104A an interesting future inhibitor.



### Pyrazolo[3,4-c]isoquinoline-based inhibitors

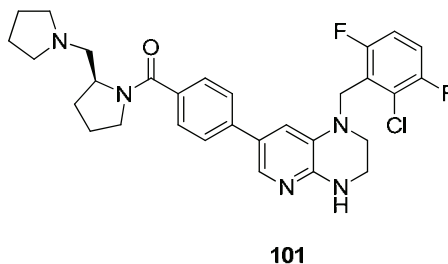
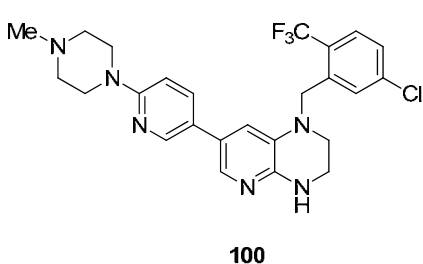
One structurally new class of ALK inhibitors is the pyrazolo[3,4-c]isoquinolines (compound **99** as a representative example).<sup>325</sup> To date, the only available information for this class of ALK

inhibitors can be found in the patent, where the structures for over 240 pyrazolo[3,4-*c*]isoquinolines are presented. The IC<sub>50</sub> values of the compounds are reported to be “less or equal to 99 nM” but also “greater than 2000 nM”.



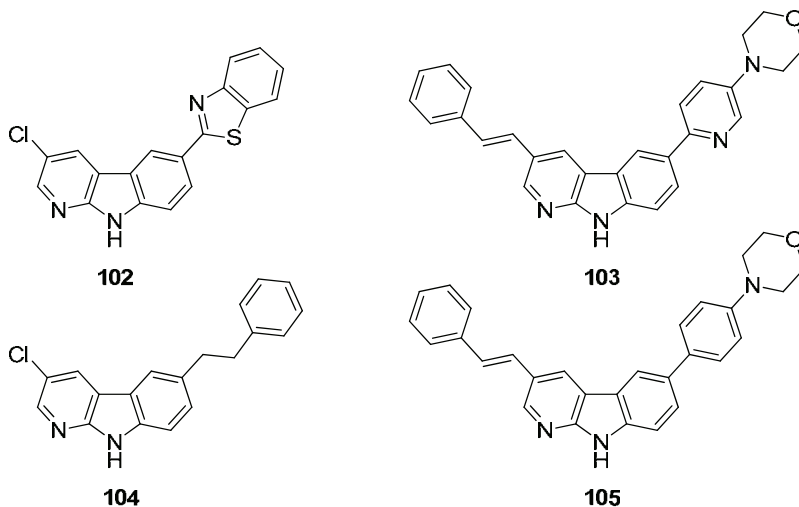
#### *Tetrahydropyrido[2,3-*b*]pyrazines*

Another new class of ALK inhibitors is the tetrahydropyrido[2,3-*b*]pyrazines.<sup>326</sup> Cephalon scientists made a rigid derivative of crizotinib (**76**) by fusing the  $\alpha$ -amino pyridinyl ring found in crizotinib (**76**). Inhibitor **100** showed an IC<sub>50</sub> value of 10 nM for ALK and also inhibited ALK phosphorylation in Karpas 299 cells with an IC<sub>50</sub> value of 200 nM. Importantly, compound **100** showed selectivity over IR in particular (IC<sub>50</sub> value > 3000 nM of IR), and over other kinases in general. Furthermore, when compound **100** was screened at 1  $\mu$ M across a panel of 400 kinases, including representative kinases from all the known kinase families, it inhibited only 2.2% of the kinases by more than 90%. Another tetrahydropyrido[2,3-*b*]pyrazine inhibitor by Cephalon is compound **101**, which displayed an even better IC<sub>50</sub> value for ALK (3 nM).<sup>327</sup>



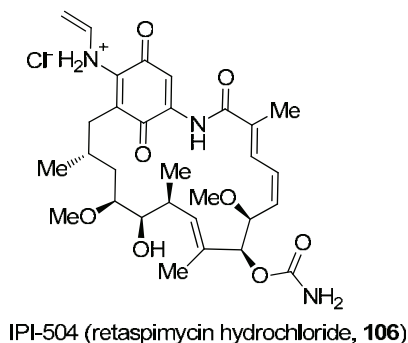
#### *$\alpha$ -Carbolines*

The  $\alpha$ -carbolines (**102-105**) are another new group of ALK inhibitors.<sup>328</sup> The only information available for these compounds is the patent where the compounds are reported as NPM-ALK, RET and Bcr-Abl inhibitors, with the IC<sub>50</sub> values of ALK starting from 0.4  $\mu$ M (compound **102**). The same researchers have also reported the synthesis of these kinds of compounds.<sup>329, 330</sup>



#### IPI-504

IPI-504 (retaspimycin hydrochloride, **106**),<sup>331</sup> a novel intravenous (IV)-administered Hsp90 chaperone inhibitor, was recently shown in a phase II study to demonstrate clinical activity in NSCLC patients, particularly among those with oncogenic ALK gene rearrangements.<sup>332</sup> IPI-504 (**106**) is a semisynthetic inhibitor, prepared in two steps from the antibiotic geldanamycin (**108**, *vide infra*).<sup>331,333</sup> In 2011, IPI-504 (**106**) will be further investigated in a phase II study by Infinity Pharmaceuticals as an inhibitor in NSCLC patients with ALK translocations.<sup>33</sup>



#### AP26113

An ALK inhibitor with no structural information available is AP26113.<sup>34,334,335</sup> Discovered by scientists of Ariad Pharmaceuticals, AP26113 is a very potent ( $IC_{50} = 0.58$  nM), orally available ALK inhibitor with a broad therapeutic index including the potential for once-daily oral dosing.



In addition, AP26113 is claimed to show approximately 100-fold selectivity for ALK-positive cell lines compared to ALK-negative cell lines and maintenance of significant selectivity over the highly similar IGF-1R and IRK (IC<sub>50</sub> of 38 and 262 nM, respectively). Compared to crizotinib (**76**), AP26113 has shown in vitro to have 10-fold greater potency, a 10-fold broader therapeutic index, and an in vivo efficacy equivalent to crizotinib (**76**) at 4- to 10-fold lower levels of exposure. Ariad Pharmaceuticals expects to advance AP26113 into clinical development in 2011.

### *Summary of the synthetic compounds targeting ALK*

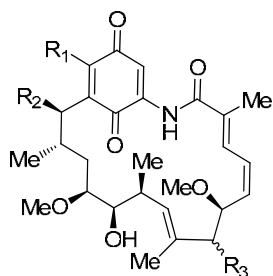
Several rationally designed inhibitors of ALK and its fusion products can be found in the literature. One of the recent drug candidates is crizotinib (**76**),<sup>292</sup> which is in clinical trials for the treatment of lung cancer.<sup>33</sup> Since the catalytic domain is highly conserved among PKs, target specificity of the compounds is required. In particular, selectivity over the IR superfamily is crucial, since dysregulation of normal metabolic pathways should be avoided.

Among the most selective inhibitors targeting ALK or its fusion products are crizotinib (**76**),<sup>33</sup> NVP-TAE684 (**73**),<sup>299</sup> the tetrahydropyrido[2,3-*b*]pyrazines (e.g. **100**)<sup>326</sup> and AP26113, however, with no structural data available.<sup>34, 334, 335</sup> The Leu1198 of ALK, compared to generally bulkier amino acids in other kinases, was suggested to be the structural basis for the selectivity among the 2,4-diaminopyrimidine-based inhibitors having an *ortho* methoxy group attached to the 2-aniline substituent.<sup>299</sup>

## **2.3.4 Natural compounds as anaplastic lymphoma kinase inhibitors**

### *Ansamycins*

To date, only a few inhibitors of ALK activity from natural sources have been reported. The fusion product NPM-ALK shows sensitivity in ALCLs to the antibiotics herbimycin A (**107**),<sup>336</sup> geldanamycin (**108**)<sup>337</sup> and 17-allylamino-17-demethoxygeldanamycin (17-AAG, **109**).<sup>278</sup> These ansamycin antibiotics **107-109** display their activity in the ALCLs via the inhibition of the Hsp90/NPM-ALK complex formation, enhancing the proteasome-enhanced degradation of ALK.<sup>278</sup> Because Hsp90 chaperones have many client proteins, these Hsp90 inhibitors are not specific for ALK inhibition. However, the ansamycin antibiotics **107-109** have been in clinical trials for the treatment of various cancers.<sup>33</sup>



R <sub>1</sub>	R <sub>2</sub>	R <sub>3</sub>	Compound
H	MeO	( <i>R</i> )-O <sub>2</sub> CNH <sub>2</sub>	Herbimycin A ( <b>107</b> )
MeO	H	( <i>S</i> )-O <sub>2</sub> CNH <sub>2</sub>	Geldanamycin ( <b>108</b> )
H <sub>2</sub> C=CHNH	H	( <i>S</i> )-O <sub>2</sub> CNH <sub>2</sub>	17-AAG ( <b>109</b> )

### *Staurosporine and 7-hydroxystaurosporine*

Staurosporine (**74**) is an antibiotic isolated from bacterium *Streptomyces staurosporeus*.<sup>338</sup>

Staurosporine (**74**) is an ATP-competitive inhibitor that unselectively inhibits many kinases.<sup>339</sup>

Not surprisingly, staurosporine (**74**) was shown also to inhibit ALK with an IC<sub>50</sub> value of approximately 130 nM in the presence of 30 μM ATP.<sup>340</sup> The IC<sub>50</sub> value for staurosporine (**74**) increased to approximately 700 nM when the ATP concentration was increased 10-fold, reflecting well an ATP-competitive inhibition.

Anti-tumor activity in a patient with an ALK-positive ALCL was reported in a phase I clinical trial in response to 7-hydroxystaurosporine (UCN-01, **75**).<sup>341</sup> However, 7-hydroxystaurosporine (**75**) showed a relatively high IC<sub>50</sub> value of 5 μM in the presence of 30 μM ATP and no inhibition when it was tested in the presence of 300 μM ATP.<sup>340</sup>

### 3 Aims of the study

During the past decades, it has become clear that malfunctioning PKs cause cancer. One way of combating this problem has been to develop ligands that target these PKs and consequently prevent this harmful disease. However, lack of suitable ligands, gene mutations, resistant cancer lines and the constant discovery of new target kinases are the main driving forces that keeps cancer research ongoing.

The primary objective in this study was to design and synthesize novel inhibitors and activators targeting either the regulatory domain of PKC or the kinase domain of ALK. Another primary objective was to synthesize bistramide A analogs. Potent lead compounds, which had been identified by computational methods, were used as templates in the design. Therefore, one of the aims of this study was to design and synthesize compound libraries with hit compound-based derivatives for the investigation of SARs of the PK ligands.

The more specific aims of the research were

- to synthesize a new class of compounds that induce apoptosis in leukemia cells (**I**);
- to design and synthesize a compound library based on the hit compound targeted to the C1 domain of PKC and to study the SAR of these compounds (**II**);
- to design and synthesize bistramide A and some of its isomers for biological studies (**III**);
- to design and synthesize inhibitors based on lead templates targeted at the kinase domain of ALK and to study the SAR of these compounds (**IV**).

## 4 Experimental

A detailed presentation of the materials, synthetic, and analytical methods can be found in the original publications **I-IV** and in the supporting information for original publications **II**, **III** and **IV**.

The supporting information for original publications **II**, **III** and **IV** is not included in this thesis book. This material is available from the author or via the Internet at <http://pubs.acs.org> for original publication **II** (46 pages) and at <http://onlinelibrary.wiley.com/> for original publications **III** (78 pages) and **IV** (16 pages).

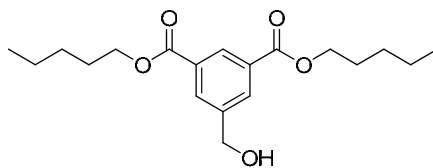
## 5 Results and discussion

The design, synthesis and SAR of PK ligands are described in the following chapters; dialkyl (5-hydroxymethyl)isophthalates and isophthalic acid derivatives (Chapter 5.1), bistramide A and its derivatives (Chapter 5.2) and urea-based inhibitors (Chapter 5.3). None of the reaction conditions presented here was systematically optimized since more emphasis was put on producing derivatives than optimizing reaction yields. Primarily those reactions which cannot be found in the original publications **I-IV** are presented here.

### 5.1 Synthesis of isophthalic acid derivatives and SAR of the compounds (I and II)

#### *Identification of dialkyl (5-hydroxymethyl)isophthalates as compounds inducing apoptosis (I)*

At the beginning of this research project, dipentyl (5-hydroxymethyl)isophthalate (**110**) among other hit compounds, had been discovered<sup>II</sup> using molecular modeling and the crystal structure of the PKC $\delta$  C1b domain (Figure 32A).<sup>81</sup> This  $C_2$ -symmetric compound (**110**) was used as a template for the design of a compound library for the SAR of the compounds.



**110**

First, the hit compound (**110**) was docked into the crystal structure of the C1b domain of PKC $\delta$  (Figure 32A).<sup>81</sup> As can be seen, compound **110** fits deeply in the binding cleft and forms similar hydrogen bonds to the protein as does phorbol 13-*O*-acetate (**7**) (Figure 32B, Figure 8 and Chapter 2.2.2.). Encouraged by these results, a number of derivatives of the hit compound (**110**) were designed.

In order to find the optimal ester groups for activity, synthesis of derivatives of the hit compound (**110**) was required. As the structurally related diethyl (5-hydroxymethyl)isophthalate (**111**) is commercially available, it was logical that it could serve as a starting material in the synthesis of the analogs.<sup>I, II</sup> Using **111** as a starting material, a set of ten symmetric diesters (compounds **110**, **112-119**, and **127**) could be prepared in only four reaction steps with overall yields of 22-46% (Figure 33).<sup>I</sup> None of the reaction conditions were systematically optimized since the main aim was to produce derivatives for biological activity assays.

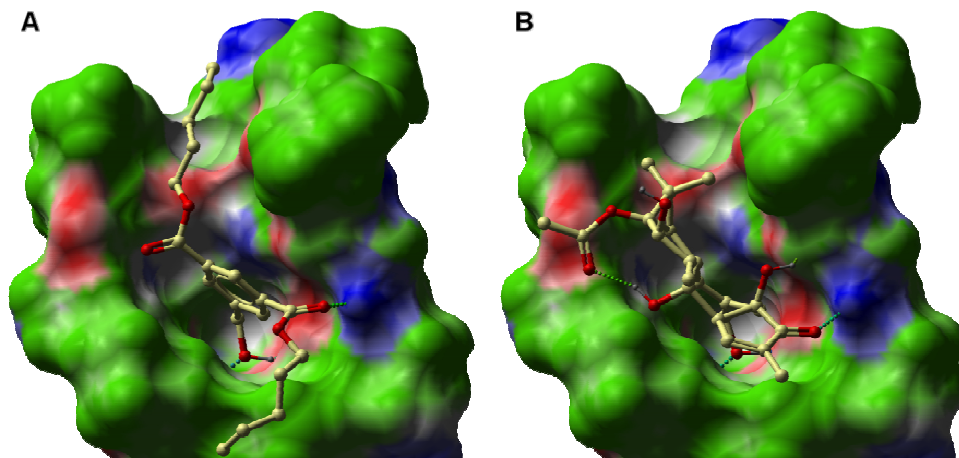


**Figure 32** *A)* The hit compound (**110**) docked into the crystal structure (PDB ID: 1PTR)<sup>81</sup> of the C1b domain of PKC $\delta$ . The hit compound (**110**) is presented in ball and stick representation and colored by atom type. The binding pocket is colored as follows: oxygen atoms (red), nitrogen atoms (blue), carbon atoms (green), hydrophobic groups (grey) and rest of the protein (green). Hydrogen bonds are denoted with green spheres. *B)* Phorbol 13-O-acetate (**7**) in the crystal structure (PubID: 1PTR) of the C1b domain of PKC $\delta$ .<sup>81</sup> Colored as in *A*). The figures were created using ICM Molsoft software 3.7.

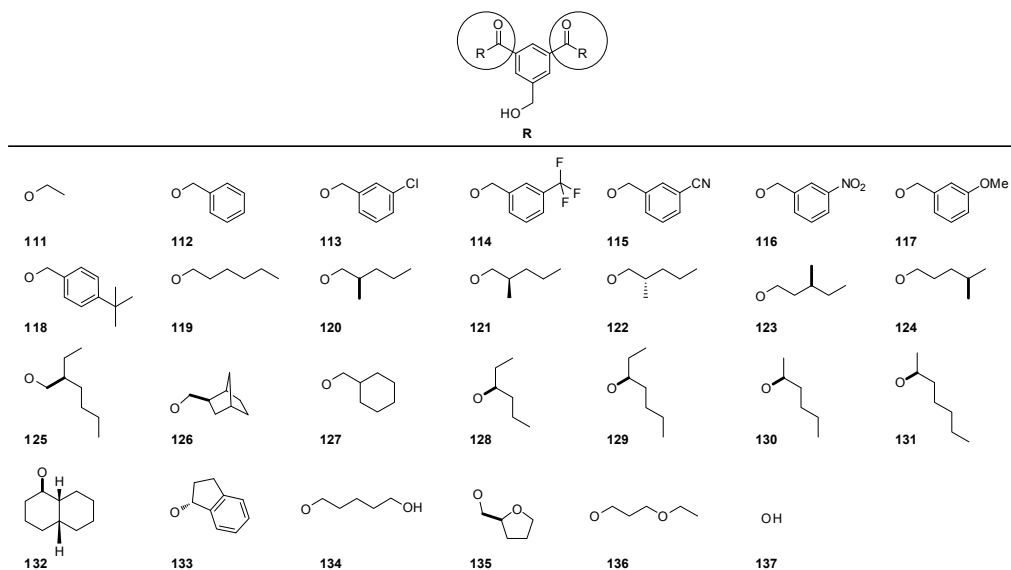


**Figure 33** Synthesized dialkyl (5-hydroxymethyl)isophthalates (**112-136**), the starting material (**111**) and the negative control compound (**137**). The modified position of the hit compound (**110**) is indicated with a circle.

The first set of compounds (**110**, **112-119**, and **127**) was tested for proapoptotic activity in HL-60 leukemia cells and in Swiss 3T3 fibroblasts (Figure 34). Compounds **114** and **119** were found to be the most promising of the studied compounds; they induced apoptosis on HL-60 leukemia cells (43 and 47%, respectively, of apoptotic cells at 20  $\mu\text{M}$ ) and their effects on fibroblasts at these concentrations were insignificant ( $< 5\%$  at 20  $\mu\text{M}$ ). In addition, reduction in mitochondrial membrane potential ( $\Delta\psi\text{m}$ ) and increase in caspase-3 activity already during the first 2 hours confirmed these results. Compounds **114** and **119** showed  $\text{IC}_{50}$  values (for HL-60 cells) of 41 and 23  $\mu\text{M}$ , respectively. The other compounds had weaker apoptosis-inducing effects in leukemia cells or they were non-selective. Interestingly, the hit compound (**110**), structurally different from compound **119** by only one carbon in both ester side chains, showed only a moderate apoptotic activity in leukemia cells (15% at 20  $\mu\text{M}$ ) and little effect on fibroblasts. Importantly, compounds **114** and **119** were not cytotoxic or mutagenic, shown by a lactate dehydrogenase assay and with a miniaturized Ames test.

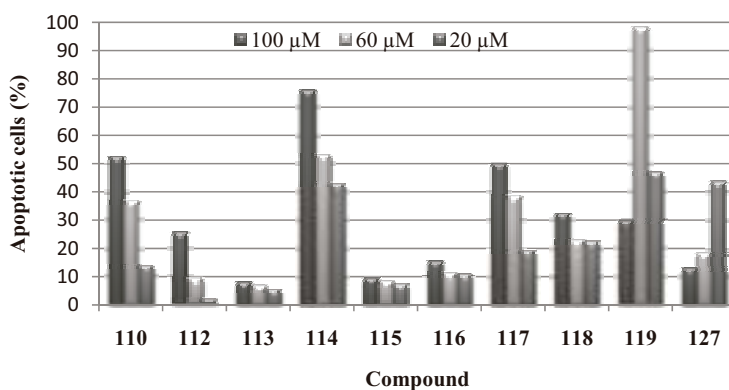


**Figure 34** Apoptotic activity in HL-60 leukemia cells for the tested compounds. The compounds were tested at concentrations of 100  $\mu\text{M}$  (black bars), 60  $\mu\text{M}$  (light grey bars) and 20  $\mu\text{M}$  (dark grey bars).

#### Structure-activity relationship of isophthalic acid derivatives (**I** and **II**)

In a second round of synthesis, the diesters **120-126** and **128-136**, and the negative control compound **137** were prepared (Figure 33).<sup>11</sup> The ester groups of the compounds were chosen to investigate: i) the optimal ester group for activity; ii) the optimal  $\text{clog}P$  value for activity and whether the  $\text{clog}P$  value could be increased and iii) the structure of the binding pocket. The syntheses of the analogs **120-126** and **128-136** were completed as for the previous compounds and with 8-78% overall yields. Subsequently, the diesters **113-114** and **118-137** were screened

for binding activity to PKC $\alpha$  and PKC $\delta$  using a filtration method in a 96-well plate format.<sup>342</sup> The diesters **113-114** and **118-133** (tested at 0.1-20  $\mu$ M concentrations) replaced [ $^3$ H]PDBu (25 nM concentration) from PKC $\alpha$  and PKC $\delta$  with 32-67% and 48-77%, respectively (Figure 35). Compounds **134-137** were not able to replace [ $^3$ H]PDBu from PKC $\alpha$  or PKC $\delta$ . In addition, the diesters replaced [ $^3$ H]PDBu in a concentration-dependent manner (Figure 36, partly unpublished results, Talman et al.).<sup>11, 343</sup> When comparing their ability to replace [ $^3$ H]PDBu from PKC $\delta$ , the best derivatives (**128-131**) generally had ester groups derived from secondary alcohols with 6-7 carbons. Furthermore, a modest selectivity between PKC $\alpha$  and PKC $\delta$  could be obtained; the compounds seemed to replace [ $^3$ H]PDBu better from PKC $\delta$  than PKC $\alpha$  in most cases (Figure 35). Compounds **114**, **128**, and **129** displayed  $K_i$  values of 205 and 590 nM, 661 and 915 nM, and 319 and 529 nM for PKC $\alpha$  and PKC $\delta$ , respectively.

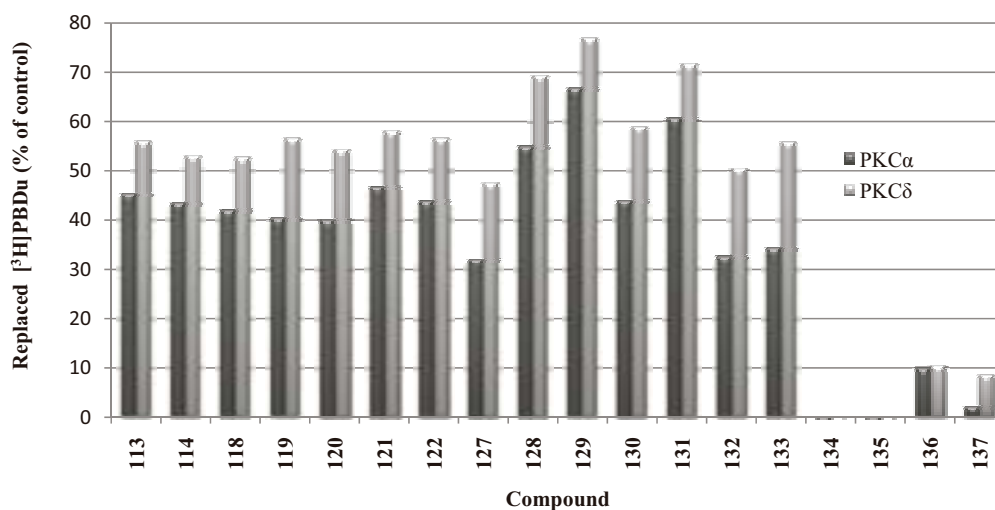


**Figure 35** The bars represent the percentage of the replaced [ $^3$ H]PDBu from PKC $\alpha$  (black bars) and PKC $\delta$  (grey bars) when 20  $\mu$ M of the compounds were tested, expressed as percentage of control ( $n = 1-8$ ). The concentration of [ $^3$ H]PDBu was kept at 25 nM.

The  $\log P$  of C1-domain binding compounds seem to affect, at least to a certain degree, the ability of replacing [ $^3$ H]PDBu from the C1 domain because the C1 domain is thought to be in close proximity to the bilayer.<sup>81, 230</sup> Analysis of the binding activity for PKC $\delta$  vs. the  $\log P$  of the synthesized compounds revealed an optimum  $\log P$ -value of greater than 5.5 (Figure 37). Compounds **134-136** were designed and synthesized in an attempt to reduce the hydrophobicity of the compounds keeping in mind not to change the overall structure too much (compare the structure of these compounds to compounds **110** and **119**). However, introducing an additional oxygen atom to the ester substituents decreased binding activity (Figure 35 and Figure 37). The



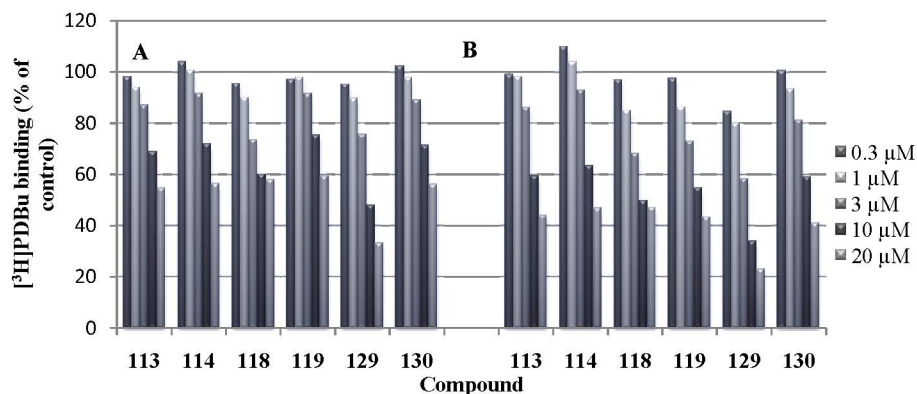


**Figure 36** Representative examples showing a concentration-dependent binding of the synthesized compounds. *A)* The bars represent the remaining  $[^3\text{H}]\text{PDBu}$  bound to PKC $\alpha$  (% of control,  $n = 2-5$ ). The compounds were tested at concentrations of 0.3, 1, 3, 10 and 20  $\mu\text{M}$ . The concentration of  $[^3\text{H}]\text{PDBu}$  was kept at 25 nM. *B)* The bars represent the remaining  $[^3\text{H}]\text{PDBu}$  bound to PKC $\delta$  (% of control,  $n = 1-3$ ). Concentrations as in A). Partly unpublished results, Talman et al.<sup>II,343</sup>

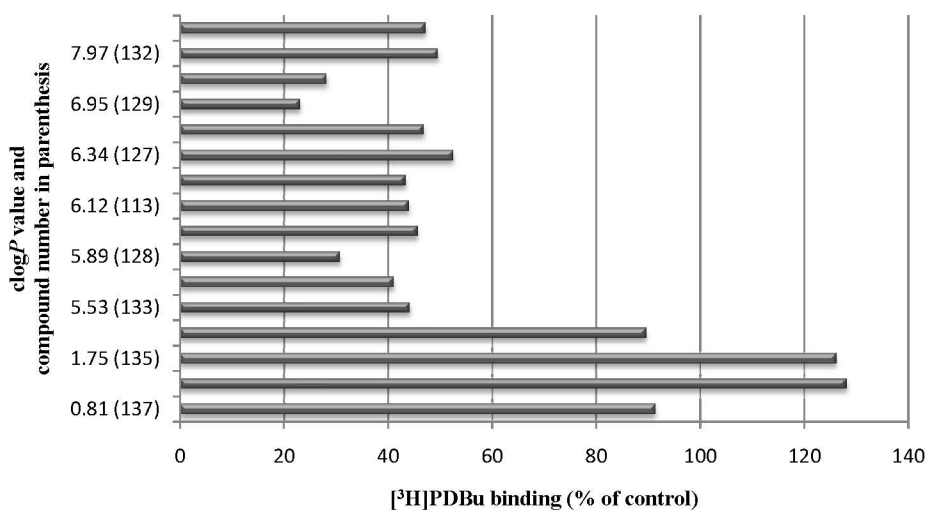


**Figure 37** Dependence of the  $\text{clog}P$ -value on the ability of replacing  $[^3\text{H}]\text{PDBu}$  bound to PKC $\delta$  (compound numbers in parenthesis). The bars represent the remaining  $[^3\text{H}]\text{PDBu}$  bound to PKC $\delta$  (% of control). The compounds were tested at 20  $\mu\text{M}$  against 25 nM solutions of  $[^3\text{H}]\text{PDBu}$ .

decreased binding affinity of these compounds with relatively more hydrophilic ester groups may be due to unfavorable interactions within the bilayer.<sup>100, 344</sup> Because activated PKC C1 domains translocate partly into the membrane, using hydrophilic side chains in the compounds may be one possibility for development of specific C1 domain-targeted ligands.<sup>345</sup> However, in the case of dialkyl 5-(hydroxymethyl)isophthalates this remains to be seen.

In a next round of SAR study we investigated how important the hydroxymethyl group found in the template (**110**) is for binding activity. To do this, we designed a series of compounds (**138-143**) having the same ester groups as in compounds **114** or **120** but the hydroxymethyl group was substituted with a proton, methyl, nitro or amino group (Figure 38).

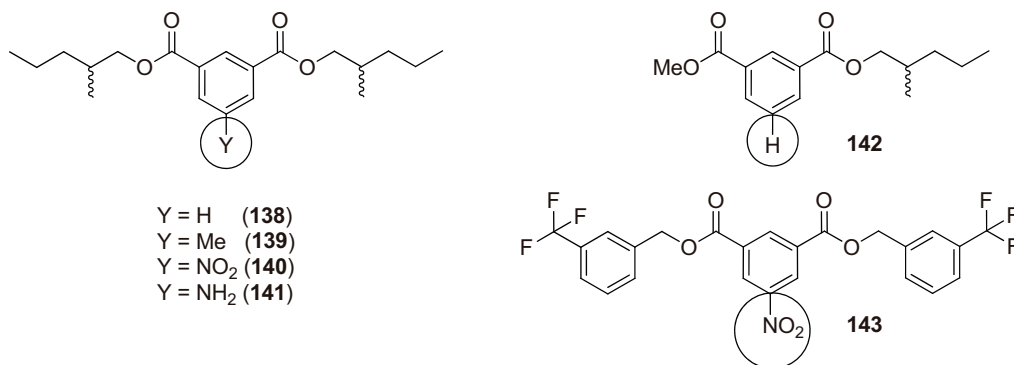
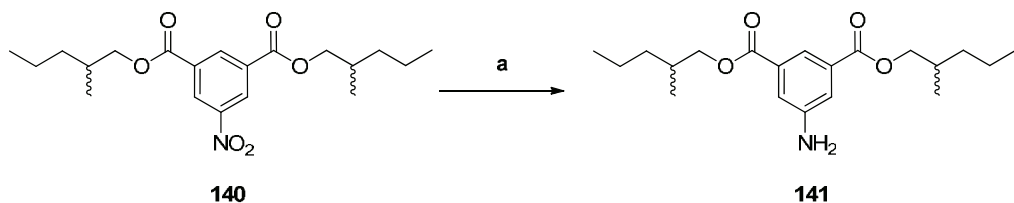


**Figure 38** Analogs (**138-143**) lacking the hydroxymethyl group of the hit compound **110** but having instead a proton (compounds **138** and **142**), methyl (compound **139**), nitro (compounds **140** and **143**), or amino (compound **141**) group. The modified position of the hit compound (**110**) is indicated with a circle.

These analogs were conveniently synthesized in only one step with 28-76% yields.<sup>II</sup> The amino analog **141** was prepared by catalytic hydrogenation of the nitro group in **140** with a 77% yield (Scheme 1, unpublished results, Boije af Gennäs et al.).<sup>346</sup>

#### Scheme 1<sup>a</sup>.



<sup>a</sup> Conditions: (a) Pd/ C (10%), EtOH, rt, 18 h, 77%. Unpublished results.<sup>346</sup>

The results from the biological assays clearly showed that the hydroxymethyl group of the hit compound (**110**) is needed for binding activity since the derivatives **138-143** were not able to replace [<sup>3</sup>H]PDBu from the C1 domain of PKC $\alpha$  or PKC $\delta$  (Figure 39, partly unpublished results, Talman et al.).<sup>11, 343</sup>

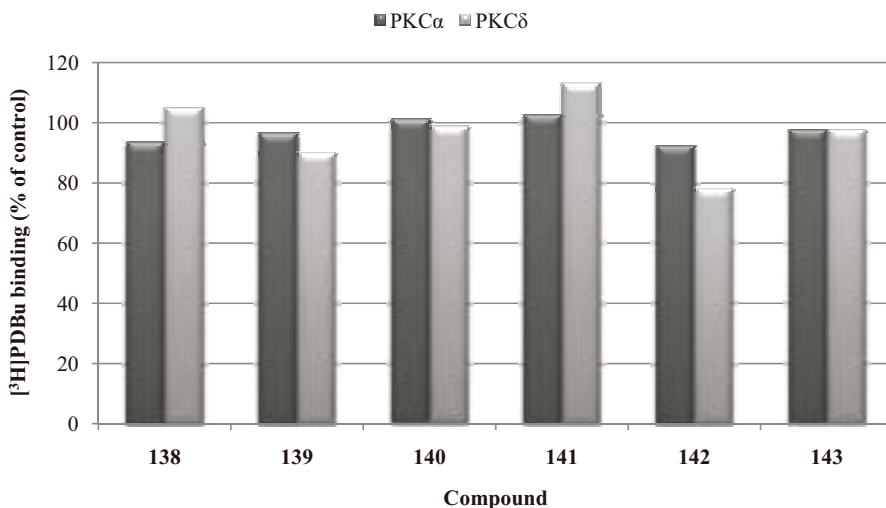


**Figure 39** The bars represent the remaining [<sup>3</sup>H]PDBu bound to PKC $\alpha$  (black bars) and PKC $\delta$  (grey bars), expressed as percentage of control ( $n = 1-3$ ). The concentrations of the compounds were 20  $\mu$ M and the concentration of [<sup>3</sup>H]PDBu was 25 nM. Partly unpublished data, Talman et al.<sup>11, 343</sup>

Since amide groups are more hydrophilic than ester groups, and amides are also more stable than esters in the cells,<sup>347</sup> the substitution of one or both of the ester groups of the hit compound (**110**) with amide group(s) or reverse amide group(s) was pursued. In addition, nonsymmetric compounds could also increase the binding affinities to the binding site of the C1 domain. Compounds **114** and **119** were chosen as templates for the amides because they had previously shown good binding activity and the respective amides were readily synthesizable, hence compounds **144** and **145** were prepared (Figure 40). The reverse amide **146** was synthesized to investigate the effect of moving the carbonyl group, which was thought to be important for activity, one atom away from the aromatic ring. In addition, compounds **147-151** and **152** were designed to study the binding potency of nonsymmetric monoester and -amide compounds (Figure 40). In these compounds one pivotal ester group was kept and the other one substituted with an amide group.

Unfortunately, all of these compounds bound less strongly than the diesters (Figure 41). The binding activity results were surprising, taking into account that the only difference in the

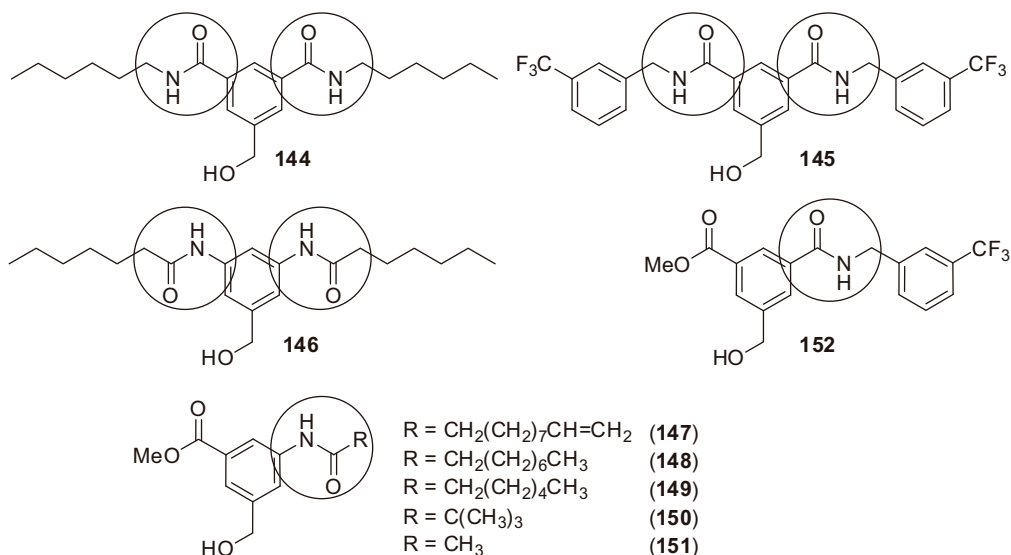


**Figure 40** Compounds with one (152) or two (144 and 145) amide or reverse amide (146-151) groups. The modified position of the hit compound (110) is indicated with a circle.

structure of the amides compared to the esters is the amide groups (compare e.g. 144 and 145 to 119 and 114). Structurally, the amide groups are more rigid than the ester groups, which may contribute negatively/unfavorably to the overall binding activity. However, inspection of the crystal structure does not confirm why these amides would not bind the regulatory domain. Interestingly, compound 147, having the longest and most hydrophobic amide group of the monoamine series (compounds 147-152), showed the best ability to replace [<sup>3</sup>H]PDBu from

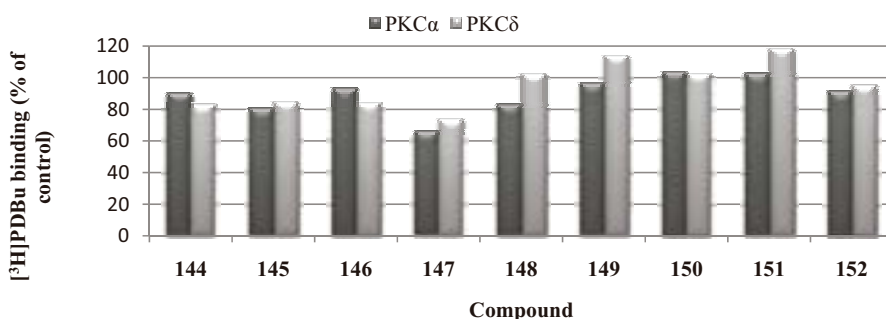


**Figure 41** Representation of the remaining [<sup>3</sup>H]PDBu bound to PKCα (black bars) and PKCδ (grey bars), expressed as percentage of control ( $n = 3$ ). The compounds were assayed at a concentration of 20  $\mu\text{M}$  and the concentration of [<sup>3</sup>H]PDBu was 25 nM.

PKC $\alpha$  and PKC $\delta$ . One explanation of these binding results may again be the interactions of the ligands within the bilayer; a more hydrophilic amide group may result in unfavorable interactions.<sup>100, 344</sup>

In the next rounds of SAR studies we wanted to investigate analogs of the hit compound that contain only one ester group. Hence, two series of compounds were synthesized; one series (compounds **153-155**)<sup>ii</sup> where the compounds lack one of the ester groups and another series (compounds **156-159**), where the compounds have only one ester group but instead one additional hydroxy or ether group inserted (Figure 42, partly unpublished results, Boije af Gennäs et al.).<sup>ii, 346</sup> Compounds **156-159** were synthesized in two or three steps starting from 5-formyl-2-hydroxybenzoic acid (**160**, Scheme 2). The phenol **156** was prepared by monoalkylation of **160** by 1-hexyl bromide and KHCO<sub>3</sub> in DMF at 80 °C for 4 h and subsequent NaBH<sub>4</sub> reduction of the intermediate (**161**) to give the product in 56% yield (two steps, unpublished data).<sup>346</sup> Derivatives **157** and **158** were obtained after dialkylation of **160** by alkyl bromide, KI and K<sub>2</sub>CO<sub>3</sub> in DMF at 110-130 °C for 17-18 h and subsequent NaBH<sub>4</sub> reduction of the intermediates (**162** and **163**) to give the products in 62-71% yields (two steps, unpublished data).<sup>346</sup> Analogue **159** was prepared from **161**, benzyl bromide, KI, K<sub>2</sub>CO<sub>3</sub> in DMF under microwaves at 130 °C for 1 hour and subsequent NaBH<sub>4</sub> reduction of the intermediate (**164**) to give the product in 34% yield (two steps, unpublished data, Boije af Gennäs et al.).<sup>346</sup>

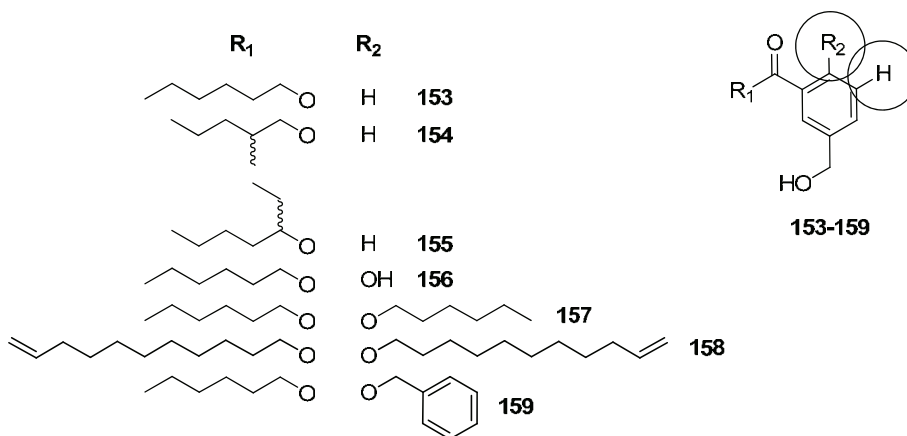
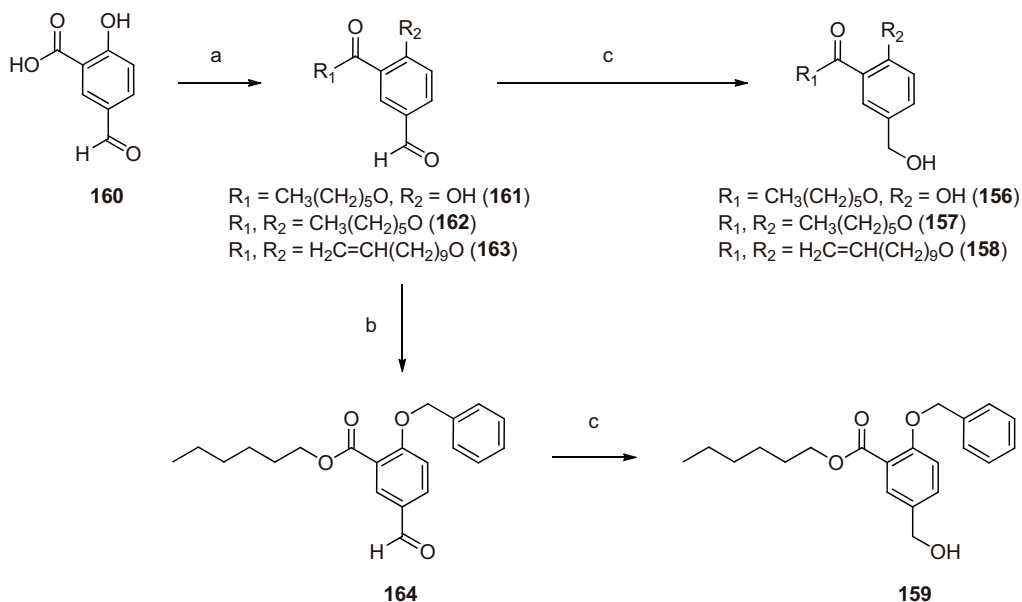


**Figure 42** Compounds **153-159** carrying only one ester group. The modified positions of the hit compound (**110**) are indicated with circles. Partly unpublished compounds, Boije af Gennäs et al.<sup>ii, 346</sup>

**Scheme 2<sup>a</sup>.**



<sup>a</sup> Conditions: (a) alkyl bromide (1.1 equiv.),  $\text{KHCO}_3$ , DMF, 80 °C, 4 h, 57% (**161**) or alkyl bromide (2.0-2.5 equiv.),  $\text{K}_2\text{CO}_3$ , KI, DMF, 110-130 °C, 17-18 h, 86-90% (**162** and **163**); (b) benzyl bromide (2.0 equiv.),  $\text{K}_2\text{CO}_3$ , KI, DMF, 130 °C, 1 h, 60% (**164**); (c)  $\text{NaBH}_4$ , MeOH (and THF), 0 °C, 2-4 h, 56-99%. Unpublished data, Boije af Gennäs et al.<sup>346</sup>

The compounds were screened for binding activity and as expected, the monoesters **153-155** did not show any activity (Figure 43).<sup>11</sup> In addition, phenol **156**, with a hydroxy group *ortho* to the ester group, did not show any binding activity (unpublished results, Talman et al.).<sup>343</sup> Instead, compound **157**, with an *ortho* 1-hexyl ether group, replaced [<sup>3</sup>H]PDBu effectively from PKC $\delta$  and less effectively from PKC $\alpha$  (Figure 43, unpublished results, Talman et al.).<sup>343</sup> These results suggest that a polar group is unfavorable at this position, underlining the hypothesis that PKC C1-domain modulators create a hydrophobic surface over the binding cleft.<sup>62</sup> In contrast, compound **159** with a benzyl ether group instead of the 1-hexyl ether group present in **157**, could not replace [<sup>3</sup>H]PDBu from PKC $\alpha$  and PKC $\delta$ . The reason for this difference in binding activities between these two compounds is hard to explain, one explanation may be that the benzylic ether group of **159** forms unfavorable interactions with the Leu254 of the C1 domain. Compound **158**, with longer alkyl chains than **157** and **159**, also showed weak binding activity. All together, these results demonstrate that two ester groups are not needed for binding activity to the C1 domain of PKC $\alpha$  and PKC $\delta$  but if the derivative only has one ester group an (*ortho*) ether group is required.

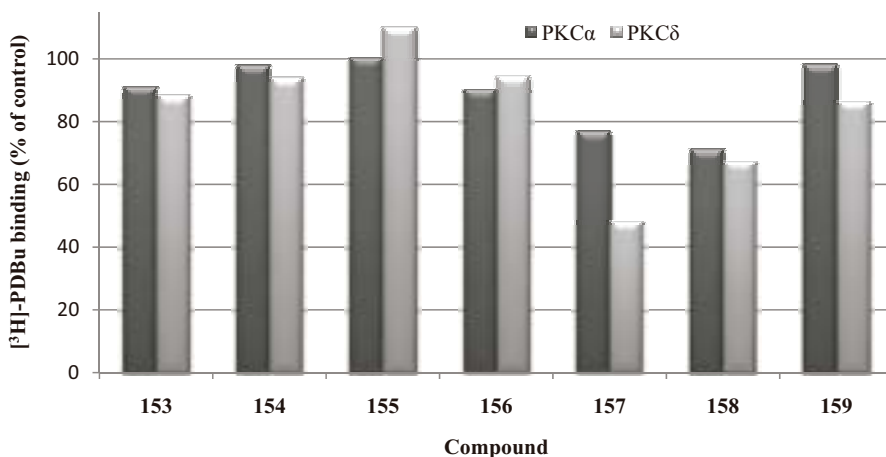


**Figure 43** The bars represent remaining [ $^3\text{H}$ ]PDBu bound to PKC $\alpha$  (black bars) and PKC $\delta$  (grey bars). The compounds were assayed at a concentration of 20  $\mu\text{M}$  in the presence of 25 nM [ $^3\text{H}$ ]PDBu, and are % of control ( $n = 3$ ). Partly unpublished results, Talman et al. <sup>11,343</sup>

To conclude, the SAR results gave the following information (Figure 44): i) at least one carbonyl of **110** is needed for activity, however, ii) if one of the ester groups of **110** is replaced by hydrogen, a hydrophobic group next to the second ester group is needed for activity, iii) the 5-hydroxymethyl group of **110** is needed for activity, iv) the best compounds have ester groups consisting of secondary alkoxy groups of 6-7 carbons, v) an additional oxygen atom in the side chains of the ester groups is not tolerated and, vi) one or both of the ester groups cannot be substituted with amide or reverse amide groups.

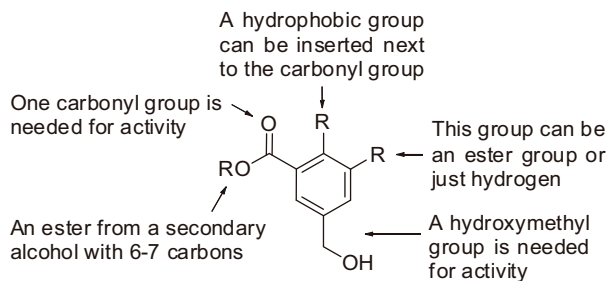


**Figure 44** Results from the SAR studies.

## 5.2 Synthesis of bistramide A and its derivatives, and the biological outcome of the compounds (III)

At the beginning of this project, there was little consensus on the activation of PKC $\delta$  by bistramide A (**30**). While PKC $\delta$  was initially discovered to be activated by bistramide A (**30**) in HL-60 and MM96E cells,<sup>170</sup> more recently another group has identified that the main target of bistramide A (**30**) is actin.<sup>172</sup> Therefore, the synthesis of analogs of bistramide A (**30**) to study the biological outcome of these structural modifications was pursued.

As bistramide A (**30**) possesses two amide groups, it was logical that its analogs could be obtained from the corresponding carboxylic acids and amines (Figure 45). Three building blocks were assigned; the south fragment (**165**), the central fragment (**166**) and the north fragment (**167**). These fragments were synthesized as a collaboration between three research groups; the south (**165**) and north (**167**) fragments were prepared in the University of Lyon (France) by two research groups and the central fragment (**166**) as part of this investigation in Helsinki. The couplings of the fragments were performed in the French laboratories.

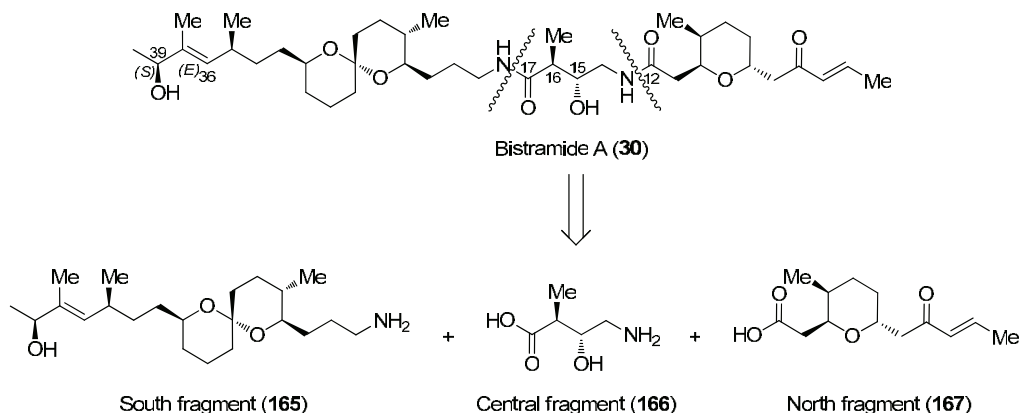


**Figure 45** Retrosynthesis of bistramide A (**30**) giving the south (**165**), the central (**166**) and the north (**167**) fragments.

Depending on the coupling strategy used in the synthesis of bistramide A (**30**), the protections and activations of the functional groups of the south (**165**), the central (**166**) and the north (**167**) fragments have to be carefully chosen. Among previously performed total syntheses of bistramide A (**30**), the most common protocol has been to couple first the north fragment (**167**) with the central fragment (**168**) followed by the coupling of the south fragment (**171**) (Figure 46).<sup>177-179</sup> Hence, the secondary hydroxy and carboxyl groups of the south (**171**) and central (**168**) fragments have been protected with *tert*-butyldimethylsilyl (TBS) and triisopropylsilyl (TIPS) groups.



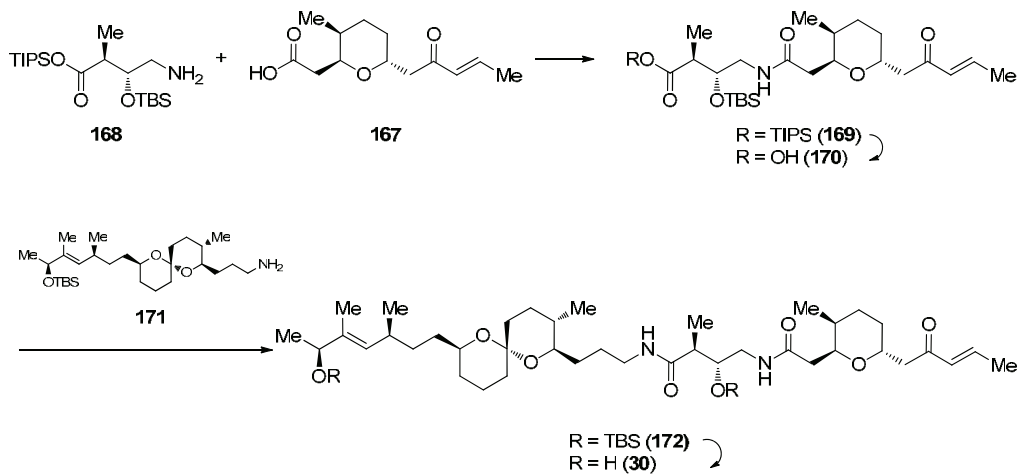


**Figure 46** Coupling strategy of fragments in the synthesis of bistramide A (**30**).<sup>177-179</sup>

In contrast to the above-mentioned coupling strategy in the synthesis of bistramide A (**30**), the groups of Kozmin<sup>175</sup> and Crimmins<sup>176</sup> performed the coupling reaction first with the south (**165**) and the central (**173**) fragments followed by the condensation of the north fragment (**176**)

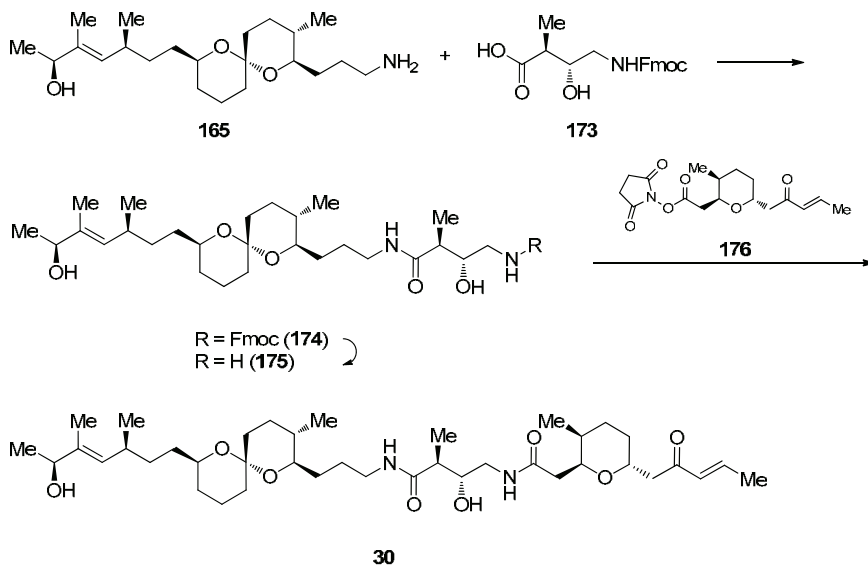


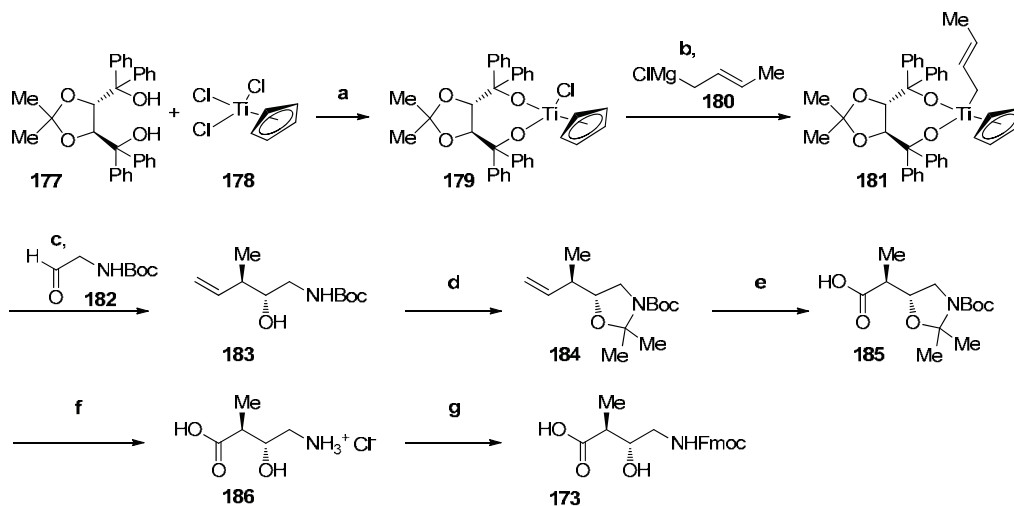
**Figure 47** Coupling strategy of Kozmin<sup>175</sup> and Crimmins<sup>176</sup> of the fragments in the synthesis of bistramide A (**30**).

(Figure 47). In this strategy, only the amino group of the central fragment (**173**) needs to be protected as a fluorenylmethyl carbamate (Fmoc, compound **173**) and consequently, the number of required deprotection steps is reduced. Therefore, we decided to use this coupling strategy in the synthesis of bistramide A (**30**) as well as its analogues.

The central fragment (**173**) was prepared in seven steps with an overall yield of 21% using the modified Kozmin synthesis route (Scheme 3).<sup>175</sup> Instead of the Brown crotylboration<sup>348</sup> of the amino aldehyde (**182**) used in the Kozmin route, we performed an asymmetric crotyltitanation<sup>349</sup> of the aldehyde (**182**).<sup>350</sup> In this reaction, the highly face-selective crotyltitanium complex (**181**),<sup>351</sup> which was synthesized from (4*R*,5*R*)-2,2-dimethyl- $\alpha,\alpha',\alpha'$ -tetraphenyldioxolane-4,5-dimethanol (TADDOL, **177**), cyclopentadienyltitanium(IV) trichloride (**178**) and 2-butenylmagnesium chloride (**180**), allowed the introduction of the desired stereochemistry of the amino alcohol (**183**). The use of a crotyltitanation instead of a crotylboration allowed us to avoid the usage of the highly volatile *trans*-2-butene used in the Kozmin route.<sup>175</sup> While having the right stereochemistry in hand, the amino alcohol (**183**) was protected as the 1,3-oxazolidine (**184**) and subsequent ruthenium chloride - periodate catalyzed oxidative cleavage of the double bond under Sharpless conditions<sup>352</sup> gave the carboxylic acid (**185**). The optical purity of the carboxylic acid (**185**) was confirmed by diazomethane derivatization and chiral GC-MS. Acidic deprotection of the 1,3-oxazolidine (**185**) to the amino acid (**186**) and subsequent introduction of a Fmoc group gave the *N*-protected amino acid **173**. Optical rotations measured of the products were in good agreement with those previously reported.<sup>175</sup>

Inspection of the crystal structure of actin complexed with bistramide A (**30**) reveals hydrogen bonds between the ligand and the protein (Figure 48).<sup>180</sup> Two hydrogen bonds between the protein and the central fragment (**166**) region of bistramide A (**30**) can be obtained; one between the phenol group of Tyr133 and the C17 carbonyl group and another between the backbone amide proton of Ile136 and the C15 hydroxy group. In addition, the two other hydrogen bonds which can be obtained in the binding complex interact with the amide groups of bistramide A (**30**). The first hydrogen bond is between the phenol group of Tyr143 and the amide proton of the south fragment (**165**) region and the second is between the backbone amide proton of Ala170 and the C12 carbonyl of the north fragment (**167**) region. Three additional hydrogen bonds between bistramide A (**30**) and actin residues can be obtained via bridging water molecules (Figure 48 and Figure 49). In addition, the C16 methyl group of the central fragment (**166**) appears to point towards a hydrophobic cave in the binding pocket. All in all, the central fragment (**166**) region appears to play an important role in the overall binding affinity of bistramide A (**30**) to the protein.

Scheme 3<sup>a</sup>.



<sup>a</sup> Conditions: (a) Et<sub>3</sub>N, Et<sub>2</sub>O, rt, 24 h; (b) 2-Butenylmagnesium chloride (**180**) (2 M in THF), Et<sub>2</sub>O, 0 °C, 80 min; (c) i) *tert*-Butyl *N*-(2-oxoethyl)carbamate (**182**), THF, -78 °C, 20 h; ii) NH<sub>4</sub>F (40%, aq.), -78 °C → rt, 24 h, 57% (three steps); (d) *p*-Toluenesulfonic acid monohydrate, 2,2-dimethoxypropane, acetone, rt, 10 min, 70%; (e) NaIO<sub>4</sub>, RuCl<sub>3</sub>, CCl<sub>4</sub>:MeCN:H<sub>2</sub>O (2:2:3), rt, 17 h, 66%; (f) HCl (3 M, aq.), EtOAc, rt, 3 h, 100%; (g) *N*-(9-Fluorenylmethoxycarbonyloxy) succinimide, Na<sub>2</sub>CO<sub>3</sub>, H<sub>2</sub>O:1,4-dioxane (1:1), rt, 2 h, 80%.

A closer look at the crystal structure of actin complexed with bistramide A (**30**) showed that the C39 hydroxy of bistramide A forms a hydrogen bond with the carbonyl of Tyr143 via a bridging water molecule (Figure 49A). By inverting the stereochemistry of the double bond, the same hydroxy may be placed in close proximity to the Tyr143 carbonyl, which would allow a direct hydrogen bond formation (Figure 49B). Therefore, bistramide A (**30**) as well as the 36(*Z*)-39(*R*) (**187**) and 36(*Z*)-39(*S*) (**188**) isomers of bistramide A (**30**) were prepared in order to test this hypothesis. <sup>III</sup>

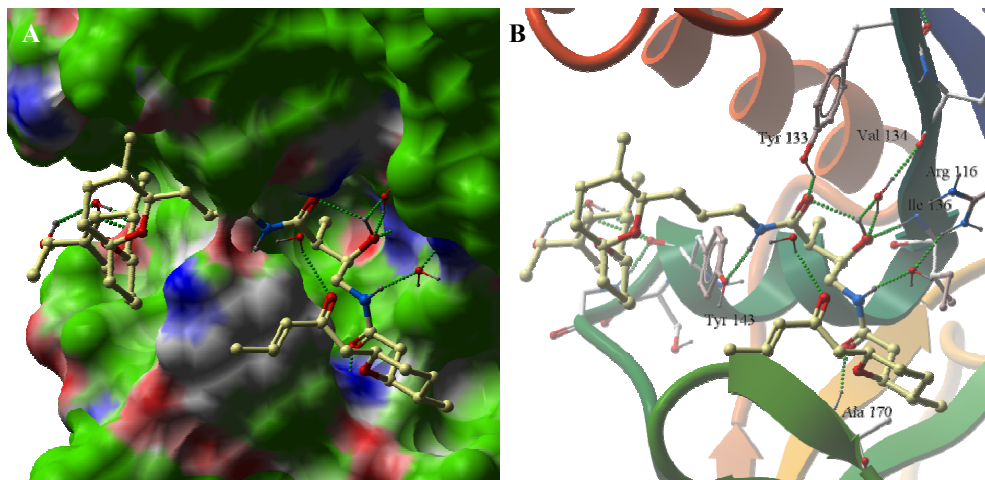
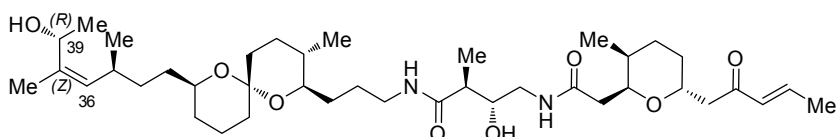
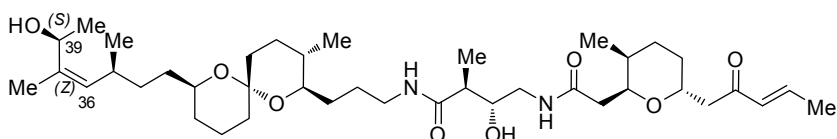


**Figure 48** *The crystal structure of actin complexed with bistramide A (30) (1.35 Å resolution, PDB ID: 2FXU).<sup>180</sup> A) The binding pocket is presented as a surface and is colored as follows: oxygen atoms (red), nitrogen atoms (blue), carbon atoms (green), hydrophobic groups (grey) and rest of the surface is colored green. Bistramide A (30) and water molecules are presented in ball and stick representation and colored by atom type. Hydrogen bonds are denoted with green spheres. B) Residues Tyr133, Ile136, Tyr143 and Ala170 that contribute to the binding of bistramide A is shown in ball and stick representation and are colored as in A). Secondary structures of the protein are colored with different colors and hydrogen bonds are denoted with green spheres. The figures were created using ICM Molsoft software 3.7.*



36(Z)-39(R) analogue (187)



36(Z)-39(S) analogue (188)

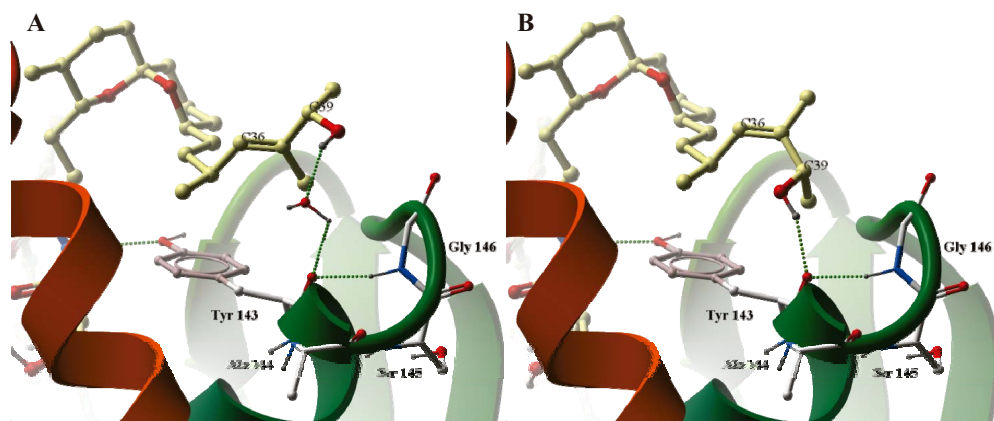


**Figure 49** *A)* The crystal structure of actin complexed with bistramide A (**30**) (PDB ID: 2FXU).<sup>180</sup> The C39 hydroxy of bistramide A (**30**) is forming a hydrogen bond with Tyr143 via a bridging water molecule. Bistramide A (**30**) and residues Tyr143, Ala144, Ser145 and Gly146 are presented in ball and stick representation and colored by atom type. Secondary structures of the protein are colored orange and green, and hydrogen bonds are denoted with green spheres. *B)* The 36(Z)-39(S) isomer **188** of bistramide A (**30**) obtained by substitution in the X-ray structure of the bistramide A-actin complex, showing the expected hydrogen bond of the C39 hydroxy to the carbonyl of Tyr143. Colored as in A). The figures were created using ICM Molsoft software 3.7.

First, to determine the effects of the natural product (**30**) and the 36(Z)-isomers (**187**) and (**188**) on cell viability, they were tested in HL-60 cells using the MTS assay. The MTS assay is a colorimetric assay used in detecting living, but not dead cells, and can therefore be used to measure cytotoxicity, proliferation or activation of cells.<sup>353</sup> This overall antiproliferative assay showed slightly weaker activities for the Z isomers **187** and **188** compared to bistramide A (**30**); the concentrations required to inhibit growth by 50% (IG<sub>50</sub>) were 1.6, 7.8 and 3.7  $\mu$ M for bistramide A (**30**), the 36(Z)-39(R) and the 36(Z)-39(S) isomers **187** and **188**, respectively. As the observed growth inhibition can be attributed to a combination of inhibition of cell cycling (antimitotic effect), proapoptotic effect, and induction of differentiation, a more detailed cell cycle analysis by flow cytometry was performed on the HL-60 cells. Indeed, while the isomers showed similar overall antiproliferative activities, flow cytometry analyses showed significant differences regarding the origin of this activity. Each compound showed a distinct distribution of antimitotic effect presumably via actin binding, proapoptotic effect most likely via PKC $\delta$ , and pro-differentiation effect as evidenced by CD11b expression.

The results of bistramide A (**30**) were consistent with inhibition of cytokinesis via actin as previously reported,<sup>172</sup> however, at high concentrations (100  $\mu$ M) the results were consistent with the induction of apoptosis. The results for the 36(Z)-39(R) isomer **187** show a similar strong accumulation in 4n polyploid cells, with no corresponding accumulation in sub-G<sub>0</sub> phase of the cell cycle, and thus no corresponding contribution of proapoptotic activity. Interestingly, the

36(Z)-39(S) isomer **188**, which has almost identical overall antiproliferative activity to **187**, shows a marked apoptotic effect at 100  $\mu$ M.

In order to evaluate the proapoptotic effect of the three compounds more accurately, Annexin V/Sytox experiments were performed. The Annexin V affinity assay can be used to determine the number of cells undergoing apoptosis since negatively charged Ptd-L-Ser (**3**), which Annexin V binds to, becomes available in apoptosis.<sup>353</sup> Similarly, the Sytox experiment uses a high affinity nucleic acid stain (Sytox) which does not penetrate membranes of live eukaryotic cells.<sup>354</sup> The results showed a mild apoptotic effect for bistramide A (**30**, 77% viable cells at 100  $\mu$ M), while little or no apoptosis was induced by the 36(Z)-39(S) isomer **188** (85% viable cells at 100  $\mu$ M). On the other hand, a definite apoptotic effect was seen for the 36(Z)-39(R) isomer **187** (57% viable cells at 100  $\mu$ M).

CD11b immunolabeling studies were performed to evaluate CD11b expression as a marker of differentiation. Bistramide A (**30**) showed a mild induction of CD11b expression at lower concentrations (36% of CD11b positive cells at 10  $\mu$ M). Interestingly, the 36(Z)-39(R) isomer **187**, which showed little or no proapoptotic effect, induced a marked expression of CD11b (66% of cells at 100  $\mu$ M). Conversely, the 36(Z)-39(S) isomer **188**, showed only a weak expression of CD11b (24% of cells at 100  $\mu$ M). These results suggest that CD11b expression may also be an indirect effect of actin binding.

In conclusion, these results confirm the existence of all three reported effects, and confirm that accumulation of 4n polyploid cells represents the primary mode of action of the natural compound. However, the results also show that the antimitotic and proapoptotic are independent effects of bistramide A (**30**), as opposed to secondary effects of actin binding. Furthermore, to determine whether induction of differentiation is dependent or independent of actin binding additional analogs have to be investigated.

### 5.3 Synthesis of urea-based anaplastic lymphoma kinase inhibitors and SAR of the compounds (IV)

At the beginning of the project, lead templates (**189-194**) had been discovered in a virtual screening of the ZINC database using a homology model of ALK (Figure 50).<sup>IV</sup> These lead templates were subjected to two in vitro assays; an inhibition assay using the isolated enzyme and a proliferation inhibition assay using NPM-ALK-transduced BaF3 cells. Non-transduced BaF3 cell lines were used as a control. Using the results from these initial biological studies of the leads **189-192** and a careful investigation of why doramapimod (**78**)<sup>294</sup> only weakly binds to ALK and why sorafenib (**79**)<sup>295</sup> does not, a set of novel ureas was designed. The compounds were designed to investigate possible gatekeeper interactions as modeling suggested that ring 2 of the lead templates **189-194** is in close proximity to the gatekeeper residue Leu1196. In addition, we wanted to design compounds that would form hydrogen bonds to the hinge region

backbone residues Glu1197, Met1199 or Ala1200 by inserting a polar group at ring 1. As the initial results from the biological screening showed low cellular activity, one additional aim was to increase the cell penetration of the compounds while keeping the non-transduced BaF3 cells untouched. Furthermore, we wanted to enhance the inhibition potency by substituting rings 1-4 with different substituents or varying the linker length of **189-194**. Keeping these aims in mind, a set of 24 ureas was designed, synthesized and assayed for inhibition activity (Tables 2-4).<sup>IV</sup>

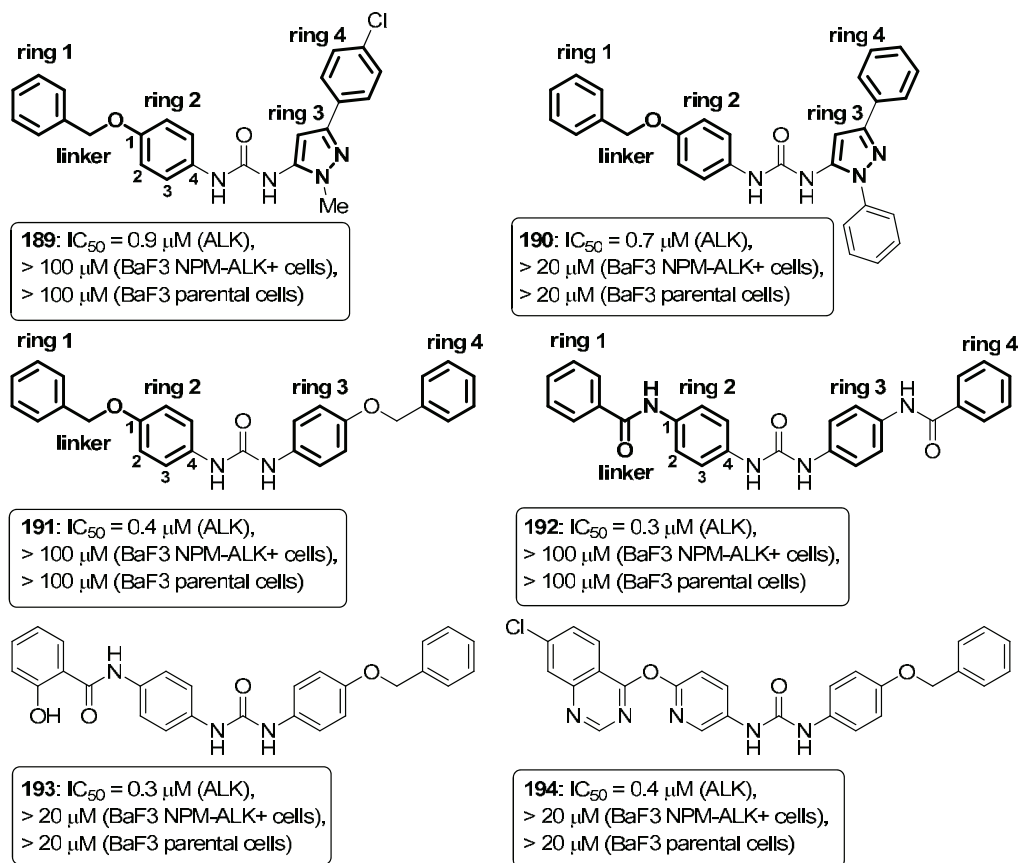


**Figure 50** Lead templates (**189-194**) discovered by virtual screening.  $IC_{50}$  values of ALK, BaF3 NPM-ALK+ cells and BaF3 parental cells are shown.

Figure 51 shows three methods used in the synthesis of nonsymmetric ureas (**197**). Method A was used in the cases when the isocyanate (**195**) and the amine (**196**) were commercially available. However, in other cases we explored various urea formation methods. Method B represents urea formation by the reaction of phosgene (**199**) with an aniline (**198**) and subsequent

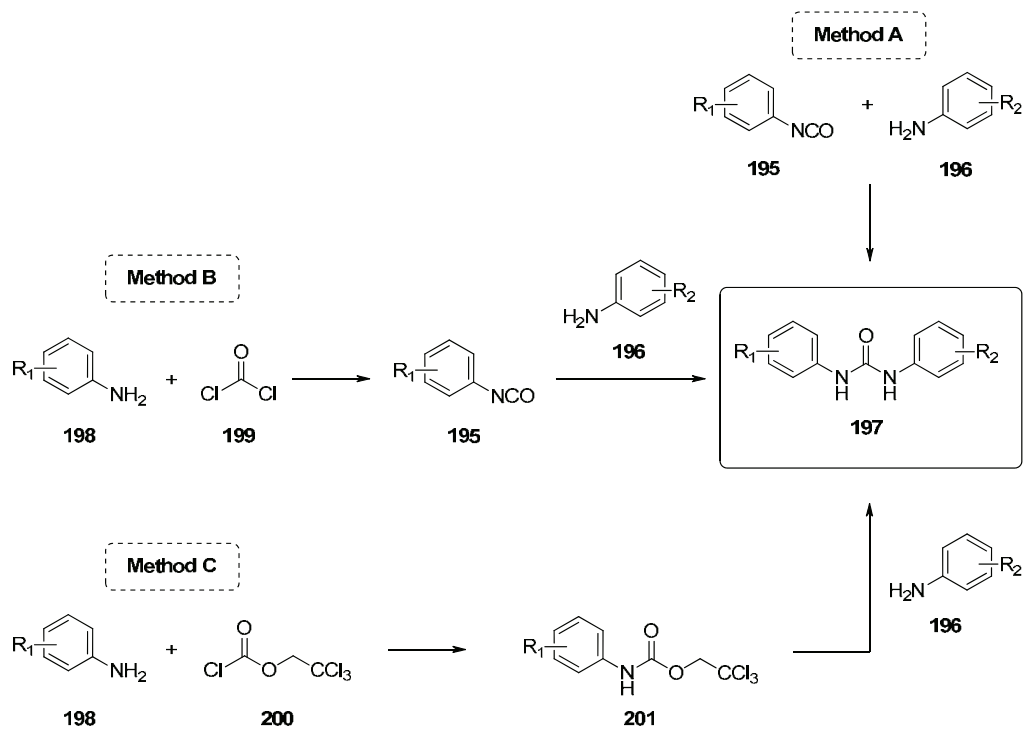


**Figure 51** Methods used in the synthesis of the nonsymmetric ureas presented in this investigation.

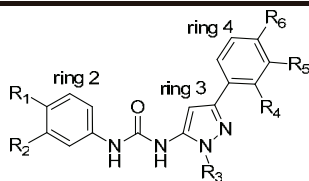
condensation of the other aniline (**196**). However, this method was found to give low yields of the desired products and required extensive purification.<sup>IV</sup> In method C the amine (**198**) is activated as the 2,2,2-trichloroethylcarbamate (**201**) followed by condensation of the second amine (**196**) to yield the urea (**197**). This method proved to be convenient since the carbamates were stable, easily isolable and yielded the desired ureas after subsequent microwave irradiation of the second amines.<sup>IV</sup> Therefore, method C was used in the syntheses of most of the ureas where commercially available isocyanates were not available. The reaction conditions presented in original publication **IV** were not systematically optimized since more emphasis was put on producing derivatives than optimizing reaction yields. The rest of the methods used in the syntheses of the compounds can be found in the original publication **IV**.

The IC<sub>50</sub> values of ureas **189** and **202-204** showed that a *para* chlorine at ring 4 of the lead template **189** was the best substituent at this position of the tested ones (chlorine, methyl, methoxy and hydrogen, Table 2, see lead template **189** in Figure 50 for the atom numbering). Even though a methoxy group at the *para* position (compound **204**) led to a slightly decreased binding potency, it remarkably enhanced (by > 20 times) the cellular activity. Interestingly, compound **205**, which otherwise has the same structure as urea **204** but the methyl of the



pyrazole ring (ring 3) is missing, did not show any cellular activity. In compound **206** the *para* chlorine at ring 4 was kept and another chlorine was inserted at C2 of ring 2 to potentially create an interaction with the gatekeeper residue Leu1196 (see Figure 30). Again, good cellular activity could be obtained but the IC<sub>50</sub> value of the isolated enzyme slightly increased. The slightly increased value may be due to the protein having to undergo a small conformational change to get the chlorine of **206** to fit or then ring 2 has to undergo a small tilt. By moving the C2 chlorine of ring 2 in **206** to the *para* position of ring 1 (compound **207**), the inhibition activity improved, however, no cellular activity was obtained. In urea **208**, the *para* chlorine of ring 4 was moved to the *meta* position. Although this small structural difference, compared to lead template **189**, did not improve the inhibition of enzyme activity, it remarkably improved the cellular activity by more than 70 times. In lead compound **190**, the *para* chlorine found in **189** is missing, however, the enzymatic activity of **190** is better than that of **189** (IC<sub>50</sub> of 0.7 and 0.9 μM, respectively).

**Table 2.** IC<sub>50</sub> values of the pyrazolyl urea derivatives **189**, **190** and **202-214** determined in cell-free assays using purified recombinant ALK kinase and in cell proliferation. The values are expressed as the mean ± sem (n = 3).



Cmpd	R <sub>1</sub>	R <sub>2</sub>	R <sub>3</sub>	R <sub>4</sub>	R <sub>5</sub>	R <sub>6</sub>	ALK IC <sub>50</sub> (μM)	BaF3 Parental IC <sub>50</sub> (μM)	BaF3 NPM-ALK IC <sub>50</sub> (μM)
<b>189</b>	BnO	H	Me	H	H	Cl	0.87 ± 0.11	> 100	> 100
<b>190</b>	BnO	H	Ph	H	H	H	0.71 ± 0.02	> 20	> 20
<b>202</b>	BnO	H	Me	H	H	H	2.3 ± 0.3	74 ± 4	49 ± 3
<b>203</b>	BnO	H	Me	H	H	Me	4.3 ± 1.9	> 100	> 100
<b>204</b>	BnO	H	Me	H	H	OMe	4.5 ± 1.2	4.1 ± 0.1	4.6 ± 1.1
<b>205</b>	BnO	H	H	H	H	OMe	1.8 ± 0.5	> 100	> 100
<b>206</b>	BnO	Cl	Me	H	H	Cl	2.6 ± 0.2	3.1 ± 1.4	1.8 ± 1.4
<b>207</b>	4-Cl-BnO	H	Me	H	H	Cl	0.79 ± 0.07	> 100	> 100
<b>208</b>	BnO	H	Me	H	Cl	H	0.82 ± 0.03	3.0 ± 0.6	1.4 ± 0.1
<b>209</b>	BnO	H	Ph	H	H	Cl	1.7 ± 0.1	8.4 ± 2.2	1.4 ± 0.4
<b>210</b>	BnO	H	Ph	Cl	H	H	0.61 ± 0.28	5.4 ± 1.5	0.70 ± 0.22
<b>211</b>	PhO	H	Me	H	H	Cl	2.5 ± 0.05	16 ± 7	5 ± 2
<b>212</b>	PhCO	H	Me	H	H	Cl	4.1 ± 2.1	0.6 ± 0.04	2.6 ± 0.4
<b>213</b>	H	Bn	Me	H	H	Cl	2.3 ± 0.8	25 ± 3	32 ± 2
<b>214</b> <sup>a</sup>	[5-(4-Cl-Ph)-2-Me-2H-pyrazol-3-yl] <sub>2</sub> CO						0.87 ± 0.11	> 100	> 100

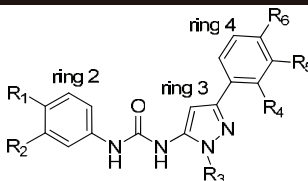
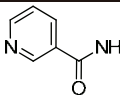
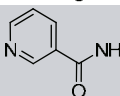
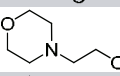
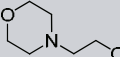
<sup>a</sup> Compound **214** is a C<sub>2</sub>-symmetric urea.

Since compound **189** showed a better  $IC_{50}$  than **202** and it has a chlorine in the *para* position of ring 4, the incorporation of a *para* chlorine into ring 4 of the lead compound **190** was pursued. However, the urea **209** showed a decrease in enzymatic activity but a good cellular activity with an increased specificity. Interestingly, when the chlorine in ring 4 was moved from the *para* position of **209** to the *ortho* position of **210**, the enzymatic ( $IC_{50}$  of 0.61  $\mu$ M) and the cellular activity, ( $IC_{50}$  of 0.70  $\mu$ M of BaF3 NPM-ALK-positive cells) as well as the specificity increased ( $IC_{50}$  of 5.4  $\mu$ M for parental BaF3 cells). Results from proliferation and apoptosis assays further illustrated the anti-tumor effects of compound **210**. The  $IC_{50}$  value for the human ALCL-derived cell line SU-DHL-1 (NPM-ALK-positive) was 0.8  $\mu$ M and it induced apoptosis in the same cell line. In contrast to the NPM-ALK-positive cells, compound **210** was significantly less toxic to the NPM-ALK-negative human leukemic cells U937. The obtained  $IC_{50}$  value was only 3.2  $\mu$ M.

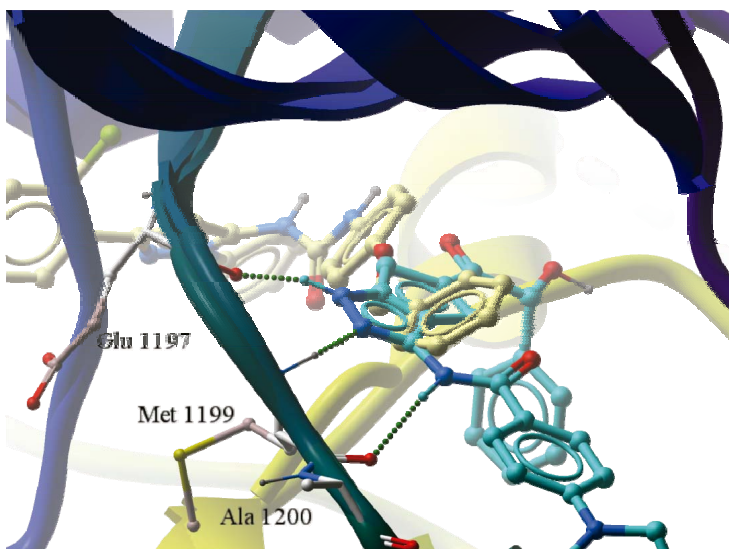
Compounds **211** and **212** were designed to investigate how a shorter linker of the lead template **189** would affect activity. Both compounds showed an increased cellular activity, however, the enzymatic activity decreased. Urea **213**, with a benzyl substituent at C2, also showed a slight decrease in binding affinity, apparently for the same reason as compound **206** (*vide supra*). However, **213** showed worse cellular activity than **206**.

Compounds **215-218** were designed and synthesized in an attempt to establish a hydrogen bond in the hinge region of ALK (Table 3). The nitrogen of the pyridine ring in **215** and **216**, and

**Table 3.**  $IC_{50}$  values of pyrazolyl urea derivatives **215-218** determined in cell-free assays using purified recombinant ALK kinase and in cell proliferation. The values are expressed as the mean  $\pm$  sem ( $n = 3$ ).

Cmpd							ALK	BaF3	BaF3
	R <sub>1</sub>	R <sub>2</sub>	R <sub>3</sub>	R <sub>4</sub>	R <sub>5</sub>	R <sub>6</sub>	$IC_{50}$ ( $\mu$ M)	Parental $IC_{50}$ ( $\mu$ M)	NPM-ALK $IC_{50}$ ( $\mu$ M)
<b>215</b>		H	Me	H	H	Cl	15 $\pm$ 2	0.14 $\pm$ 0.05	0.38 $\pm$ 0.04
<b>216</b>		H	Me	H	H	H	> 100	3.5 $\pm$ 0.2	7.1 $\pm$ 1.1
<b>217</b>		H	Me	H	H	H	> 100	22 $\pm$ 7	27 $\pm$ 7
<b>218</b>		H	Me	H	H	Cl	41 $\pm$ 2	5.0 $\pm$ 1.0	3.2 $\pm$ 1.3

the oxygen in the morpholino group of **217** and **218** were suggested by modeling to form the same kind of hydrogen bond with Met1199 of the backbone as can be obtained for PHA-E429 (**72**) in the crystal structure of ALK, for example (Figure 52). However, compounds **215-218** showed weak binding to ALK but may target some other kinases in the cells, particularly **215**, which showed high cellular activity ( $IC_{50}$  of 0.14  $\mu\text{M}$  for parental BaF3 cells). Interestingly, the cellular activity of urea **215**, with a *para* chlorine in ring 4, was 25 times higher than for urea **216**, which has an unsubstituted ring 4.

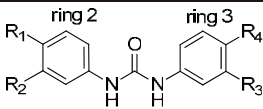
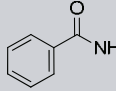
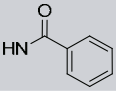
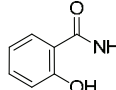
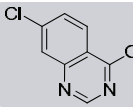
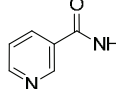
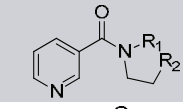
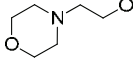
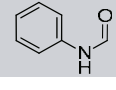


**Figure 52** An enlargement of compound **210** docked into the kinase domain of the homology model of ALK superimposed on the crystal structure of ALK in complex with PHA-E429 (**72**) (PDB ID: 2XBA).<sup>281</sup> The compounds are presented in ball and stick representations and colored by atom type; carbons (**210**: beige and PHA-E429 (**72**): turquoise), nitrogens (blue), oxygens (red) and chlorines (light green). The Glu1197, Met1199 and Ala1200 residues of the hinge region are shown in ball and sticks and are colored by atom type. Hydrogen bonds between the hinge region residues and PHA-E429 (**72**) are denoted with green spheres. The figure was created using ICM Molsoft software 3.7.

The lead templates **191-192** were also modified in an attempt to increase their enzymatic and cellular activities. Noticeably, from the initial screening results of these candidates, the amide groups of **192** were not involved in hydrogen bonding to the protein as the  $IC_{50}$  values of **191** and **192** were similar (0.4 and 0.3  $\mu\text{M}$ , respectively). Therefore, in a similar way as the modifications done for lead templates **189-190**, the possibility of forming hydrogen bonds to the hinge region by adding a hydrogen acceptor group to the ring 1 of **191** and **192** was investigated. However, compounds **219-221** showed a slightly decreased binding affinity for ALK compared to lead templates **191** and **192** (Table 4). Compounds **223-225** were synthesized and tested for binding affinity in an attempt to find additional interactions with the gatekeeper Leu1196 or to

investigate the required linker length of the compounds. Again, the enzymatic activities could not be improved but the cellular activities increased for compounds **224** and **225**. It is hard to speculate on the binding modes of these compounds since the structures and the relative symmetry of the compounds allows them to bind in several ways. In conclusion, the enzymatic activity could not be improved; however, the cellular activity was increased significantly.

**Table 4.** *IC<sub>50</sub> values of phenyl urea derivatives 191-194 and 219-225 determined using purified ALK kinase domain and the effects of these compounds on cell proliferation. The values are expressed as the mean ± sem (n = 3).*

Cmpd					ALK IC <sub>50</sub> (μM)	BaF3 Parental IC <sub>50</sub> (μM)	BaF3 NPM-ALK IC <sub>50</sub> (μM)
	R <sub>1</sub>	R <sub>2</sub>	R <sub>3</sub>	R <sub>4</sub>			
<b>191</b>	BnO	H	H	OBn	0.44 ± 0.08	> 100	> 100
<b>192</b>		H	H		0.3 ± 0.03	> 100	> 100
<b>193</b>		H	H	OBn	0.26 ± 0.09	> 20	> 20
<b>194<sup>a</sup></b>		-	H	OBn	0.38 ± 0.08	> 20	> 20
<b>219</b>		H	H	OBn	0.80 ± 0.12	61 ± 13	42 ± 5
<b>220</b>		H	H	OBn	3.6 ± 0.7	> 100	86 ± 1
<b>221</b>		H	H	OBn	8.9 ± 3.2	> 100	> 100
<b>222</b>		H	H	OBn	0.39 ± 0.1	> 100	> 100
<b>223</b>	BnO	Cl	Cl	OBn	1.7 ± 0.2	44 ± 6	50 ± 8
<b>224</b>	PhO	H	H	OBn	5.0 ± 0.2	10 ± 5	1.5 ± 0.9
<b>225</b>	H	Bn	H	OBn-4-Cl	2.0 ± 0.4	7.1 ± 0.2	11 ± 1

<sup>a</sup> Compound **194** has a 6-[(7-chloroquinazolin-4-yl)oxy]pyridin-3-yl ring as ring 2, see Figure 50.

## 6 Summary and conclusions

A totally new class of compounds binding the regulatory domain of PKC was identified in this study. The set of 31 dialkyl 5-(hydroxymethyl)isophthalates presented here were conveniently synthesized in only four steps and with overall yields of 8-78%. The compounds were shown to displace radioactively labeled [ $^3\text{H}$ ]PDBu from PKC $\alpha$  and PKC $\delta$  in a concentration-dependent manner, thus providing evidence that they target the C1 domain. The best compounds (**114**, **128**, and **129**, with 3-(trifluoromethyl)benzyl, 3-hexyl and 3-heptyl ester groups, respectively) showed  $K_i$  values in the 200-900 nM range. Comparing the  $K_i$  values obtained between PKC $\alpha$  and PKC $\delta$  there was a modest selectivity in the binding affinities for PKC $\alpha$ . However, compound **114** was able to displace a substantially smaller proportion of [ $^3\text{H}$ ]PDBu from PKC $\alpha$  than from PKC $\delta$ . SAR studies of the synthesized compounds demonstrated not only the important functional groups for binding to the C1 domain, but also that modifications of these groups diminished binding activity. Interestingly, while derivatives **114** and **128** induced PKC-dependent ERK phosphorylation in HeLa cells, compound **129**, structurally different from **128** only by one carbon in the side chains, was unable to induce ERK phosphorylation. Instead, derivative **129** inhibited phorbol-induced ERK phosphorylation. The reason why the isophthalates **114** and **128** functioned as PKC agonists but the very similar analog **129** as an antagonist remained unclear.

Derivatives **114** and **119** (with 3-(trifluoromethyl)benzyl and 1-hexyl ester groups, respectively) were shown to induce apoptosis already during the first two hours in HL-60 leukemia cells while they were not cytotoxic or mutagenic in Swiss 3T3 fibroblasts. Future work should focus on the pharmacology of these ligands, making them more drug-like. Emphasis should be put on improving the binding affinity and the specificity among C1 domain containing proteins.

In this study the total syntheses of the natural compound bistramide A (**30**) and the new 36(*Z*)-39(*R*) (**187**) and 36(*Z*)-39(*S*) (**188**) isomers of bistramide A were finished in co-operation between three laboratories. The central fragment (**173**) of bistramide A (**30**) prepared in this investigation was successfully performed in seven steps with an overall yield of 21%. The synthesis route of the central fragment (**173**) relied on an asymmetric crotyltitanation, allowing us to avoid the use of highly volatile *trans*-2-butene used in the Kozmin route. The highly face-selective crotyltitanium complex (**181**) used in the introduction of the right stereochemistry of the central fragment (**173**) was found to work well in this reaction.

The overall antiproliferative activities of the isomers were shown to be similar, however, each compound showed a distinct distribution of antimetabolic effect, proapoptotic effect, and pro-differentiation effect. Accumulation of 4n polyploid cells was confirmed to represent the primary mode of action for the antiproliferative effect of bistramide A (**30**). In addition, it was shown that the antimetabolic and proapoptotic effects of bistramide A (**30**) were independent effects and not secondary to actin binding. However, whether the induction of differentiation is dependent or independent of actin binding remains to be seen.

A third aim in this study was to design and synthesize a new class of type II inhibitors targeted at the kinase domain of ALK. Most of the compounds were conveniently prepared in only one reaction step using commercially available isocyanates and amines. In addition, urea formation was performed by activating one of the amines and subsequent condensation of the other. Of the activation methods investigated, activating the amines as 2,2,2-trichloroethylcarbamates was found to be the superior method, since the carbamates were isolable and cleanly yielded the desired ureas with the second amines after subsequent microwave irradiation.

The set of twenty-five 1,3-disubstituted ureas presented here showed  $IC_{50}$  values as low as 390 nM and, more importantly, selective antiproliferative activity on ALK-positive cells was achieved. The best inhibitor (**210**) inhibited the cell growth of ALK-positive cell lines BaF3 (NPM-ALK-positive) and SU-DHL-1 with  $IC_{50}$  values of 0.6 and 0.8  $\mu$ M, respectively. The compound **210** was less toxic to the NPM-ALK-negative human leukemic cells U937 ( $IC_{50}$  = 3.2  $\mu$ M) and BaF3 parental cells ( $IC_{50}$  = 5.4  $\mu$ M). SAR studies of the synthesized compounds revealed functional groups and positions of the scaffold, which enhanced the enzymatic and cellular activities. Even though these inhibitors were modeled to mainly bind outside the ATP-binding pocket, attempts to create interactions with the hinge region of these type II inhibitors did not succeed. Indeed, future inhibitors should be designed to explore possible interactions with the hinge region and also to improve the drug-like properties.

Unfortunately, the results of this study do not resolve the cancer problem. However, the more realistic aims were to contribute new knowledge into the field. Even though the achieved binding affinities of the PKC regulatory domain-targeted compounds presented in this study were not in the low nanomolar range, which some natural compounds display, the compounds are widely sought new chemical entities of the C1 domain. As there are no clinically available C1 domain-targeted drugs on the market and natural compounds are generally laborious to prepare, the newly synthesized compounds as well as the SAR information provided by this investigation may be useful in the future for researchers developing potential cancer drugs. Analogues of prostratin, bryostatins, aplysiatoxin, indo- and benzolactams and DAG-lactones may be among these.

The results from the other kinase studied, ALK, are very promising since we were able to develop an inhibitor with submicromolar in vitro activity, growth inhibitory activity on cancer cell lines as well as selectivity of 10-fold in favor of BaF3 NPM-ALK-positive cells compared to BaF3 parental cells. In addition, since the inhibitors were designed to target the inactive conformation of the catalytic domain of ALK, they may prove to show selectivity among other enzymes. However, this remains to be seen.

## 7 References

1. Manning, G.; Whyte, D. B.; Martinez, R.; Hunter, T.; Sudarsanam, S. The protein kinase complement of the human genome. *Science* **2002**, *298*, 1912-1934.
2. Matthews, D. A.; Gerritsen, M. E. 1.2 Kinases and Cancer. In *Targeting Protein Kinases for Cancer Therapy*; John Wiley & Sons, Inc.: New Jersey, USA, **2010**; 3-8.
3. Finnish Cancer Registry *Cancer in Finland 2006 and 2007*. *Cancer Society of Finland Publication Helsinki*; **2009**; 76.
4. American Cancer Society *Cancer Facts & Figures 2010*. *Atlanta: American Cancer Society*; **2010**; 1-66.
5. Takai, Y.; Kishimoto, A.; Inoue, M.; Nishizuka, Y. Studies on a cyclic nucleotide-independent protein kinase and its proenzyme in mammalian tissues. I. Purification and characterization of an active enzyme from bovine cerebellum. *J. Biol. Chem.* **1977**, *252*, 7603-7609.
6. Inoue, M.; Kishimoto, A.; Takai, Y.; Nishizuka, Y. Studies on a cyclic nucleotide-independent protein kinase and its proenzyme in mammalian tissues. II. Proenzyme and its activation by calcium-dependent protease from rat brain. *J. Biol. Chem.* **1977**, *252*, 7610-7616.
7. Takai, Y.; Kishimoto, A.; Iwasa, Y.; Kawahara, Y.; Mori, T.; Nishizuka, Y. Calcium-dependent activation of a multifunctional protein kinase by membrane phospholipids. *J. Biol. Chem.* **1979**, *254*, 3692-3695.
8. Takai, Y.; Kishimoto, A.; Kikkawa, U.; Mori, T.; Nishizuka, Y. Unsaturated diacylglycerol as a possible messenger for the activation of calcium-activated, phospholipid-dependent protein kinase system. *Biochem. Biophys. Res. Commun.* **1979**, *91*, 1218-1224.
9. Nishizuka, Y. The role of protein kinase C in cell surface signal transduction and tumour promotion. *Nature* **1984**, *308*, 693-698.
10. Hofmann, J. Protein kinase C isozymes as potential targets for anticancer therapy. *Curr. Cancer. Drug Targets* **2004**, *4*, 125-146.
11. Griner, E. M.; Kazanietz, M. G. Protein kinase C and other diacylglycerol effectors in cancer. *Nat. Rev. Cancer.* **2007**, *7*, 281-294.
12. Battaini, F. Protein kinase C isoforms as therapeutic targets in nervous system disease states. *Pharmacol. Res.* **2001**, *44*, 353-361.
13. Pascale, A.; Amadio, M.; Govoni, S.; Battaini, F. The aging brain, a key target for the future: the protein kinase C involvement. *Pharmacol. Res.* **2007**, *55*, 560-569.
14. Olariu, A.; Yamada, K.; Nabeshima, T. Amyloid pathology and protein kinase C (PKC): possible therapeutic effects of PKC activators. *J. Pharmacol. Sci.* **2005**, *97*, 1-5.
15. Alkon, D. L.; Sun, M. K.; Nelson, T. J. PKC signaling deficits: a mechanistic hypothesis for the origins of Alzheimer's disease. *Trends Pharmacol. Sci.* **2007**, *28*, 51-60.
16. Baier, G.; Wagner, J. PKC inhibitors: potential in T cell-dependent immune diseases. *Curr. Opin. Cell Biol.* **2009**, *21*, 262-267.
17. Hayashi, K.; Altman, A. Protein kinase C theta (PKC $\theta$ ): a key player in T cell life and death. *Pharmacol. Res.* **2007**, *55*, 537-544.
18. Sabri, A.; Steinberg, S. F. Protein kinase C isoform-selective signals that lead to cardiac hypertrophy and the progression of heart failure. *Mol. Cell. Biochem.* **2003**, *251*, 97-101.
19. Churchill, E.; Budas, G.; Vallentin, A.; Koyanagi, T.; Mochly-Rosen, D. PKC isozymes in chronic cardiac disease: possible therapeutic targets? *Annu. Rev. Pharmacol. Toxicol.* **2008**, *48*, 569-599.
20. Chou, W. H.; Messing, R. O. Protein kinase C isozymes in stroke. *Trends Cardiovasc. Med.* **2005**, *15*, 47-51.

21. Jirousek, M. R.; Gillig, J. R.; Gonzalez, C. M.; Heath, W. F.; McDonald, J. H.,3rd; Neel, D. A.; Rito, C. J.; Singh, U.; Stramm, L. E.; Melikian-Badalian, A.; Baevsky, M.; Ballas, L. M.; Hall, S. E.; Winneroski, L. L.; Faul, M. M. (*S*)-13-[(Dimethylamino)methyl]-10,11,14,15-tetrahydro-4,9:16, 21-dimetheno-1*H*, 13*H*-dibenzo[*e,k*]pyrrolo[3,4-*h*][1,4,13]oxadiazacyclohexadecene-1,3(2*H*)-dione (LY333531) and related analogues: isozyme selective inhibitors of protein kinase C  $\beta$ . *J. Med. Chem.* **1996**, *39*, 2664-2671.
22. Faul, M. M.; Gillig, J. R.; Jirousek, M. R.; Ballas, L. M.; Schotten, T.; Kahl, A.; Mohr, M. Acyclic N-(azacycloalkyl)bisindolylmaleimides: isozyme selective inhibitors of PKC $\beta$ . *Bioorg. Med. Chem. Lett.* **2003**, *13*, 1857-1859.
23. Clarke, M.; Dodson, P. M. PKC inhibition and diabetic microvascular complications. *Best Pract. Res. Clin. Endocrinol. Metab.* **2007**, *21*, 573-586.
24. Herbst, R. S.; Oh, Y.; Wagle, A.; Lahn, M. Enzastaurin, a protein kinase C $\beta$ -selective inhibitor, and its potential application as an anticancer agent in lung cancer. *Clin. Cancer Res.* **2007**, *13*, 4641-4646.
25. Fischer, P.; Nacheva, E.; Mason, D. Y.; Sherrington, P. D.; Hoyle, C.; Hayhoe, F. G.; Karpas, A. A Ki-1 (CD30)-positive human cell line (Karpas 299) established from a high-grade non-Hodgkin's lymphoma, showing a 2;5 translocation and rearrangement of the T-cell receptor beta-chain gene. *Blood* **1988**, *72*, 234-240.
26. Benz-Lemoine, E.; Brizard, A.; Huret, J. L.; Babin, P.; Guilhot, F.; Couet, D.; Tanzer, J. Malignant histiocytosis: a specific t(2;5)(p23;q35) translocation? Review of the literature. *Blood* **1988**, *72*, 1045-1047.
27. Morris, S. W.; Kirstein, M. N.; Valentine, M. B.; Dittmer, K. G.; Shapiro, D. N.; Saltman, D. L.; Look, A. T. Fusion of a kinase gene, ALK, to a nucleolar protein gene, NPM, in non-Hodgkin's lymphoma. *Science* **1994**, *263*, 1281-1284.
28. Shiota, M.; Fujimoto, J.; Semba, T.; Satoh, H.; Yamamoto, T.; Mori, S. Hyperphosphorylation of a novel 80 kDa protein tyrosine kinase similar to Ltk in a human Ki-1 lymphoma cell line, AMS3. *Oncogene* **1994**, *9*, 1567-1574.
29. Ardini, E.; Magnaghi, P.; Orsini, P.; Galvani, A.; Menichincheri, M. Anaplastic Lymphoma Kinase: Role in specific tumours, and development of small molecule inhibitors for cancer therapy. *Cancer Lett.* **2010**, *299*, 81-94.
30. Iwahara, T.; Fujimoto, J.; Wen, D.; Cupples, R.; Bucay, N.; Arakawa, T.; Mori, S.; Ratzkin, B.; Yamamoto, T. Molecular characterization of ALK, a receptor tyrosine kinase expressed specifically in the nervous system. *Oncogene* **1997**, *14*, 439-449.
31. Chiarle, R.; Voena, C.; Ambrogio, C.; Piva, R.; Inghirami, G. The anaplastic lymphoma kinase in the pathogenesis of cancer. *Nat. Rev. Cancer.* **2008**, *8*, 11-23.
32. Drexler, H. G.; Gignac, S. M.; von Wasielewski, R.; Werner, M.; Dirks, W. G. Pathobiology of NPM-ALK and variant fusion genes in anaplastic large cell lymphoma and other lymphomas. *Leukemia* **2000**, *14*, 1533-1559.
33. US National Institutes of Health. Clinicaltrials.gov. <http://clinicaltrials.gov/> (accessed September, 2010).
34. Zhang, S.; Wang, F.; Keats, J.; Ning, Y.; Wardwell, S. D.; Moran, L.; Mohemmad, Q. K.; Ye, E.; Anjum, R.; Wang, Y.; Zhu, X.; Miret, J. J.; Dalgarno, D.; Narasimhan, N. I.; Clackson, T.; Shakespeare, W. C.; Rivera, V. M. AP26113, a potent ALK inhibitor, overcomes mutations in EML4-ALK that confer resistance to PF-02341066. *AACR (Annual Meeting)* **2010**.
35. Getlik, M.; Grutter, C.; Simard, J. R.; Kluter, S.; Rabiller, M.; Rode, H. B.; Robubi, A.; Rauh, D. Hybrid compound design to overcome the gatekeeper T338M mutation in cSrc. *J. Med. Chem.* **2009**, *52*, 3915-3926.
36. Simard, J. R.; Kluter, S.; Grutter, C.; Getlik, M.; Rabiller, M.; Rode, H. B.; Rauh, D. A new screening assay for allosteric inhibitors of cSrc. *Nat. Chem. Biol.* **2009**, *5*, 394-396.



37. Alton, G. R.; Lunney, E. A. Targeting the unactivated conformations of protein kinases for small molecule drug discovery. *Expert Opin. Drug Discov.* **2008**, *3*, 595-605.
38. Matthews, D. A.; Gerritsen, M. E. 1.1 A Brief History of Protein Phosphorylation. In *Targeting Protein Kinases for Cancer Therapy*; John Wiley & Sons, Inc.: New Jersey, USA, **2010**; 1-3.
39. Matthews, D. A.; Gerritsen, M. E. 2.3 Catalytic Activity of Protein Kinases. In *Targeting Protein Kinases for Cancer Therapy*; John Wiley & Sons, Inc.: New Jersey, USA, **2010**; 87-91.
40. Ubersax, J. A.; Ferrell, J. E. Mechanisms of specificity in protein phosphorylation. *Nat. Rev. Mol. Cell Biol.* **2007**, *8*, 530-541.
41. Steinberg, S. F. Structural basis of protein kinase C isoform function. *Physiol. Rev.* **2008**, *88*, 1341-1378.
42. Valiev, M.; Yang, J.; Adams, J. A.; Taylor, S. S.; Weare, J. H. Phosphorylation reaction in cAPK protein kinase-free energy quantum mechanical/molecular mechanics simulations. *J. Phys. Chem. B* **2007**, *111*, 13455-13464.
43. Madhusudan; Trafny, E. A.; Xuong, N. H.; Adams, J. A.; Ten Eyck, L. F.; Taylor, S. S.; Sowadski, J. M. cAMP-dependent protein kinase: crystallographic insights into substrate recognition and phosphotransfer. *Protein Sci.* **1994**, *3*, 176-187.
44. Adams, J. A.; Taylor, S. S. Phosphorylation of peptide substrates for the catalytic subunit of cAMP-dependent protein kinase. *J. Biol. Chem.* **1993**, *268*, 7747-7752.
45. Zheng, J.; Trafny, E. A.; Knighton, D. R.; Xuong, N. H.; Taylor, S. S.; Ten Eyck, L. F.; Sowadski, J. M. 2.2 A refined crystal structure of the catalytic subunit of cAMP-dependent protein kinase complexed with MnATP and a peptide inhibitor. *Acta Crystallogr. D Biol. Crystallogr.* **1993**, *49*, 362-365.
46. Nishizuka, Y. Protein kinase C and lipid signaling for sustained cellular responses. *FASEB J.* **1995**, *9*, 484-496.
47. Newton, A. C.; Keranen, L. M. Phosphatidyl-L-serine is necessary for protein kinase C's high-affinity interaction with diacylglycerol-containing membranes. *Biochemistry* **1994**, *33*, 6651-6658.
48. Nishizuka, Y. Intracellular signaling by hydrolysis of phospholipids and activation of protein kinase C. *Science* **1992**, *258*, 607-614.
49. Oude Weernink, P. A.; Han, L.; Jakobs, K. H.; Schmidt, M. Dynamic phospholipid signaling by G protein-coupled receptors. *Biochim. Biophys. Acta* **2007**, *1768*, 888-900.
50. Rhee, S. G. Regulation of phosphoinositide-specific phospholipase C. *Annu. Rev. Biochem.* **2001**, *70*, 281-312.
51. Meyer-Bertenrath, J. G. 150 Years of croton oil research. *Experientia* **1969**, *25*, 1-5.
52. Castagna, M.; Takai, Y.; Kaibuchi, K.; Sano, K.; Kikkawa, U.; Nishizuka, Y. Direct activation of calcium-activated, phospholipid-dependent protein kinase by tumor-promoting phorbol esters. *J. Biol. Chem.* **1982**, *257*, 7847-7851.
53. Kraft, A. S.; Anderson, W. B.; Cooper, H. L.; Sando, J. J. Decrease in cytosolic calcium/phospholipid-dependent protein kinase activity following phorbol ester treatment of EL4 thymoma cells. *J. Biol. Chem.* **1982**, *257*, 13193-13196.
54. Ashendel, C. L. The phorbol ester receptor: a phospholipid-regulated protein kinase. *Biochim. Biophys. Acta* **1985**, *822*, 219-242.
55. Cho, W. Membrane targeting by C1 and C2 domains. *J. Biol. Chem.* **2001**, *276*, 32407-32410.
56. Wang, Q. J.; Bhattacharyya, D.; Garfield, S.; Nacro, K.; Marquez, V. E.; Blumberg, P. M. Differential localization of protein kinase C  $\delta$  by phorbol esters and related compounds using a fusion protein with green fluorescent protein. *J. Biol. Chem.* **1999**, *274*, 37233-37239.

57. Hu, T.; Exton, J. H. Protein kinase C $\alpha$  translocates to the perinuclear region to activate phospholipase D1. *J. Biol. Chem.* **2004**, *279*, 35702-35708.
58. Kashiwagi, K.; Shirai, Y.; Kuriyama, M.; Sakai, N.; Saito, N. Importance of C1B domain for lipid messenger-induced targeting of protein kinase C. *J. Biol. Chem.* **2002**, *277*, 18037-18045.
59. Duan, D.; Sigano, D. M.; Kelley, J. A.; Lai, C. C.; Lewin, N. E.; Kedei, N.; Peach, M. L.; Lee, J.; Abeyweera, T. P.; Rotenberg, S. A.; Kim, H.; Kim, Y. H.; El Kazzouli, S.; Chung, J. U.; Young, H. A.; Young, M. R.; Baker, A.; Colburn, N. H.; Haimovitz-Friedman, A.; Truman, J. P.; Parrish, D. A.; Deschamps, J. R.; Perry, N. A.; Surawski, R. J.; Blumberg, P. M.; Marquez, V. E. Conformationally constrained analogues of diacylglycerol. 29. Cells sort diacylglycerol-lactone chemical zip codes to produce diverse and selective biological activities. *J. Med. Chem.* **2008**, *51*, 5198-5220.
60. Blumberg, P. M.; Kedei, N.; Lewin, N. E.; Yang, D.; Czifra, G.; Pu, Y.; Peach, M. L.; Marquez, V. E. Wealth of opportunity - the C1 domain as a target for drug development. *Curr. Drug Targets* **2008**, *9*, 641-652.
61. Budas, G. R.; Churchill, E. N.; Mochly-Rosen, D. Cardioprotective mechanisms of PKC isozyme-selective activators and inhibitors in the treatment of ischemia-reperfusion injury. *Pharmacol. Res.* **2007**, *55*, 523-536.
62. Newton, A. C. Protein kinase C: structural and spatial regulation by phosphorylation, cofactors, and macromolecular interactions. *Chem. Rev.* **2001**, *101*, 2353-2364.
63. Tsutakawa, S. E.; Medzihradsky, K. F.; Flint, A. J.; Burlingame, A. L.; Koshland, D. E., Jr Determination of in vivo phosphorylation sites in protein kinase C. *J. Biol. Chem.* **1995**, *270*, 26807-26812.
64. Keranen, L. M.; Dutil, E. M.; Newton, A. C. Protein kinase C is regulated in vivo by three functionally distinct phosphorylations. *Curr. Biol.* **1995**, *5*, 1394-1403.
65. Cenni, V.; Doppler, H.; Sonnenburg, E. D.; Maraldi, N.; Newton, A. C.; Toker, A. Regulation of novel protein kinase C  $\epsilon$  by phosphorylation. *Biochem. J.* **2002**, *363*, 537-545.
66. Parekh, D.; Ziegler, W.; Yonezawa, K.; Hara, K.; Parker, P. J. Mammalian TOR controls one of two kinase pathways acting upon nPKC $\delta$  and nPKC $\epsilon$ . *J. Biol. Chem.* **1999**, *274*, 34758-34764.
67. House, C.; Kemp, B. E. Protein kinase C contains a pseudosubstrate prototope in its regulatory domain. *Science* **1987**, *238*, 1726-1728.
68. Newton, A. C. Regulation of the ABC kinases by phosphorylation: protein kinase C as a paradigm. *Biochem. J.* **2003**, *370*, 361-371.
69. Leonard, T. A.; Rózycki, B.; Saidi, L. F.; Hummer, G.; Hurley, J. H. Crystal Structure and Allosteric Activation of Protein Kinase C  $\beta$ II. *Cell* **2011**, *144*, 55-66.
70. Dutil, E. M.; Keranen, L. M.; DePaoli-Roach, A. A.; Newton, A. C. In vivo regulation of protein kinase C by trans-phosphorylation followed by autophosphorylation. *J. Biol. Chem.* **1994**, *269*, 29359-29362.
71. Hansra, G.; Garcia-Paramio, P.; Prevostel, C.; Whelan, R. D.; Bornancin, F.; Parker, P. J. Multisite dephosphorylation and desensitization of conventional protein kinase C isotypes. *Biochem. J.* **1999**, *342*, 337-344.
72. Prevostel, C.; Alice, V.; Joubert, D.; Parker, P. J. Protein kinase C $\alpha$  actively downregulates through caveolae-dependent traffic to an endosomal compartment. *J. Cell. Sci.* **2000**, *113*, 2575-2584.
73. Lee, H. W.; Smith, L.; Pettit, G. R.; Smith, J. B. Bryostatin 1 and phorbol ester down-modulate protein kinase C- $\alpha$  and - $\epsilon$  via the ubiquitin/proteasome pathway in human fibroblasts. *Mol. Pharmacol.* **1997**, *51*, 439-447.

74. Lu, Z.; Liu, D.; Hornia, A.; Devonish, W.; Pagano, M.; Foster, D. A. Activation of protein kinase C triggers its ubiquitination and degradation. *Mol. Cell. Biol.* **1998**, *18*, 839-845.
75. Gao, T.; Newton, A. C. The turn motif is a phosphorylation switch that regulates the binding of Hsp70 to protein kinase C. *J. Biol. Chem.* **2002**, *277*, 31585-31592.
76. Szallasi, Z.; Bögi, K.; Gohari, S.; Biro, T.; Acs, P.; Blumberg, P. M. Non-equivalent roles for the first and second zinc fingers of protein kinase C $\delta$ . Effect of their mutation on phorbol ester-induced translocation in NIH 3T3 cells. *J. Biol. Chem.* **1996**, *271*, 18299-18301.
77. Bögi, K.; Lorenzo, P. S.; Acs, P.; Szallasi, Z.; Wagner, G. S.; Blumberg, P. M. Comparison of the roles of the C1a and C1b domains of protein kinase C alpha in ligand induced translocation in NIH 3T3 cells. *FEBS Lett.* **1999**, *456*, 27-30.
78. Stahelin, R. V.; Digman, M. A.; Medkova, M.; Ananthanarayanan, B.; Rafter, J. D.; Melowic, H. R.; Cho, W. Mechanism of diacylglycerol-induced membrane targeting and activation of protein kinase C $\delta$ . *J. Biol. Chem.* **2004**, *279*, 29501-29512.
79. Giorgione, J. R.; Lin, J. H.; McCammon, J. A.; Newton, A. C. Increased membrane affinity of the C1 domain of protein kinase C $\delta$  compensates for the lack of involvement of its C2 domain in membrane recruitment. *J. Biol. Chem.* **2006**, *281*, 1660-1669.
80. Dries, D. R.; Gallegos, L. L.; Newton, A. C. A single residue in the C1 domain sensitizes novel protein kinase C isoforms to cellular diacylglycerol production. *J. Biol. Chem.* **2007**, *282*, 826-830.
81. Zhang, G.; Kazanietz, M. G.; Blumberg, P. M.; Hurley, J. H. Crystal structure of the cys2 activator-binding domain of protein kinase C  $\delta$  in complex with phorbol ester. *Cell* **1995**, *81*, 917-924.
82. Xu, R. X.; Pawelczyk, T.; Xia, T. H.; Brown, S. C. NMR structure of a protein kinase C- $\gamma$  phorbol-binding domain and study of protein-lipid micelle interactions. *Biochemistry* **1997**, *36*, 10709-10717.
83. Hommel, U.; Zurini, M.; Luyten, M. Solution structure of a cysteine rich domain of rat protein kinase C. *Nat. Struct. Biol.* **1994**, *1*, 383-387.
84. Lomize, A. L.; Pogozheva, I. D.; Lomize, M. A.; Mosberg, H. I. The role of hydrophobic interactions in positioning of peripheral proteins in membranes. *BMC Struct. Biol.* **2007**, *7*, 44.
85. Sugita, K.; Neville, C. F.; Sodeoka, M.; Sasai, H. and Shibasaki, M. Stereocontrolled Syntheses of Phorbol Analogs and Evaluation of their Binding Affinity to PKC. *Tetrahedron Lett.* **1995**, *36*, 1067-1070.
86. Sodeoka, M.; Uotsu, K. and Shibasaki, M. Photoaffinity Labeling of PKC with a Phorbol Derivative Importance of the 13-Acyl Group in Phorbol Ester-PKC Interaction. *Tetrahedron Lett.* **1995**, *36*, 8795-8798.
87. Kazanietz, M. G.; Barchi, J. J.; Omichinski, J.G. and Blumberg, P.M. Low Affinity Binding of Phorbol Esters to Protein Kinase C and Its Recombinant Cysteine-rich Region in Absence of Phospholipids. *J. Biol. Chem.* **1995**, *270*, 14679-14684.
88. Yeh, E.; Sharkey, N. A.; Blumberg, P. M. Influence of side chains on phorbol ester binding to protein kinase C. *Phytother. Res.* **1987**, *1*, 135-139.
89. Kang, J. H.; Peach, M. L.; Pu, Y.; Lewin, N. E.; Nicklaus, M. C.; Blumberg, P. M.; Marquez, V. E. Conformationally constrained analogues of diacylglycerol (DAG). 25. Exploration of the sn-1 and sn-2 carbonyl functionality reveals the essential role of the sn-1 carbonyl at the lipid interface in the binding of DAG-lactones to protein kinase C. *J. Med. Chem.* **2005**, *48*, 5738-5748.
90. Hritz, J.; Ulicny, J.; Laaksonen, A.; Jancura, D.; Miskovsky, P. Molecular interaction model for the C1B domain of protein kinase C- $\gamma$  in the complex with its activator phorbol-12-myristate-13-acetate in water solution and lipid bilayer. *J. Med. Chem.* **2004**, *47*, 6547-6555.

91. Fischer, S. M.; Patrick, K. E.; Lee, M. L.; Cameron, G. S. 4- $\beta$ - and 4- $\alpha$ -12-O-tetradecanoylphorbol-13-acetate elicit arachidonate release from epidermal cells through different mechanisms. *Cancer Res.* **1991**, *51*, 850-856.
92. Watanabe, H.; Davis, J. B.; Smart, D.; Jerman, J. C.; Smith, G. D.; Hayes, P.; Vriens, J.; Cairns, W.; Wissenbach, U.; Prenen, J.; Flockerzi, V.; Droogmans, G.; Benham, C. D.; Nilius, B. Activation of TRPV4 channels (hVRL-2/mTRP12) by phorbol derivatives. *J. Biol. Chem.* **2002**, *277*, 13569-13577.
93. Klausen, T. K.; Pagani, A.; Minassi, A.; Ech-Chahad, A.; Prenen, J.; Owsianik, G.; Hoffmann, E. K.; Pedersen, S. F.; Appendino, G.; Nilius, B. Modulation of the transient receptor potential vanilloid channel TRPV4 by 4- $\alpha$ -phorbol esters: a structure-activity study. *J. Med. Chem.* **2009**, *52*, 2933-2939.
94. Tanaka, M.; Irie, K.; Nakagawa, Y.; Nakamura, Y.; Ohigashi, H.; Wender, P. A. The C4 hydroxyl group of phorbol esters is not necessary for protein kinase C binding. *Bioorg. Med. Chem. Lett.* **2001**, *11*, 719-722.
95. Takimura, T.; Kamata, K.; Fukasawa, K.; Ohsawa, H.; Komatani, H.; Yoshizumi, T.; Takahashi, I.; Kotani, H.; Iwasawa, Y. Structures of the PKC- $\iota$  kinase domain in its ATP-bound and apo forms reveal defined structures of residues 533-551 in the C-terminal tail and their roles in ATP binding. *Acta Crystallogr. D Biol. Crystallogr.* **2010**, *66*, 577-583.
96. Canagarajah, B.; Leskow, F. C.; Ho, J. Y.; Mischak, H.; Saidi, L. F.; Kazanietz, M. G.; Hurley, J. H. Structural mechanism for lipid activation of the Rac-specific GAP,  $\beta$ 2-chimaerin. *Cell* **2004**, *119*, 407-418.
97. Colon-Gonzalez, F.; Kazanietz, M. G. C1 domains exposed: from diacylglycerol binding to protein-protein interactions. *Biochim. Biophys. Acta* **2006**, *1761*, 827-837.
98. Yang, C.; Kazanietz, M. G. Divergence and complexities in DAG signaling: looking beyond PKC. *Trends Pharmacol. Sci.* **2003**, *24*, 602-608.
99. Parker, P. J.; Coussens, L.; Totty, N.; Rhee, L.; Young, S.; Chen, E.; Stabel, S.; Waterfield, M. D.; Ullrich, A. The complete primary structure of protein kinase C—the major phorbol ester receptor. *Science* **1986**, *233*, 853-859.
100. Boije af Gennäs, G.; Talman, V.; Tuominen, R.; Yli-Kauhaluoma, J.; Ekokoski, E. Recent Developments in Compounds Targeted at the Regulatory Domain of Protein Kinase C. *Curr. Top. Med. Chem.* **2011**, *11*, 1370-1392.
101. Gustafson, K. R.; Cardellina, J. H., 2nd; McMahan, J. B.; Gulakowski, R. J.; Ishitoya, J.; Szallasi, Z.; Lewin, N. E.; Blumberg, P. M.; Weislow, O. S.; Beutler, J. A. A nonpromoting phorbol from the samoan medicinal plant *Homalanthus nutans* inhibits cell killing by HIV-1. *J. Med. Chem.* **1992**, *35*, 1978-1986.
102. Wender, P. A.; Kee, J. M.; Warrington, J. M. Practical synthesis of prostratin, DPP, and their analogs, adjuvant leads against latent HIV. *Science* **2008**, *320*, 649-652.
103. Marquez, N.; Calzado, M. A.; Sanchez-Duffhues, G.; Perez, M.; Minassi, A.; Pagani, A.; Appendino, G.; Diaz, L.; Munoz-Fernandez, M. A.; Munoz, E. Differential effects of phorbol-13-monoesters on human immunodeficiency virus reactivation. *Biochem. Pharmacol.* **2008**, *75*, 1370-1380.
104. Szallasi, Z.; Krausz, K. W.; Blumberg, P. M. Non-promoting 12-deoxyphorbol 13-esters as potent inhibitors of phorbol 12-myristate 13-acetate-induced acute and chronic biological responses in CD-1 mouse skin. *Carcinogenesis* **1992**, *13*, 2161-2167.
105. Gulakowski, R. J.; McMahan, J. B.; Buckheit, R. W., Jr; Gustafson, K. R.; Boyd, M. R. Antireplicative and anticypathic activities of prostratin, a non-tumor-promoting phorbol ester, against human immunodeficiency virus (HIV). *Antiviral Res.* **1997**, *33*, 87-97.
106. Kulkosky, J.; Culnan, D. M.; Roman, J.; Dornadula, G.; Schnell, M.; Boyd, M. R.; Pomerantz, R. J. Prostratin: activation of latent HIV-1 expression suggests a potential inductive adjuvant therapy for HAART. *Blood* **2001**, *98*, 3006-3015.

107. Hezareh, M.; Moukil, M. A.; Szanto, I.; Pondarzewski, M.; Mouche, S.; Cherix, N.; Brown, S. J.; Carpentier, J. L.; Foti, M. Mechanisms of HIV receptor and co-receptor down-regulation by prostratin: role of conventional and novel PKC isoforms. *Antivir. Chem. Chemother.* **2004**, *15*, 207-222.
108. Williams, S. A.; Chen, L. F.; Kwon, H.; Fenard, D.; Bisgrove, D.; Verdin, E.; Greene, W. C. Prostratin antagonizes HIV latency by activating NF- $\kappa$ B. *J. Biol. Chem.* **2004**, *279*, 42008-42017.
109. Hohmann, J.; Evanics, F.; Berta, L.; Bartok, T. Diterpenoids from *Euphorbia peplus*. *Planta Med.* **2000**, *66*, 291-294.
110. Jassbi, A. R. Chemistry and biological activity of secondary metabolites in *Euphorbia* from Iran. *Phytochemistry* **2006**, *67*, 1977-1984.
111. Ogbourne, S. M.; Hampson, P.; Lord, J. M.; Parsons, P.; De Witte, P. A.; Suhrbier, A. Proceedings of the First International Conference on PEP005. *Anti-cancer Drugs* **2007**, *18*, 357-362.
112. Kedei, N.; Lundberg, D. J.; Toth, A.; Welburn, P.; Garfield, S. H.; Blumberg, P. M. Characterization of the interaction of ingenol 3-angelate with protein kinase C. *Cancer Res.* **2004**, *64*, 3243-3255.
113. Hasler, C. M.; Acs, G.; Blumberg, P. M. Specific binding to protein kinase C by ingenol and its induction of biological responses. *Cancer Res.* **1992**, *52*, 202-208.
114. Ogbourne, S. M.; Suhrbier, A.; Jones, B.; Cozzi, S. J.; Boyle, G. M.; Morris, M.; McAlpine, D.; Johns, J.; Scott, T. M.; Sutherland, K. P.; Gardner, J. M.; Le, T. T.; Lenarczyk, A.; Aylward, J. H.; Parsons, P. G. Antitumor activity of 3-ingenyl angelate: plasma membrane and mitochondrial disruption and necrotic cell death. *Cancer Res.* **2004**, *64*, 2833-2839.
115. Hampson, P.; Chahal, H.; Khanim, F.; Hayden, R.; Mulder, A.; Assi, L. K.; Bunce, C. M.; Lord, J. M. PEP005, a selective small-molecule activator of protein kinase C, has potent antileukemic activity mediated via the delta isoform of PKC. *Blood* **2005**, *106*, 1362-1368.
116. Hampson, P.; Kavanagh, D. S.,E.; Wang, K.; Lord, J. M.; Rainger, E. G. The anti-tumor agent, ingenol-3-angelate (PEP005), promotes the recruitment of cytotoxic neutrophils by activation of vascular endothelial cells in a PKC- $\delta$  dependent manner. *Cancer Immunol Immunother.* **2008**, *57*, 1241-1251.
117. Pettit, G. R.; Herald, C. L.; Doubek, D. L.; Herald, D. L. Isolation and Structure of Bryostatin 1. *J. Am. Chem. Soc.* **1982**, *104*, 6846-6848.
118. Davidson, S. K.; Allen, S. W.; Lim, G. E.; Anderson, C. M.; Haygood, M. G. Evidence for the biosynthesis of bryostatins by the bacterial symbiont "*Candidatus Endobugula sertula*" of the bryozoan *Bugula neritina*. *Appl. Environ. Microbiol.* **2001**, *67*, 4531-4537.
119. Hale, K. J.; Manaviazar, S. New approaches to the total synthesis of the bryostatin antitumor macrolides. *Chem. Asian J.* **2010**, *5*, 704-754.
120. Wender, P. A.; Verma, V. A. The Design, Synthesis, and Evaluation of C7 Diversified Bryostatin Analogs Reveals a Hot Spot for PKC Affinity. *Org. Lett.* **2008**, *10*, 3331-3334.
121. Mutter, R.; Wills, M. Chemistry and clinical biology of the bryostatins. *Bioorg. Med. Chem.* **2000**, *8*, 1841-1860.
122. Evans, D. A.; Carter, P. H.; Carreira, E. M.; Charette, A. B.; Prunet, J. A.; Lautens, M. Total Synthesis of Bryostatin 2. *J. Am. Chem. Soc.* **1999**, *121*, 7540-7552.
123. Dell'Aquila, M. L.; Nguyen, H. T.; Herald, C. L.; Pettit, G. R.; Blumberg, P. M. Inhibition by bryostatin 1 of the phorbol ester-induced blockage of differentiation in hexamethylene bisacetamide-treated Friend erythroleukemia cells. *Cancer Res.* **1987**, *47*, 6006-6009.
124. Kato, Y.; Scheuer, P. J. Aplysiatoxin and debromoaplysiatoxin, constituents of the marine mollusk *Stylocheilus longicauda* (Quoy and Gaimard, 1824). *J. Am. Chem. Soc.* **1974**, *96*, 2245-2246.

125. Horowitz, A. D.; Fujiki, H.; Weinstein, I. B. Comparative effects of aplysiatoxin, debromoaplysiatoxin, and teleocidin on receptor binding and phospholipid metabolism. *Cancer Res.* **1983**, *43*, 1529-1535.
126. Fujiki, H.; Suganuma, M.; Nakayasu, M.; Hoshino, H.; Moore, R. E.; Sugimura, T. The third class of new tumor promoters, polyacetates (debromoaplysiatoxin and aplysiatoxin), can differentiate biological actions relevant to tumor promoters. *Jpn. J. Cancer Res. (Gann)* **1982**, *73*, 495-497.
127. Nakagawa, Y.; Yanagita, R. C.; Hamada, N.; Murakami, A.; Takahashi, H.; Saito, N.; Nagai, H.; Irie, K. A simple analogue of tumor-promoting aplysiatoxin is an antineoplastic agent rather than a tumor promoter: development of a synthetically accessible protein kinase C activator with bryostatin-like activity. *J. Am. Chem. Soc.* **2009**, *131*, 7573-7579.
128. Nakamura, H.; Kishi, Y.; Pajares, M. A.; Rando, R. R. Structural basis of protein kinase C activation by tumor promoters. *Proc. Natl. Acad. Sci. U. S. A.* **1989**, *86*, 9672-9676.
129. Takashima, M.; Sakai, H. A new toxic substance, teleocidin produced by *Streptomyces*. Part I. Production, isolation, and chemical studies. *Bull. Agric. Chem. Soc. Jpn.* **1960**, *24*, 647-651.
130. Fujiki, H.; Mori, M.; Nakayasu, M.; Terada, M.; Sugimura, T.; Moore, R. E. Indole alkaloids: dihydroteleocidin B, teleocidin, and lyngbyatoxin A as members of a new class of tumor promoters. *Proc. Natl. Acad. Sci. U. S. A.* **1981**, *78*, 3872-3876.
131. Umezawa, K.; Weinstein, I. B.; Horowitz, A.; Fujiki, H.; Matsushima, T.; Sugimura, T. Similarity of teleocidin B and phorbol ester tumour promoters in effects on membrane receptors. *Nature* **1981**, *290*, 411-413.
132. Fujiki, H.; Suganuma, M.; Nakayasu, M.; Tahira, T.; Endo, Y.; Shudo, K.; Sugimura, T. Structure-activity Studies on Synthetic Analogues (Indolactams) of the Tumor Promoter Teleocidin. *Jpn. J. Cancer Res. (Gann)* **1984**, *75*, 866-870.
133. Endo, Y.; Takehana, S.; Ohno, M.; Driedger, P. E.; Stabel, S.; Mizutani, M. Y.; Tomioka, N.; Itai, A.; Shudo, K. Clarification of the binding mode of teleocidin and benzolactams to the Cys2 domain of protein kinase C $\delta$  by synthesis of hydrophobically modified, teleocidin-mimicking benzolactams and computational docking simulation. *J. Med. Chem.* **1998**, *41*, 1476-1496.
134. Rong, S. B.; Enyedy, I. J.; Qiao, L.; Zhao, L.; Ma, D.; Pearce, L. L.; Lorenzo, P. S.; Stone, J. C.; Blumberg, P. M.; Wang, S.; Kozikowski, A. P. Structural basis of RasGRP binding to high-affinity PKC ligands. *J. Med. Chem.* **2002**, *45*, 853-860.
135. Yanagita, R. C.; Nakagawa, Y.; Yamanaka, N.; Kashiwagi, K.; Saito, N.; Irie, K. Synthesis, conformational analysis, and biological evaluation of 1-hexylindolactam-V10 as a selective activator for novel protein kinase C isozymes. *J. Med. Chem.* **2008**, *51*, 46-56.
136. Nakagawa, Y.; Irie, K.; Yanagita, R. C.; Ohigashi, H.; Tsuda, K. Indolactam-V is involved in the CH/ $\pi$  interaction with Pro-11 of the PKC $\delta$  C1B domain: application for the structural optimization of the PKC $\delta$  ligand. *J. Am. Chem. Soc.* **2005**, *127*, 5746-5747.
137. Arcamone, F.; Cassinelli, G.; Fantini, G.; Grein, A.; Orezzi, P.; Pol, C.; Spalla, C. Adriamycin, 14-hydroxydaunomycin, a new antitumor antibiotic from *S. peucetius* var. *caesius*. *Biotechnol. Bioeng.* **1969**, *11*, 1101-1110.
138. Frederick, C. A.; Williams, L. D.; Ughetto, G.; van der Marel, G. A.; van Boom, J. H.; Rich, A.; Wang, A. H. Structural comparison of anticancer drug-DNA complexes: adriamycin and daunomycin. *Biochemistry* **1990**, *29*, 2538-2549.
139. Roaten, J. B.; Kazanietz, M. G.; Caloca, M. J.; Bertics, P. J.; Lothstein, L.; Parrill, A. L.; Israel, M.; Sweatman, T. W. Interaction of the novel anthracycline antitumor agent N-benzyladriamycin-14-valerate with the C1-regulatory domain of protein kinase C: structural requirements, isoform specificity, and correlation with drug cytotoxicity. *Mol. Cancer Ther.* **2002**, *1*, 483-492.

140. Minotti, G.; Menna, P.; Salvatorelli, E.; Cairo, G.; Gianni, L. Anthracyclines: molecular advances and pharmacologic developments in antitumor activity and cardiotoxicity. *Pharmacol. Rev.* **2004**, *56*, 185-229.
141. Kobayashi, E.; Nakano, H.; Morimoto, M.; Tamaoki, T. Calphostin C (UCN-1028C), a novel microbial compound, is a highly potent and specific inhibitor of protein kinase C. *Biochem. Biophys. Res. Commun.* **1989**, *159*, 548-553.
142. Iida, T.; Kobayashi, E.; Yoshida, M.; Sano, H. Calphostins, novel and specific inhibitors of protein kinase C. II. Chemical structures. *J. Antibiot.* **1989**, *42*, 1475-1481.
143. Kobayashi, E.; Ando, K.; Nakano, H.; Iida, T.; Ohno, H.; Morimoto, M.; Tamaoki, T. Calphostins (UCN-1028), novel and specific inhibitors of protein kinase C. I. Fermentation, isolation, physico-chemical properties and biological activities. *J. Antibiot.* **1989**, *42*, 1470-1474.
144. Rotenberg, S. A.; Huang, M. H.; Zhu, J.; Su, L.; Riedel, H. Deletion analysis of protein kinase C inactivation by calphostin C. *Mol. Carcinog.* **1995**, *12*, 42-49.
145. Gopalakrishna, R.; Chen, Z. H.; Gundimeda, U. Irreversible oxidative inactivation of protein kinase C by photosensitive inhibitor calphostin C. *FEBS Lett.* **1992**, *314*, 149-154.
146. Bruns, R. F.; Miller, F. D.; Merriman, R. L.; Howbert, J. J.; Heath, W. F.; Kobayashi, E.; Takahashi, I.; Tamaoki, T.; Nakano, H. Inhibition of protein kinase C by calphostin C is light-dependent. *Biochem. Biophys. Res. Commun.* **1991**, *176*, 288-293.
147. Lown, J. W. 1996 Hoffman-LaRoche Award Lecture Photochemistry and photobiology of perylenequinones. *Can. J. Chem.* **1997**, *75*, 99-119.
148. Merlic, C. A.; Aldrich, C. C.; Albaneze-Walker, J.; Saghatelian, A. Carbene Complexes in the Synthesis of Complex Natural Products: Total Synthesis of the Calphostins. *J. Am. Chem. Soc.* **2000**, *122*, 3224-3225.
149. Merlic, C. A.; Aldrich, C. C.; Albaneze-Walker, J.; Saghatelian, A.; Mammen, J. Total synthesis of the calphostins: application of fischer carbene complexes and thermodynamic control of atropisomers. *J. Org. Chem.* **2001**, *66*, 1297-1309.
150. Chiarini, A.; Whitfield, J. F.; Pacchiana, R.; Armato, U.; Dal Pra, I. Photoexcited calphostin C selectively destroys nuclear lamin B1 in neoplastic human and rat cells - a novel mechanism of action of a photodynamic tumor therapy agent. *Biochim. Biophys. Acta* **2008**, *1783*, 1642-1653.
151. Dubauskas, Z.; Beck, T. P.; Chmura, S. J.; Kovar, D. A.; Kadkhodaiyan, M. M.; Shrivastav, M.; Chung, T.; Stadler, W. M.; Rinker-Schaeffer, C. W. Activated calphostin C cytotoxicity is independent of p53 status and in vivo metastatic potential. *Clin. Cancer Res.* **1998**, *4*, 2391-2398.
152. Pollack, I. F.; Kawecki, S. The effect of calphostin C, a potent photodependent protein kinase C inhibitor, on the proliferation of glioma cells in vitro. *J. Neurooncol.* **1997**, *31*, 255-266.
153. Chiarini, A.; Whitfield, J. F.; Pacchiana, R.; Marconi, M.; Armato, U.; Dal Pra, I. Calphostin C, a remarkable multimodal photodynamic killer of neoplastic cells by selective nuclear lamin B1 destruction and apoptosis (Review). *Oncol. Rep.* **2010**, *23*, 887-892.
154. Marner, F.; Krick, W.; Gellrich, B.; Jaenicke, L. Iridogermanal and Iridogermanal: Two New Triterpenoids from Rhizomes of *Iris germanica* L. *J. Org. Chem.* **1982**, *47*, 2531-2536.
155. Takahashi, K.; Suzuki, S.; Hano, Y.; Nomura, T. Protein kinase C activation by iridal type triterpenoids. *Biol. Pharm. Bull.* **2002**, *25*, 432-436.
156. Shao, L.; Lewin, N. E.; Lorenzo, P. S.; Hu, Z.; Enyedy, I. J.; Garfield, S. H.; Stone, J. C.; Marner, F. J.; Blumberg, P. M.; Wang, S. Iridals are a novel class of ligands for phorbol ester receptors with modest selectivity for the RasGRP receptor subfamily. *J. Med. Chem.* **2001**, *44*, 3872-3880.

157. Bonfils, J. P.; Pinguet, F.; Culine, S.; Sauvaire, Y. Cytotoxicity of iridals, triterpenoids from Iris, on human tumor cell lines A2780 and K562. *Planta Med.* **2001**, *67*, 79-81.
158. Corbu, A.; Aquino, M.; Pratap, T. V.; Retailleau, P.; Arseniyadis, S. Enantioselective synthesis of iridal, the parent molecule of the iridal triterpenoid class. *Org. Lett.* **2008**, *10*, 1787-1790.
159. Appendino, G.; Jakupovic, S.; Tron, G. C.; Jakupovic, J.; Milon, V.; Ballero, M. Macrocytic diterpenoids from Euphorbia semiperfoliata. *J. Nat. Prod.* **1998**, *61*, 749-756.
160. Bedoya, L. M.; Marquez, N.; Martinez, N.; Gutierrez-Eisman, S.; Alvarez, A.; Calzado, M. A.; Rojas, J. M.; Appendino, G.; Munoz, E.; Alcamí, J. SJ23B, a jatrophone diterpene activates classical PKCs and displays strong activity against HIV in vitro. *Biochem. Pharmacol.* **2009**, *77*, 965-978.
161. Gouiffès, D.; Moreau, S.; Helbecque, N.; Bernier, J. L.; Hénichart, J. P.; Barbin, Y.; Laurent, D.; Verbist, J. F. Proton Nuclear Magnetic Study of Bistramide A, a new cytotoxic drug isolated from *Lissoclinum Bistratum* Sluiter. *Tetrahedron* **1988**, *44*, 451-459.
162. Biard, J. F.; Roussakis, C.; Kornprobst, J. M.; Gouiffès-Barbin, D.; Verbist, J. F.; Cotelle, P.; Foster, M. P.; Ireland, C. M.; Debitus, C. Bistramides A, B, C, D, and K: a new class of bioactive cyclic polyethers from *Lissoclinum Bistratum*. *J. Nat. Prod.* **1994**, *57*, 1336-1345.
163. Riou, D.; Roussakis, C.; Robillard, N.; Biard, J. F.; Verbist, J. F. Bistramide A-induced irreversible arrest of cell proliferation in a non-small-cell bronchopulmonary carcinoma is similar to induction of terminal maturation. *Biol. Cell.* **1993**, *77*, 261-264.
164. Gouiffès, D.; Juge, M.; Grimaud, N.; Welin, L.; Sauviat, M. P.; Barbin, Y.; Laurent, D.; Roussakis, C.; Henichart, J. P.; Verbist, J. F. Bistramide A, a new toxin from the urochordata *Lissoclinum bistratum* Sluiter: isolation and preliminary characterization. *Toxicon* **1988**, *26*, 1129-1136.
165. Sauviat, M.-P.; Gouiffès-Barbin, D.; Ecault, E.; Verbist, J.-F. Blockade of sodium channels by bistramide A in voltage-clamped frog skeletal muscle fibres. *Biochim. Biophys. Acta, Biomembr.* **1992**, *1103*, 109-114.
166. Sauviat, M. P.; Verbist, J. F. Alteration of the voltage-dependence of the twitch tension in frog skeletal muscle fibres by a polyether, Bistramide A. *Gen. Physiol. Biophys.* **1993**, *12*, 465-471.
167. Stanwell, C.; Gescher, A.; Watters, D. Cytostatic and cytotoxic properties of the marine product bistratene A and analysis of the role of protein kinase C in its mode of action. *Biochem. Pharmacol.* **1993**, *45*, 1753-1761.
168. Gautret, P.; Le Pape, P.; Biard, J. F.; Menard, D.; Verbist, J. F.; Marjolet, M. The effects of bistramides on rodent malaria. *Acta Parasitol.* **1998**, *43*, 50-53.
169. Mann, V. H.; Law, M. H.; Watters, D.; Saul, A. The effects of bistratene A on the development of *Plasmodium falciparum* in culture. *Int. J. Parasitol.* **1996**, *26*, 117-121.
170. Griffiths, G.; Garrone, B.; Deacon, E.; Owen, P.; Pongracz, J.; Mead, G.; Bradwell, A.; Watters, D.; Lord, J. The polyether bistratene A activates protein kinase C- $\delta$  and induces growth arrest in HL60 cells. *Biochem. Biophys. Res. Commun.* **1996**, *222*, 802-808.
171. Watters, D.; Garrone, B.; Coomer, J.; Johnson, W. E.; Brown, G.; Parsons, P. Stimulation of melanogenesis in a human melanoma cell line by bistratene A. *Biochem. Pharmacol.* **1998**, *55*, 1691-1699.
172. Statsuk, A. V.; Bai, R.; Baryza, J. L.; Verma, V. A.; Hamel, E.; Wender, P. A.; Kozmin, S. A. Actin is the primary cellular receptor of bistramide A. *Nat. Chem. Biol.* **2005**, *1*, 383-388.
173. Rizvi, S. A.; Courson, D. S.; Keller, V. A.; Rock, R. S.; Kozmin, S. A. The dual mode of action of bistramide A entails severing of filamentous actin and covalent protein modification. *Proc. Natl. Acad. Sci. U. S. A.* **2008**, *105*, 4088-4092.



174. Watters, D.; Garrone, B.; Gobert, G.; Williams, S.; Gardiner, R.; Lavin, M. Bistratene A causes phosphorylation of talin and redistribution of actin microfilaments in fibroblasts: possible role for PKC- $\delta$ . *Exp. Cell Res.* **1996**, *229*, 327-335.
175. Statsuk, A. V.; Liu, D.; Kozmin, S. A. Synthesis of bistramide A. *J. Am. Chem. Soc.* **2004**, *126*, 9546-9547.
176. Crimmins, M. T.; DeBaillie, A. C. Enantioselective total synthesis of bistramide A. *J. Am. Chem. Soc.* **2006**, *128*, 4936-4937.
177. Lowe, J. T.; Wrona, I. E.; Panek, J. S. Total synthesis of bistramide A. *Org. Lett.* **2007**, *9*, 327-330.
178. Wrona, I. E.; Lowe, J. T.; Turbyville, T. J.; Johnson, T. R.; Beignet, J.; Beutler, J. A.; Panek, J. S. Synthesis of a 35-member stereoisomer library of bistramide A: evaluation of effects on actin state, cell cycle and tumor cell growth. *J. Org. Chem.* **2009**, *74*, 1897-1916.
179. Yadav, J. S.; Chetia, L. Stereoselective total synthesis of bistramide A. *Org. Lett.* **2007**, *9*, 4587-4589.
180. Rizvi, S. A.; Tereshko, V.; Kossiakoff, A. A.; Kozmin, S. A. Structure of bistramide A-actin complex at a 1.35 angstroms resolution. *J. Am. Chem. Soc.* **2006**, *128*, 3882-3883.
181. Rizvi, S. A.; Liu, S.; Chen, Z.; Skau, C.; Pytynia, M.; Kovar, D. R.; Chmura, S. J.; Kozmin, S. A. Rationally simplified bistramide analog reversibly targets actin polymerization and inhibits cancer progression in vitro and in vivo. *J. Am. Chem. Soc.* **2010**, *132*, 7288-7290.
182. Wipf, P.; Uto, Y.; Yoshimura, S. Total Synthesis of a Stereoisomer of Bistramide C and Assignment of Configuration of the Natural Product. *Chem. Eur. J.* **2002**, *8*, 1670-1681.
183. Wipf, P.; Hopkins, T. D. Total synthesis and structure validation of (+)-bistramide C. *Chem. Commun.* **2005**, *27*, 3421-3423.
184. Swannie, H. C.; Kaye, S. B. Protein kinase C inhibitors. *Curr. Oncol. Rep.* **2002**, *4*, 37-46.
185. Kortmansky, J.; Schwartz, G. K. Bryostatins: a novel PKC inhibitor in clinical development. *Cancer Invest.* **2003**, *21*, 924-936.
186. Siller, G.; Gebauer, K.; Welburn, P.; Katsamas, J.; Ogbourne, S. M. PEP005 (ingenol mebutate) gel, a novel agent for the treatment of actinic keratosis: results of a randomized, double-blind, vehicle-controlled, multicentre, phase IIa study. *Australas. J. Dermatol.* **2009**, *50*, 16-22.
187. Anderson, L.; Schmieder, G. J.; Werschler, W. P.; Tschen, E. H.; Ling, M. R.; Stough, D. B.; Katsamas, J. Randomized, double-blind, double-dummy, vehicle-controlled study of ingenol mebutate gel 0.025% and 0.05% for actinic keratosis. *J. Am. Acad. Dermatol.* **2009**, *60*, 934-943.
188. Wender, P. A.; Heumann, L. V.; Kramer, R.; Gauntlett, C.; Mieuli, E.; Fournogerakis, D.; Boudreault, P.; Schrier, A.; Dechristopher, B. Prostratin analogs, bryostatins, produgs, synthetic methods, and methods of use. U.S. Pat. Appl. 2011/0014699A1.
189. Krauter, G.; Von der Lieth, C. W.; Schmidt, R.; Hecker, E. Structure/activity relationships of polyfunctional diterpenes of the tiglane type. A pharmacophore model for protein-kinase-C activators based on structure/activity studies and molecular modeling of the tumor promoters 12-O-tetradecanoylphorbol 13-acetate and 3-O-tetradecanoylingenol. *Eur. J. Biochem.* **1996**, *242*, 417-427.
190. Winkler, J. D.; Hong, B.; Bahador, A.; Kazanietz, M. G.; Blumberg, P. M. Synthesis of ingenol analogues with affinity for protein kinase C. *Bioorg. Med. Chem. Lett.* **1993**, *3*, 577-580.
191. Hecker, E. Three stage carcinogenesis in mouse skin—recent results and present status of an advanced model system of chemical carcinogenesis. *Toxicol. Pathol.* **1987**, *15*, 245-258.

192. Blanco-Molina, M.; Tron, G. C.; Macho, A.; Lucena, C.; Calzado, M. A.; Munoz, E.; Appendino, G. Ingenol esters induce apoptosis in Jurkat cells through an AP-1 and NF- $\kappa$ B independent pathway. *Chem. Biol.* **2001**, *8*, 767-778.
193. Mason, S. A.; Cozzi, S. J.; Pierce, C. J.; Pavey, S. J.; Parsons, P. G.; Boyle, G. M. The induction of senescence-like growth arrest by protein kinase C-activating diterpene esters in solid tumor cells. *Invest New Drugs* **2010**, *28*, 575-586.
194. Pavlick, A. C.; Wu, J.; Roberts, J.; Rosenthal, M. A.; Hamilton, A.; Wadler, S.; Farrell, K.; Carr, M.; Fry, D.; Murgo, A. J.; Oratz, R.; Hochster, H.; Liebes, L.; Muggia, F. Phase I study of bryostatin 1, a protein kinase C modulator, preceding cisplatin in patients with refractory non-hematologic tumors. *Cancer Chemother. Pharmacol.* **2009**, *64*, 803-810.
195. Barr, P. M.; Lazarus, H. M.; Cooper, B. W.; Schluchter, M. D.; Panneerselvam, A.; Jacobberger, J. W.; Hsu, J. W.; Janakiraman, N.; Simic, A.; Dowlati, A.; Remick, S. C. Phase II study of bryostatin 1 and vincristine for aggressive non-Hodgkin lymphoma relapsing after an autologous stem cell transplant. *Am. J. Hematol.* **2009**, *84*, 484-487.
196. Lam, A. P.; Sparano, J. A.; Vinciguerra, V.; Ocean, A. J.; Christos, P.; Hochster, H.; Camacho, F.; Goel, S.; Mani, S.; Kaubisch, A. Phase II Study of Paclitaxel Plus the Protein Kinase C Inhibitor Bryostatin-1 in Advanced Pancreatic Carcinoma. *Am. J. Clin. Oncol.* **2010**, *33*, 121-124.
197. Ku, G. Y.; Ilson, D. H.; Schwartz, L. H.; Capanu, M.; O'Reilly, E.; Shah, M. A.; Kelsen, D. P.; Schwartz, G. K. Phase II trial of sequential paclitaxel and 1 h infusion of bryostatin-1 in patients with advanced esophageal cancer. *Cancer Chemother. Pharmacol.* **2008**, *62*, 875-880.
198. Roberts, J. D.; Smith, M. R.; Feldman, E. J.; Cragg, L.; Millenson, M. M.; Roboz, G. J.; Honeycutt, C.; Thune, R.; Padavic-Shaller, K.; Carter, W. H.; Ramakrishnan, V.; Murgo, A. J.; Grant, S. Phase I study of bryostatin 1 and fludarabine in patients with chronic lymphocytic leukemia and indolent (non-Hodgkin's) lymphoma. *Clin. Cancer Res.* **2006**, *12*, 5809-5816.
199. El-Rayes, B. F.; Gadgeel, S.; Shields, A. F.; Manza, S.; Lorusso, P.; Philip, P. A. Phase I study of bryostatin 1 and gemcitabine. *Clin. Cancer Res.* **2006**, *12*, 7059-7062.
200. Peterson, A. C.; Harlin, H.; Karrison, T.; Vogelzang, N. J.; Knost, J. A.; Kugler, J. W.; Lester, E.; Vokes, E.; Gajewski, T. F.; Stadler, W. M. A randomized phase II trial of interleukin-2 in combination with four different doses of bryostatin-1 in patients with renal cell carcinoma. *Invest. New Drugs* **2006**, *24*, 141-149.
201. Ajani, J. A.; Jiang, Y.; Faust, J.; Chang, B. B.; Ho, L.; Yao, J. C.; Rousey, S.; Dakhil, S.; Cherny, R. C.; Craig, C.; Bleyer, A. A multi-center phase II study of sequential paclitaxel and bryostatin-1 (NSC 339555) in patients with untreated, advanced gastric or gastroesophageal junction adenocarcinoma. *Invest. New Drugs* **2006**, *24*, 353-357.
202. Wender, P. A.; Baryza, J. L.; Bennett, C. E.; Bi, F. C.; Brenner, S. E.; Clarke, M. O.; Horan, J. C.; Kan, C.; Lacôte, E.; Lippa, B.; Nell, P. G.; Turner, T. M. The Practical Synthesis of a Novel and Highly Potent Analogue of Bryostatin. *J. Am. Chem. Soc.* **2002**, *124*, 13648-13649.
203. Wender, P. A.; Baryza, J. L.; Brenner, S. E.; Clarke, M. O.; Craske, M. L.; Horan, J.C. and Meyer, T. Function Oriented Synthesis: The Design, Synthesis, PKC Binding and Translocation Activity of a New Bryostatin Analogue. *Curr. Drug Discovery Technol.* **2004**, *1*, 1-11.
204. Wender, P. A.; Brabander, J. D.; Harran, P. G.; Jimenez, J.; Koehler, M. F. T.; Lippa, B.; Park, C.; Shiozaki, M. Synthesis of the First Members of a New Class of Biologically Active Bryostatin Analogues. *J. Am. Chem. Soc.* **1998**, *120*, 4534-4535.
205. Keck, G. E.; Poudel, Y. B.; Welch, D. S.; Kraft, M. B.; Truong, A. P.; Stephens, J. C.; Keddi, N.; Lewin, N. E.; Blumberg, P. M. Substitution on the A-ring confers to bryopyran

- analogues the unique biological activity characteristic of bryostatins and distinct from that of the phorbol esters. *Org. Lett.* **2009**, *11*, 593-596.
206. Wender, P. A.; Dechristopher, B. A.; Schrier, A. J. Efficient synthetic access to a new family of highly potent bryostatin analogues via a Prins-driven macrocyclization strategy. *J. Am. Chem. Soc.* **2008**, *130*, 6658-6659.
207. Endo, Y.; Ohno, M.; Hirano, M.; Itai, A.; Shudo, K. Synthesis, Conformation, and Biological Activity of Teleocidin Mimics, Benzolactams. A Clarification of the Conformational Flexibility Problem in Structure-Activity Studies of Teleocidins. *J. Am. Chem. Soc.* **1996**, *118*, 1841-1855.
208. Irie, K.; Nakagawa, Y.; Ohigashi, H. Toward the development of new medicinal leads with selectivity for protein kinase C isozymes. *Chem. Rec.* **2005**, *5*, 185-195.
209. Kozikowski, A. P.; Chen, Y.; Subhasish, T.; Lewin, N. E.; Blumberg, P. M.; Zhong, Z. D.M.A.; Wang, W.; Shen, Y. L.,B. Searching for disease modifiers-PKC activation and HDAC inhibition - a dual drug approach to Alzheimer's disease that decreases A $\beta$  production while blocking oxidative stress. *ChemMedChem.* **2009**, *4*, 1095-1105.
210. Irie, K.; Nakagawa, Y.; Ohigashi, H. Indolactam and benzolactam compounds as new medicinal leads with binding selectivity for C1 domains of protein kinase C isozymes. *Curr. Pharm. Des.* **2004**, *10*, 1371-1385.
211. Kozikowski, A. P.; Wang, S.; Ma, D.; Yao, J.; Ahmad, S.; Glazer, R. I.; Bögi, K.; Acs, P.; Modarres, S.; Lewin, N. E.; Blumberg, P. M. Modeling, chemistry, and biology of the benzolactam analogues of indolactam V (ILV). 2. Identification of the binding site of the benzolactams in the CRD2 activator-binding domain of PKC $\delta$  and discovery of an ILV analogue of improved isozyme selectivity. *J. Med. Chem.* **1997**, *40*, 1316-1326.
212. Ma, D.; Tang, G.; Kozikowski, A. P. Synthesis of 7-substituted benzolactam-V8s and their selectivity for protein kinase C isozymes. *Org. Lett.* **2002**, *4*, 2377-2380.
213. Nakagawa, Y.; Irie, K.; Masuda, A.; Ohigashi, H. Synthesis, conformation and PKC isozyme surrogate binding of new lactone analogues of benzolactam-V8s. *Tetrahedron* **2002**, *58*, 2101-2115.
214. Nakagawa, Y.; Irie, K.; Yanagita, R. C.; Ohigashi, H.; Tsuda, K.; Kashiwagi, K.; Saito, N. Design and synthesis of 8-octyl-benzolactam-V9, a selective activator for protein kinase C  $\epsilon$  and  $\eta$ . *J. Med. Chem.* **2006**, *49*, 2681-2666.
215. Endo, Y.; Yokoyama, A. Role of the hydrophobic moiety of tumor promoters. Synthesis and activity of 2-alkylated benzolactams. *Bioorg. Med. Chem. Lett.* **2000**, *10*, 63-66.
216. Bhagavan, S.; Ibarreta, D.; Ma, D.; Kozikowski, A. P.; Etcheberrigaray, R. Restoration of TEA-induced calcium responses in fibroblasts from Alzheimer's disease patients by a PKC activator. *Neurobiol. Dis.* **1998**, *5*, 177-187.
217. Israel, M.; Seshadri, R.; Idriss, J. M. N-Benzyladriamycin-14-valerate (AD198), a promising new adriamycin (ADR) analog. *Proc. Am. Assoc. Cancer Res.* **1985**, *26*, 220.
218. Barrett, C. M.; Lewis, F. L.; Roaten, J. B.; Sweatman, T. W.; Israel, M.; Cleveland, J. L.; Lothstein, L. Novel extranuclear-targeted anthracyclines override the antiapoptotic functions of Bcl-2 and target protein kinase C pathways to induce apoptosis. *Mol. Cancer Ther.* **2002**, *1*, 469-481.
219. Roaten, J. B.; Kazanietz, M. G.; Sweatman, T. W.; Lothstein, L.; Israel, M.; Parrill, A. L. Molecular models of N-benzyladriamycin-14-valerate (AD 198) in complex with the phorbol ester-binding C1b domain of protein kinase C- $\delta$ . *J. Med. Chem.* **2001**, *44*, 1028-1034.
220. Harstrick, A.; Vanhoefer, U.; Schleucher, N.; Schroeder, J.; Baumgart, J.; Scheulen, M. E.; Wilke, H.; Seeber, S. Activity of N-benzyl-adriamycin-14-valerate (AD198), a new anthracycline derivate, in multidrug resistant human ovarian and breast carcinoma cell lines. *Anti-cancer Drugs* **1995**, *6*, 681-685.

221. Traganos, F.; Israel, M.; Silber, R.; Seshadri, R.; Kirschenbaum, S.; Potmesil, M. Effects of new N-alkyl analogues of adriamycin on in vitro survival and cell cycle progression of L1210 cells. *Cancer Res.* **1985**, *45*, 6273-6279.
222. Lothstein, L.; Savranskaya, L.; Sweatman, T. W. N-Benzyladriamycin-14-valerate (AD 198) cytotoxicity circumvents Bcr-Abl anti-apoptotic signaling in human leukemia cells and also potentiates imatinib cytotoxicity. *Leuk. Res.* **2007**, *31*, 1085-1095.
223. He, Y.; Liu, J.; Durrant, D.; Yang, H. S.; Sweatman, T.; Lothstein, L.; Lee, R. M. N-benzyladriamycin-14-valerate (AD198) induces apoptosis through protein kinase C- $\delta$ -induced phosphorylation of phospholipid scramblase 3. *Cancer Res.* **2005**, *65*, 10016-10023.
224. Ganapathi, R.; Grabowski, D.; Sweatman, T. W.; Seshadri, R.; Israel, M. N-benzyladriamycin-14-valerate versus progressively doxorubicin-resistant murine tumours: cellular pharmacology and characterisation of cross-resistance in vitro and in vivo. *Br. J. Cancer* **1989**, *60*, 819-826.
225. Lothstein, L.; Israel, M.; Sweatman, T. W. Anthracycline drug targeting: cytoplasmic versus nuclear - a fork in the road. *Drug Resist. Updat.* **2001**, *4*, 169-177.
226. Chuang, L. F.; Kung, H. F.; Israel, M.; Chuang, R. Y. Activation of human leukemia protein kinase C by tumor promoters and its inhibition by N-trifluoroacetyl adriamycin-14-valerate (AD 32). *Biochem. Pharmacol.* **1992**, *43*, 865-872.
227. Markman, M.; Homesley, H.; Norberts, D. A.; Schink, J.; Abbas, F.; Miller, A.; Soper, J.; Teng, N.; Hammond, N.; Muggia, F.; Israel, M.; Sweatman, T. Phase I trial of intraperitoneal AD-32 in gynecologic malignancies. *Gynecol. Oncol.* **1996**, *61*, 90-93.
228. Morgan, B. J.; Dey, S.; Johnson, S. W.; Kozlowski, M. C. Design, synthesis, and investigation of protein kinase C inhibitors: total syntheses of (+)-calphostin D, (+)-phleichrome, cercosporin, and new photoactive perylenequinones. *J. Am. Chem. Soc.* **2009**, *131*, 9413-9425.
229. Marquez, V. E.; Blumberg, P. M. Synthetic diacylglycerols (DAG) and DAG-lactones as activators of protein kinase C (PK-C). *Acc. Chem. Res.* **2003**, *36*, 434-443.
230. Nacro, K.; Bienfait, B.; Lee, J.; Han, K. C.; Kang, J. H.; Benzaria, S.; Lewin, N. E.; Bhattacharyya, D. K.; Blumberg, P. M.; Marquez, V. E. Conformationally constrained analogues of diacylglycerol (DAG). 16. How much structural complexity is necessary for recognition and high binding affinity to protein kinase C? *J. Med. Chem.* **2000**, *43*, 921-944.
231. Kang, J. H.; Siddiqui, M. A.; Sigano, D. M.; Krajewski, K.; Lewin, N. E.; Pu, Y.; Blumberg, P. M.; Lee, J.; Marquez, V. E. Conformationally constrained analogues of diacylglycerol. 24. Asymmetric synthesis of a chiral (R)-DAG-lactone template as a versatile precursor for highly functionalized DAG-lactones. *Org. Lett.* **2004**, *6*, 2413-2416.
232. Comin, M. J.; Czifra, G.; Kedei, N.; Telek, A.; Lewin, N. E.; Kolusheva, S.; Velasquez, J. F.; Kobylarz, R.; Jelinek, R.; Blumberg, P. M.; Marquez, V. E. Conformationally constrained analogues of diacylglycerol (DAG). 31. Modulation of the biological properties of diacylglycerol lactones (DAG-lactones) containing rigid-rod acyl groups separated from the core lactone by spacer units of different lengths. *J. Med. Chem.* **2009**, *52*, 3274-3283.
233. Pu, Y.; Perry, N. A.; Yang, D.; Lewin, N. E.; Kedei, N.; Braun, D. C.; Choi, S. H.; Blumberg, P. M.; Garfield, S. H.; Stone, J. C.; Duan, D.; Marquez, V. E. A novel diacylglycerol-lactone shows marked selectivity in vitro among C1 domains of protein kinase C (PKC) isoforms  $\alpha$  and  $\delta$  as well as selectivity for RasGRP compared with PKC $\alpha$ . *J. Biol. Chem.* **2005**, *280*, 27329-27338, and erratum *J. Biol. Chem.* **2004**, *279*, 23846.
234. Garcia-Bermejo, M. L.; Leskow, F. C.; Fujii, T.; Wang, Q.; Blumberg, P. M.; Ohba, M.; Kuroki, T.; Han, K. C.; Lee, J.; Marquez, V. E.; Kazanietz, M. G. Diacylglycerol (DAG)-lactones, a new class of protein kinase C (PKC) agonists, induce apoptosis in LNCaP prostate cancer cells by selective activation of PKC $\alpha$ . *J. Biol. Chem.* **2002**, *277*, 645-655.

235. Truman, J. P.; Rotenberg, S. A.; Kang, J. H.; Lerman, G.; Fuks, Z.; Kolesnick, R.; Marquez, V. E.; Haimovitz-Friedman, A. PKC $\alpha$  activation downregulates ATM and radio-sensitizes androgen-sensitive human prostate cancer cells in vitro and in vivo. *Cancer Biol. Ther.* **2009**, *8*, 54-63.
236. Hamer, D. H.; Bocklandt, S.; McHugh, L.; Chun, T. W.; Blumberg, P. M.; Sigano, D. M.; Marquez, V. E. Rational design of drugs that induce human immunodeficiency virus replication. *J. Virol.* **2003**, *77*, 10227-10236.
237. Stoica, G. E.; Kuo, A.; Aigner, A.; Sunitha, I.; Souttou, B.; Malerczyk, C.; Caughey, D. J.; Wen, D.; Karavanov, A.; Riegel, A. T.; Wellstein, A. Identification of anaplastic lymphoma kinase as a receptor for the growth factor pleiotrophin. *J. Biol. Chem.* **2001**, *276*, 16772-16779.
238. Stoica, G. E.; Kuo, A.; Powers, C.; Bowden, E. T.; Sale, E. B.; Riegel, A. T.; Wellstein, A. Midkine binds to anaplastic lymphoma kinase (ALK) and acts as a growth factor for different cell types. *J. Biol. Chem.* **2002**, *277*, 35990-35998.
239. Moog-Lutz, C.; Degoutin, J.; Gouzi, J. Y.; Frobert, Y.; Brunet-de Carvalho, N.; Bureau, J.; Creminon, C.; Vigny, M. Activation and inhibition of anaplastic lymphoma kinase receptor tyrosine kinase by monoclonal antibodies and absence of agonist activity of pleiotrophin. *J. Biol. Chem.* **2005**, *280*, 26039-26048.
240. Palmer, R. H.; Vernersson, E.; Grabbe, C.; Hallberg, B. Anaplastic lymphoma kinase: signalling in development and disease. *Biochem. J.* **2009**, *420*, 345-361.
241. Mourali, J.; Benard, A.; Lourenco, F. C.; Monnet, C.; Greenland, C.; Moog-Lutz, C.; Racaud-Sultan, C.; Gonzalez-Dunia, D.; Vigny, M.; Mehlen, P.; Delsol, G.; Allouche, M. Anaplastic lymphoma kinase is a dependence receptor whose proapoptotic functions are activated by caspase cleavage. *Mol. Cell. Biol.* **2006**, *26*, 6209-6222.
242. Allouche, M. ALK is a novel dependence receptor: potential implications in development and cancer. *Cell Cycle* **2007**, *6*, 1533-1538.
243. Bai, R. Y.; Dieter, P.; Peschel, C.; Morris, S. W.; Duyster, J. Nucleophosmin-anaplastic lymphoma kinase of large-cell anaplastic lymphoma is a constitutively active tyrosine kinase that utilizes phospholipase C- $\gamma$  to mediate its mitogenicity. *Mol. Cell. Biol.* **1998**, *18*, 6951-6961.
244. Motegi, A.; Fujimoto, J.; Kotani, M.; Sakuraba, H.; Yamamoto, T. ALK receptor tyrosine kinase promotes cell growth and neurite outgrowth. *J. Cell. Sci.* **2004**, *117*, 3319-3329.
245. Pulford, K.; Lamant, L.; Morris, S. W.; Butler, L. H.; Wood, K. M.; Stroud, D.; Delsol, G.; Mason, D. Y. Detection of anaplastic lymphoma kinase (ALK) and nucleolar protein nucleophosmin (NPM)-ALK proteins in normal and neoplastic cells with the monoclonal antibody ALK1. *Blood* **1997**, *89*, 1394-1404.
246. Bilsland, J. G.; Wheeldon, A.; Mead, A.; Znamenskiy, P.; Almond, S.; Waters, K. A.; Thakur, M.; Beaumont, V.; Bonnert, T. P.; Heavens, R.; Whiting, P.; McAllister, G.; Munoz-Sanjuan, I. Behavioral and neurochemical alterations in mice deficient in anaplastic lymphoma kinase suggest therapeutic potential for psychiatric indications. *Neuropsychopharmacology* **2008**, *33*, 685-700.
247. Kristoffersson, U.; Heim, S.; Heldrup, J.; Åkerman, M.; Garwicz, S.; Mitelman, F. Cytogenetic studies of childhood non-Hodgkin lymphomas. *Hereditas* **1985**, *103*, 77-84.
248. Morgan, R.; Hecht, B. K.; Sandberg, A. A.; Hecht, F.; Smith, S. D. Chromosome 5q35 breakpoint in malignant histiocytosis. *N. Engl. J. Med.* **1986**, *314*, 1322.
249. Gunby, R. H.; Sala, E.; Tartari, C. J.; Puttini, M.; Gambacorti-Passerini, C.; Mologni, L. Oncogenic fusion tyrosine kinases as molecular targets for anti-cancer therapy. *Anticancer Agents Med. Chem.* **2007**, *7*, 594-611.
250. Soda, M.; Choi, Y. L.; Enomoto, M.; Takada, S.; Yamashita, Y.; Ishikawa, S.; Fujiwara, S.; Watanabe, H.; Kurashina, K.; Hatanaka, H.; Bando, M.; Ohno, S.; Ishikawa, Y.; Aburatani,

- H.; Niki, T.; Sohara, Y.; Sugiyama, Y.; Mano, H. Identification of the transforming EML4-ALK fusion gene in non-small-cell lung cancer. *Nature* **2007**, *448*, 561-566.
251. Lin, E.; Li, L.; Guan, Y.; Soriano, R.; Rivers, C. S.; Mohan, S.; Pandita, A.; Tang, J.; Modrusan, Z. Exon array profiling detects EML4-ALK fusion in breast, colorectal, and non-small cell lung cancers. *Mol. Cancer Res.* **2009**, *7*, 1466-1476.
252. Pulford, K.; Morris, S. W.; Turturro, F. Anaplastic lymphoma kinase proteins in growth control and cancer. *J. Cell. Physiol.* **2004**, *199*, 330-358.
253. Sandlund, J. T.; Pui, C. H.; Roberts, W. M.; Santana, V. M.; Morris, S. W.; Berard, C. W.; Hutchison, R. E.; Ribeiro, R. C.; Mahmoud, H.; Crist, W. M. Clinicopathologic features and treatment outcome of children with large-cell lymphoma and the t(2;5)(p23;q35). *Blood* **1994**, *84*, 2467-2471.
254. Kadin, M. E.; Morris, S. W. The t(2;5) in human lymphomas. *Leuk. Lymphoma* **1998**, *29*, 249-256.
255. Fantl, W. J.; Johnson, D. E.; Williams, L. T. Signalling by receptor tyrosine kinases. *Annu. Rev. Biochem.* **1993**, *62*, 453-481.
256. Fass, D.; Blacklow, S.; Kim, P. S.; Berger, J. M. Molecular basis of familial hypercholesterolaemia from structure of LDL receptor module. *Nature* **1997**, *388*, 691-693.
257. Daly, N. L.; Scanlon, M. J.; Djordjevic, J. T.; Kroon, P. A.; Smith, R. Three-dimensional structure of a cysteine-rich repeat from the low-density lipoprotein receptor. *Proc. Natl. Acad. Sci. U. S. A.* **1995**, *92*, 6334-6338.
258. Loren, C. E.; Scully, A.; Grabbe, C.; Edeen, P. T.; Thomas, J.; McKeown, M.; Hunter, T.; Palmer, R. H. Identification and characterization of DAlk: a novel *Drosophila melanogaster* RTK which drives ERK activation in vivo. *Genes Cells* **2001**, *6*, 531-544.
259. Jiang, Y. P.; Wang, H.; D'Eustachio, P.; Musacchio, J. M.; Schlessinger, J.; Sap, J. Cloning and characterization of R-PTP- $\kappa$ , a new member of the receptor protein tyrosine phosphatase family with a proteolytically cleaved cellular adhesion molecule-like extracellular region. *Mol. Cell. Biol.* **1993**, *13*, 2942-2951.
260. Cismasiu, V. B.; Denes, S. A.; Reilander, H.; Michel, H.; Szedlacsek, S. E. The MAM (mephrin/A5-protein/PTPmu) domain is a homophilic binding site promoting the lateral dimerization of receptor-like protein-tyrosine phosphatase  $\mu$ . *J. Biol. Chem.* **2004**, *279*, 26922-26931.
261. Loren, C. E.; Englund, C.; Grabbe, C.; Hallberg, B.; Hunter, T.; Palmer, R. H. A crucial role for the Anaplastic lymphoma kinase receptor tyrosine kinase in gut development in *Drosophila melanogaster*. *EMBO Rep.* **2003**, *4*, 781-786.
262. Morris, S. W.; Naeve, C.; Mathew, P.; James, P. L.; Kirstein, M. N.; Cui, X.; Witte, D. P. ALK, the chromosome 2 gene locus altered by the t(2;5) in non-Hodgkin's lymphoma, encodes a novel neural receptor tyrosine kinase that is highly related to leukocyte tyrosine kinase (LTK). *Oncogene* **1997**, *14*, 2175-2188.
263. Degoutin, J.; Vigny, M.; Gouzi, J. Y. ALK activation induces Shc and FRS2 recruitment: Signaling and phenotypic outcomes in PC12 cells differentiation. *FEBS Lett.* **2007**, *581*, 727-734.
264. Turner, S. D.; Yeung, D.; Hadfield, K.; Cook, S. J.; Alexander, D. R. The NPM-ALK tyrosine kinase mimics TCR signalling pathways, inducing NFAT and AP-1 by RAS-dependent mechanisms. *Cell. Signal.* **2007**, *19*, 740-747.
265. Pulford, K.; Lamant, L.; Espinos, E.; Jiang, Q.; Xue, L.; Turturro, F.; Delsol, G.; Morris, S. W. The emerging normal and disease-related roles of anaplastic lymphoma kinase. *Cell Mol. Life Sci.* **2004**, *61*, 2939-2953.
266. Webb, T. R.; Slavish, J.; George, R. E.; Look, A. T.; Xue, L.; Jiang, Q.; Cui, X.; Rentrop, W. B.; Morris, S. W. Anaplastic lymphoma kinase: role in cancer pathogenesis and small-molecule inhibitor development for therapy. *Expert Rev. Anticancer Ther.* **2009**, *9*, 331-356.

267. Bischof, D.; Pulford, K.; Mason, D. Y.; Morris, S. W. Role of the nucleophosmin (NPM) portion of the non-Hodgkin's lymphoma-associated NPM-anaplastic lymphoma kinase fusion protein in oncogenesis. *Mol. Cell. Biol.* **1997**, *17*, 2312-2325.
268. Cordell, J. L.; Pulford, K. A.; Bigerna, B.; Roncador, G.; Banham, A.; Colombo, E.; Pelicci, P. G.; Mason, D. Y.; Falini, B. Detection of normal and chimeric nucleophosmin in human cells. *Blood* **1999**, *93*, 632-642.
269. Tartari, C. J.; Gunby, R. H.; Coluccia, A. M.; Sottocornola, R.; Cimbri, B.; Scapozza, L.; Donella-Deana, A.; Pinna, L. A.; Gambacorti-Passerini, C. Characterization of some molecular mechanisms governing autoactivation of the catalytic domain of the anaplastic lymphoma kinase. *J. Biol. Chem.* **2008**, *283*, 3743-3750.
270. Perez-Pinera, P.; Zhang, W.; Chang, Y.; Vega, J. A.; Deuel, T. F. Anaplastic lymphoma kinase is activated through the pleiotrophin/receptor protein-tyrosine phosphatase  $\beta/\zeta$  signaling pathway: an alternative mechanism of receptor tyrosine kinase activation. *J. Biol. Chem.* **2007**, *282*, 28683-28690.
271. Donella-Deana, A.; Marin, O.; Cesaro, L.; Gunby, R. H.; Ferrarese, A.; Coluccia, A. M.; Tartari, C. J.; Mologni, L.; Scapozza, L.; Gambacorti-Passerini, C.; Pinna, L. A. Unique substrate specificity of anaplastic lymphoma kinase (ALK): development of phosphoacceptor peptides for the assay of ALK activity. *Biochemistry* **2005**, *44*, 8533-8542.
272. Yang, H. L.; Eriksson, T.; Vernersson, E.; Vigny, M.; Hallberg, B.; Palmer, R. H. The ligand Jelly Belly (Jeb) activates the Drosophila Alk RTK to drive PC12 cell differentiation, but is unable to activate the mouse ALK RTK. *J. Exp. Zool. B. Mol. Dev. Evol.* **2007**, *308*, 269-282.
273. Bennisroune, A.; Mazot, P.; Boutterin, M. C.; Vigny, M. Activation of the orphan receptor tyrosine kinase ALK by zinc. *Biochem. Biophys. Res. Commun.* **2010**, *398*, 702-706.
274. Degoutin, J.; Brunet-de Carvalho, N.; Cifuentes-Diaz, C.; Vigny, M. ALK (Anaplastic Lymphoma Kinase) expression in DRG neurons and its involvement in neuron-Schwann cells interaction. *Eur. J. Neurosci.* **2009**, *29*, 275-286.
275. Richter, K.; Buchner, J. Hsp90: chaperoning signal transduction. *J. Cell. Physiol.* **2001**, *188*, 281-290.
276. Jolly, C.; Morimoto, R. I. Role of the heat shock response and molecular chaperones in oncogenesis and cell death. *J. Natl. Cancer Inst.* **2000**, *92*, 1564-1572.
277. Murphy, P. J.; Kanelakis, K. C.; Galigniana, M. D.; Morishima, Y.; Pratt, W. B. Stoichiometry, abundance, and functional significance of the hsp90/hsp70-based multiprotein chaperone machinery in reticulocyte lysate. *J. Biol. Chem.* **2001**, *276*, 30092-30098.
278. Bonvini, P.; Gastaldi, T.; Falini, B.; Rosolen, A. Nucleophosmin-anaplastic lymphoma kinase (NPM-ALK), a novel Hsp90-client tyrosine kinase: down-regulation of NPM-ALK expression and tyrosine phosphorylation in ALK(+) CD30(+) lymphoma cells by the Hsp90 antagonist 17-allylamino,17-demethoxygeldanamycin. *Cancer Res.* **2002**, *62*, 1559-1566.
279. Lüders, J.; Demand, J.; Höhfeld, J. The Ubiquitin-related BAG-1 Provides a Link between the Molecular Chaperones Hsc70/Hsp70 and the Proteasome. *J. Biol. Chem.* **2000**, *275*, 4613-4617.
280. Gunby, R. H.; Ahmed, S.; Sottocornola, R.; Gasser, M.; Redaelli, S.; Mologni, L.; Tartari, C. J.; Belloni, V.; Gambacorti-Passerini, C.; Scapozza, L. Structural insights into the ATP binding pocket of the anaplastic lymphoma kinase by site-directed mutagenesis, inhibitor binding analysis, and homology modeling. *J. Med. Chem.* **2006**, *49*, 5759-5768.
281. Bossi, R. T.; Saccardo, M. B.; Ardini, E.; Menichincheri, M.; Rusconi, L.; Magnaghi, P.; Orsini, P.; Avanzi, N.; Borgia, A. L.; Nesi, M.; Bandiera, T.; Fogliatto, G.; Bertrand, J. A. Crystal structures of anaplastic lymphoma kinase in complex with ATP competitive inhibitors. *Biochemistry* **2010**, *49*, 6813-6825.

282. Lee, C. C.; Jia, Y.; Li, N.; Sun, X.; Ng, K.; Ambing, E.; Gao, M. Y.; Hua, S.; Chen, C.; Kim, S.; Michellys, P. Y.; Lesley, S. A.; Harris, J.; Spraggon, G. Crystal structure of the anaplastic lymphoma kinase (ALK) catalytic domain. *Biochem. J.* **2010**, *430*, 425-437.
283. Deininger, M. W.; Druker, B. J. Specific targeted therapy of chronic myelogenous leukemia with imatinib. *Pharmacol. Rev.* **2003**, *55*, 401-423.
284. Huse, M.; Kuriyan, J. The conformational plasticity of protein kinases. *Cell* **2002**, *109*, 275-282.
285. Eswaran, J.; Knapp, S. Insights into protein kinase regulation and inhibition by large scale structural comparison. *Biochim. Biophys. Acta* **2010**, *1804*, 429-432.
286. Matthews, D. A.; Gerritsen, M. E. 2.2 Protein Kinase Domain Structure and Function. In *Targeting Protein Kinases for Cancer Therapy*; John Wiley & Sons, Inc.: New Jersey, USA, **2010**; 83-87.
287. Yun, C. H.; Mengwasser, K. E.; Toms, A. V.; Woo, M. S.; Greulich, H.; Wong, K. K.; Meyerson, M.; Eck, M. J. The T790M mutation in EGFR kinase causes drug resistance by increasing the affinity for ATP. *Proc. Natl. Acad. Sci. U. S. A.* **2008**, *105*, 2070-2075.
288. Adams, J. A. Activation loop phosphorylation and catalysis in protein kinases: is there functional evidence for the autoinhibitor model? *Biochemistry* **2003**, *42*, 601-607.
289. Kornev, A. P.; Haste, N. M.; Taylor, S. S.; Eyck, L. F. Surface comparison of active and inactive protein kinases identifies a conserved activation mechanism. *Proc. Natl. Acad. Sci. U. S. A.* **2006**, *103*, 17783-17788.
290. Jänne, P. A.; Gray, N.; Settleman, J. Factors underlying sensitivity of cancers to small-molecule kinase inhibitors. *Nat. Rev. Drug Discov.* **2009**, *8*, 709-723.
291. Liu, Y.; Gray, N. S. Rational design of inhibitors that bind to inactive kinase conformations. *Nat. Chem. Biol.* **2006**, *2*, 358-364.
292. Zou, H. Y.; Li, Q.; Lee, J. H.; Arango, M. E.; McDonnell, S. R.; Yamazaki, S.; Koudriakova, T. B.; Alton, G.; Cui, J. J.; Kung, P. P.; Nambu, M. D.; Los, G.; Bender, S. L.; Mroczkowski, B.; Christensen, J. G. An orally available small-molecule inhibitor of c-Met, PF-2341066, exhibits cytoreductive antitumor efficacy through antiproliferative and antiangiogenic mechanisms. *Cancer Res.* **2007**, *67*, 4408-4417.
293. Schindler, T.; Bornmann, W.; Pellicena, P.; Miller, W. T.; Clarkson, B.; Kuriyan, J. Structural mechanism for STI-571 inhibition of abelson tyrosine kinase. *Science* **2000**, *289*, 1938-1942.
294. Pargellis, C.; Tong, L.; Churchill, L.; Cirillo, P. F.; Gilmore, T.; Graham, A. G.; Grob, P. M.; Hickey, E. R.; Moss, N.; Pav, S.; Regan, J. Inhibition of p38 MAP kinase by utilizing a novel allosteric binding site. *Nat. Struct. Biol.* **2002**, *9*, 268-272.
295. Lowinger, T. B.; Riedl, B.; Dumas, J.; Smith, R. A. Design and discovery of small molecules targeting raf-1 kinase. *Curr. Pharm. Des.* **2002**, *8*, 2269-2278.
296. Kufareva, I.; Abagyan, R. Type-II kinase inhibitor docking, screening, and profiling using modified structures of active kinase states. *J. Med. Chem.* **2008**, *51*, 7921-7932.
297. Mol, C. D.; Dougan, D. R.; Schneider, T. R.; Skene, R. J.; Kraus, M. L.; Scheibe, D. N.; Snell, G. P.; Zou, H.; Sang, B. C.; Wilson, K. P. Structural basis for the autoinhibition and STI-571 inhibition of c-Kit tyrosine kinase. *J. Biol. Chem.* **2004**, *279*, 31655-31663.
298. Cavalli, A.; Dezi, C.; Folkers, G.; Scapozza, L.; Recanatini, M. Three-dimensional model of the cyclin-dependent kinase 1 (CDK1): Ab initio active site parameters for molecular dynamics studies of CDKS. *Proteins* **2001**, *45*, 478-485.
299. Galkin, A. V.; Melnick, J. S.; Kim, S.; Hood, T. L.; Li, N.; Li, L.; Xia, G.; Steensma, R.; Chopiuk, G.; Jiang, J.; Wan, Y.; Ding, P.; Liu, Y.; Sun, F.; Schultz, P. G.; Gray, N. S.; Warmuth, M. Identification of NVP-TAE684, a potent, selective, and efficacious inhibitor of NPM-ALK. *Proc. Natl. Acad. Sci. U. S. A.* **2007**, *104*, 270-275.



300. Choi, H. G.; Ren, P.; Adrian, F.; Sun, F.; Lee, H. S.; Wang, X.; Ding, Q.; Zhang, G.; Xie, Y.; Zhang, J.; Liu, Y.; Tuntland, T.; Warmuth, M.; Manley, P. W.; Mestan, J.; Gray, N. S.; Sim, T. A type-II kinase inhibitor capable of inhibiting the T315I "gatekeeper" mutant of Bcr-Abl. *J. Med. Chem.* **2010**, *53*, 5439-5448.
301. Rabindran, S. K.; Discafani, C. M.; Rosfjord, E. C.; Baxter, M.; Floyd, M. B.; Golas, J.; Hallett, W. A.; Johnson, B. D.; Nilakantan, R.; Overbeek, E.; Reich, M. F.; Shen, R.; Shi, X.; Tsou, H. R.; Wang, Y. F.; Wissner, A. Antitumor activity of HKI-272, an orally active, irreversible inhibitor of the HER-2 tyrosine kinase. *Cancer Res.* **2004**, *64*, 3958-3965.
302. Adrian, F. J.; Ding, Q.; Sim, T.; Velentza, A.; Sloan, C.; Liu, Y.; Zhang, G.; Hur, W.; Ding, S.; Manley, P.; Mestan, J.; Fabbro, D.; Gray, N. S. Allosteric inhibitors of Bcr-abl-dependent cell proliferation. *Nat. Chem. Biol.* **2006**, *2*, 95-102.
303. McDermott, U.; Sharma, S. V.; Dowell, L.; Greninger, P.; Montagut, C.; Lamb, J.; Archibald, H.; Raudales, R.; Tam, A.; Lee, D.; Rothenberg, S. M.; Supko, J. G.; Sordella, R.; Ulkus, L. E.; Iafrate, A. J.; Maheswaran, S.; Njauw, C. N.; Tsao, H.; Drew, L.; Hanke, J. H.; Ma, X. J.; Erlander, M. G.; Gray, N. S.; Haber, D. A.; Settleman, J. Identification of genotype-correlated sensitivity to selective kinase inhibitors by using high-throughput tumor cell line profiling. *Proc. Natl. Acad. Sci. U. S. A.* **2007**, *104*, 19936-19941.
304. McDermott, U.; Iafrate, A. J.; Gray, N. S.; Shioda, T.; Classon, M.; Maheswaran, S.; Zhou, W.; Choi, H. G.; Smith, S. L.; Dowell, L.; Ulkus, L. E.; Kuhlmann, G.; Greninger, P.; Christensen, J. G.; Haber, D. A.; Settleman, J. Genomic alterations of anaplastic lymphoma kinase may sensitize tumors to anaplastic lymphoma kinase inhibitors. *Cancer Res.* **2008**, *68*, 3389-3395.
305. Kawahara, E.; Miyake, T.; Roesel, J. Pyrimidine derivatives U.S. Pat. Appl. 2008/293708A1.
306. Garcia-Echeverria, C.; Kanazawa, T.; Kawahara, E.; Masuya, K.; Matsuura, N.; Miyake, T.; Ohmori, O.; Umemura, I.; Steensma, R.; Chopiuk, G.; Jiang, J.; Wan, Y.; Ding, Q.; Zhang, Q.; Gray, N. S.; Karanewsky, D. 2,4-Pyrimidinediamines useful in the treatment of neoplastic diseases, inflammatory and immune system disorders. WO 2005/016894A1.
307. Choi, Y. L.; Takeuchi, K.; Soda, M.; Inamura, K.; Togashi, Y.; Hatano, S.; Enomoto, M.; Hamada, T.; Haruta, H.; Watanabe, H.; Kurashina, K.; Hatanaka, H.; Ueno, T.; Takada, S.; Yamashita, Y.; Sugiyama, Y.; Ishikawa, Y.; Mano, H. Identification of novel isoforms of the EML4-ALK transforming gene in non-small cell lung cancer. *Cancer Res.* **2008**, *68*, 4971-4976.
308. Soda, M.; Takada, S.; Takeuchi, K.; Choi, Y. L.; Enomoto, M.; Ueno, T.; Haruta, H.; Hamada, T.; Yamashita, Y.; Ishikawa, Y.; Sugiyama, Y.; Mano, H. A mouse model for EML4-ALK-positive lung cancer. *Proc. Natl. Acad. Sci. U. S. A.* **2008**, *105*, 19893-19897.
309. Lu, L.; Ghose, A. K.; Quail, M. R.; Albom, M. S.; Durkin, J. T.; Holskin, B. P.; Angeles, T. S.; Meyer, S. L.; Ruggeri, B. A.; Cheng, M. ALK mutants in the kinase domain exhibit altered kinase activity and differential sensitivity to small molecule ALK inhibitors. *Biochemistry* **2009**, *48*, 3600-3609.
310. Sabbatini, P.; Korenchuk, S.; Rowand, J. L.; Groy, A.; Liu, Q.; Leperi, D.; Atkins, C.; Dumble, M.; Yang, J.; Anderson, K.; Kruger, R. G.; Gontarek, R. R.; Maksimchuk, K. R.; Suravajjala, S.; Lapierre, R. R.; Shotwell, J. B.; Wilson, J. W.; Chamberlain, S. D.; Rabindran, S. K.; Kumar, R. GSK1838705A inhibits the insulin-like growth factor-1 receptor and anaplastic lymphoma kinase and shows antitumor activity in experimental models of human cancers. *Mol. Cancer Ther.* **2009**, *8*, 2811-2820.
311. Chamberlain, S. D.; Redman, A. M.; Wilson, J. W.; Deanda, F.; Shotwell, J. B.; Gerding, R.; Lei, H.; Yang, B.; Stevens, K. L.; Hassell, A. M.; Shewchuk, L. M.; Leesnitzer, M. A.; Smith, J. L.; Sabbatini, P.; Atkins, C.; Groy, A.; Rowand, J. L.; Kumar, R.; Mook, R. A., Jr; Moorthy, G.; Patnaik, S. Optimization of 4,6-bis-anilino-1*H*-pyrrolo[2,3-*d*]pyrimidine IGF-

- 1R tyrosine kinase inhibitors towards JNK selectivity. *Bioorg. Med. Chem. Lett.* **2009**, *19*, 360-364.
312. Hudkins, R. L.; Zulli, A. L.; Reddy, D. R.; Gingrich, D. E.; Tao, M.; Becknell, N. C.; Diebold, J. L.; Underiner, T. L. Novel fused pyrrolocarbazoles. U.S. Pat. Appl. 2005/0143442A1.
313. Wan, W.; Albom, M. S.; Lu, L.; Quail, M. R.; Becknell, N. C.; Weinberg, L. R.; Reddy, D. R.; Holskin, B. P.; Angeles, T. S.; Underiner, T. L.; Meyer, S. L.; Hudkins, R. L.; Dorsey, B. D.; Ator, M. A.; Ruggeri, B. A.; Cheng, M. Anaplastic lymphoma kinase activity is essential for the proliferation and survival of anaplastic large-cell lymphoma cells. *Blood* **2006**, *107*, 1617-1623.
314. Passoni, L.; Longo, L.; Collini, P.; Coluccia, A. M.; Bozzi, F.; Podda, M.; Gregorio, A.; Gambini, C.; Garaventa, A.; Pistoia, V.; Del Grosso, F.; Tonini, G. P.; Cheng, M.; Gambacorti-Passerini, C.; Anichini, A.; Fossati-Bellani, F.; Di Nicola, M.; Luksch, R. Mutation-independent anaplastic lymphoma kinase overexpression in poor prognosis neuroblastoma patients. *Cancer Res.* **2009**, *69*, 7338-7346.
315. Thaimattam, R.; Daga, P. R.; Banerjee, R.; Iqbal, J. 3D-QSAR studies on c-Src kinase inhibitors and docking analyses of a potent dual kinase inhibitor of c-Src and c-Abl kinases. *Bioorg. Med. Chem.* **2005**, *13*, 4704-4712.
316. Moasser, M. M.; Srethapakdi, M.; Sachar, K. S.; Kraker, A. J.; Rosen, N. Inhibition of Src kinases by a selective tyrosine kinase inhibitor causes mitotic arrest. *Cancer Res.* **1999**, *59*, 6145-6152.
317. Nagar, B.; Bornmann, W. G.; Pellicena, P.; Schindler, T.; Veach, D. R.; Miller, W. T.; Clarkson, B.; Kuriyan, J. Crystal structures of the kinase domain of c-Abl in complex with the small molecule inhibitors PD173955 and imatinib (STI-571). *Cancer Res.* **2002**, *62*, 4236-4243.
318. Marzec, M.; Kasprzycka, M.; Ptasznik, A.; Wlodarski, P.; Zhang, Q.; Odum, N.; Wasik, M. A. Inhibition of ALK enzymatic activity in T-cell lymphoma cells induces apoptosis and suppresses proliferation and STAT3 phosphorylation independently of Jak3. *Lab. Invest.* **2005**, *85*, 1544-1554.
319. Moyer, J. D.; Barbacci, E. G.; Iwata, K. K.; Arnold, L.; Boman, B.; Cunningham, A.; DiOrio, C.; Doty, J.; Morin, M. J.; Moyer, M. P.; Neveu, M.; Pollack, V. A.; Pustilnik, L. R.; Reynolds, M. M.; Sloan, D.; Theleman, A.; Miller, P. Induction of apoptosis and cell cycle arrest by CP-358,774, an inhibitor of epidermal growth factor receptor tyrosine kinase. *Cancer Res.* **1997**, *57*, 4838-4848.
320. Wakeling, A. E.; Guy, S. P.; Woodburn, J. R.; Ashton, S. E.; Curry, B. J.; Barker, A. J.; Gibson, K. H. ZD1839 (Iressa): an orally active inhibitor of epidermal growth factor signaling with potential for cancer therapy. *Cancer Res.* **2002**, *62*, 5749-5754.
321. Shaw, A. T.; Yeap, B. Y.; Mino-Kenudson, M.; Digumarthy, S. R.; Costa, D. B.; Heist, R. S.; Solomon, B.; Stubbs, H.; Admane, S.; McDermott, U.; Settleman, J.; Kobayashi, S.; Mark, E. J.; Rodig, S. J.; Chirieac, L. R.; Kwak, E. L.; Lynch, T. J.; Iafrate, A. J. Clinical features and outcome of patients with non-small-cell lung cancer who harbor EML4-ALK. *J. Clin. Oncol.* **2009**, *27*, 4247-4253.
322. Zhu, T.; Yan, Z.; Chucholowski, A.; Webb, T. R.; Li, R. Polymer-supported synthesis of pyridone-focused libraries as inhibitors of anaplastic lymphoma kinase. *J. Comb. Chem.* **2006**, *8*, 401-409.
323. Li, R.; Xue, L.; Zhu, T.; Jiang, Q.; Cui, X.; Yan, Z.; McGee, D.; Wang, J.; Gantla, V. R.; Pickens, J. C.; McGrath, D.; Chucholowski, A.; Morris, S. W.; Webb, T. R. Design and synthesis of 5-aryl-pyridone-carboxamides as inhibitors of anaplastic lymphoma kinase. *J. Med. Chem.* **2006**, *49*, 1006-1015.

324. Gregor, V. E.; Liu, Y.; Anikin, A.; McGee, D. P. C.; Mikel, C.; McGrath, D. E.; Vavi-Lala, G. R.; Pickens, J. C.; Kadushkin, A. T., M.S.; Zozulya, S.; Vairagoundar, R.; Zhu, T.; Chucholowski, A.; Webb, T. R.; Jiang, L.; Gantla, V. R.; Yan, Z. Tricyclic compounds and its use as tyrosine kinase modulators. WO 2008/021369A3.
325. Anand, N. K.; Blazey, C. M.; Bowles, O. J.; Bussenius, J.; Costanzo, S.; Curtis, J. K.; Dubenko, L.; Kennedy, A. R.; Khoury, R. G.; Kim, A. I.; Manalo, J. L.; Peto, C. J.; Rice, K. D.; Tsang, T. H. Anaplastic Lymphoma Kinase Modulators and Methods of Use. WO 2005/009389A3.
326. Milkiewicz, K. L.; Weinberg, L. R.; Albom, M. S.; Angeles, T. S.; Cheng, M.; Ghose, A. K.; Roemmele, R. C.; Theroff, J. P.; Underiner, T. L.; Zifcick, C. A.; Dorsey, B. D. Synthesis and structure-activity relationships of 1,2,3,4-tetrahydropyrido[2,3-*b*]pyrazines as potent and selective inhibitors of the anaplastic lymphoma kinase. *Bioorg. Med. Chem.* **2010**, *18*, 4351-4362.
327. Ahmed, G.; Bohnstedt, A.; Breslin, H. J.; Burke, J.; Curry, M. A.; Diebold, J. L.; Dorsey, B.; Dugan, B. J.; Feng, D.; Gingrich, D. E.; Guo, T.; Ho, K.; Learn, K. S.; Lisko, J. G.; Liu, R.; Mesaros, E. F.; Milkiewicz, K.; Ott, G. R.; Parrish, J.; Theroff, J. P. Fused Bicyclic Derivatives of 2,4-diaminopyrimidine as ALK and c-MET Inhibitors. WO 2008/051547A1.
328. Gambacorti-Passerini, C.; Mologni, L.; Scapozza, L.; Ahmad, S.; Goekjian, P. G.; Gueyrard, D.; Popowycz, F.; Joseph, B.; Schneider, C.; Garcia, P. Alpha-carboline inhibitors of NMP-ALK, RET, and Bcr-Abl. WO 2010/025872A3.
329. Schneider, C.; Goyard, D.; Gueyrard, D.; Joseph, B.; Goekjian, P. G. Synthesis of 2-, 3-, and 4-Substituted Pyrido[2,3-*b*]indoles by C–N, C–O, and C–C(sp) Bond Formation. *Eur. J. Org. Chem.* **2010**, *2010*, 6665-6677.
330. Schneider, C.; Gueyrard, D.; Joseph, B.; Goekjian, P. G. Chemoselective functionalization of  $\alpha$ -carbolines at the C-2, C-3, C-4, and C-6 positions using Suzuki–Miyaura reactions. *Tetrahedron* **2009**, *65*, 5427-5437.
331. Ge, J.; Normant, E.; Porter, J. R.; Ali, J. A.; Dembski, M. S.; Gao, Y.; Georges, A. T.; Grenier, L.; Pak, R. H.; Patterson, J.; Sydor, J. R.; Tibbitts, T. T.; Tong, J. K.; Adams, J.; Palombella, V. J. Design, synthesis, and biological evaluation of hydroquinone derivatives of 17-amino-17-demethoxygeldanamycin as potent, water-soluble inhibitors of Hsp90. *J. Med. Chem.* **2006**, *49*, 4606-4615.
332. Sequist, L. V.; Gettinger, S.; Senzer, N. N.; Martins, R. G.; Janne, P. A.; Lilenbaum, R.; Gray, J. E.; Iafrate, A. J.; Katayama, R.; Hafeez, N.; Sweeney, J.; Walker, J. R.; Fritz, C.; Ross, R. W.; Grayzel, D.; Engelman, J. A.; Borger, D. R.; Paez, G.; Natale, R. Activity of IPI-504, a Novel Heat-Shock Protein 90 Inhibitor, in Patients With Molecularly Defined Non-Small-Cell Lung Cancer. *J. Clin. Oncol.* **2010**, *28*, 4953-4960.
333. Schnur, R. C.; Corman, M. L.; Gallaschun, R. J.; Cooper, B. A.; Dee, M. F.; Doty, J. L.; Muzzi, M. L.; DiOrio, C. I.; Barbacci, E. G.; Miller, P. E. erbB-2 oncogene inhibition by geldanamycin derivatives: synthesis, mechanism of action, and structure-activity relationships. *J. Med. Chem.* **1995**, *38*, 3813-3820.
334. Rivera, V. M.; Anjum, R.; Wang, F.; Zhang, S.; Keats, J.; Ning, Y.; Wardwell, S. D.; Moran, L.; Ye, E.; Chun, D. Y.; Mohemmad, Q. K.; Liu, S.; Huang, W.-S.; Wang, Y.; Thomas, M.; Li, F.; Qi, J.; Miret, J.; Iulicucci, J. D.; Dalgarno, D.; Narasimhan, N. I.; Clackson, T.; Shakespeare, W. C. Efficacy and pharmacodynamic analysis of AP26113, a potent and selective orally active inhibitor of Anaplastic Lymphoma Kinase (ALK). *AACR (Annual Meeting)* **2010**.
335. Shakespeare, W. C.; Fantin, V. R.; Wang, F.; Kohlmann, A.; Liu, S.; Huang, W.-S.; Wang, Y.; Zou, D.; Thomas, M.; Li, F.; Qi, J.; Cai, L.; Dwight, T.; Xu, Y.; Xu, R.; Dodd, R.; Xu, X.; Anjum, R.; Zhang, S.; Keats, J.; Xue, L.; Wardwell, S. D.; Ning, Y.; Moran, L. E.; Mohemmad, Q. K.; Zhu, X.; Narasimhan, N. I.; Rivera, V. M.; Dalgarno, D.; Clackson, T.

- Discovery of potent and selective orally active inhibitors of anaplastic lymphoma kinase (ALK). *AACR (Annual Meeting)* **2009**.
336. Turturro, F.; Arnold, M. D.; Frist, A. Y.; Pulford, K. Model of inhibition of the NPM-ALK kinase activity by herbimycin A. *Clin. Cancer Res.* **2002**, *8*, 240-245.
337. Schumacher, J. A.; Crockett, D. K.; Elenitoba-Johnson, K. S.; Lim, M. S. Proteome-wide changes induced by the Hsp90 inhibitor, geldanamycin in anaplastic large cell lymphoma cells. *Proteomics* **2007**, *7*, 2603-2616.
338. Omura, S.; Iwai, Y.; Hirano, A.; Nakagawa, A.; Awaya, J.; Tsuchya, H.; Takahashi, Y.; Masuma, R. A new alkaloid AM-2282 of Streptomyces origin. Taxonomy, fermentation, isolation and preliminary characterization. *J. Antibiot.* **1977**, *30*, 275-282.
339. Karaman, M. W.; Herrgard, S.; Treiber, D. K.; Gallant, P.; Atteridge, C. E.; Campbell, B. T.; Chan, K. W.; Ciceri, P.; Davis, M. I.; Edeen, P. T.; Faraoni, R.; Floyd, M.; Hunt, J. P.; Lockhart, D. J.; Milanov, Z. V.; Morrison, M. J.; Pallares, G.; Patel, H. K.; Pritchard, S.; Wodicka, L. M.; Zarrinkar, P. P. A quantitative analysis of kinase inhibitor selectivity. *Nat. Biotechnol.* **2008**, *26*, 127-132.
340. Gunby, R. H.; Tartari, C. J.; Porchia, F.; Donella-Deana, A.; Scapozza, L.; Gambacorti-Passerini, C. An enzyme-linked immunosorbent assay to screen for inhibitors of the oncogenic anaplastic lymphoma kinase. *Haematologica* **2005**, *90*, 988-990.
341. Sausville, E. A.; Arbuck, S. G.; Messmann, R.; Headlee, D.; Bauer, K. S.; Lush, R. M.; Murgo, A.; Figg, W. D.; Lahusen, T.; Jaken, S.; Jing, X.; Roberge, M.; Fuse, E.; Kuwabara, T.; Senderowicz, A. M. Phase I trial of 72-hour continuous infusion UCN-01 in patients with refractory neoplasms. *J. Clin. Oncol.* **2001**, *19*, 2319-2333.
342. Gopalakrishna, R.; Chen, Z. H.; Gundimeda, U.; Wilson, J. C.; Anderson, W. B. Rapid filtration assays for protein kinase C activity and phorbol ester binding using multiwell plates with fitted filtration discs. *Anal. Biochem.* **1992**, *206*, 24-35.
343. Talman, V.; Boije af Gennäs, G.; Ekokoski, E.; Aitio, O.; Yli-Kauhaluoma, J.; Tuominen, R., Unpublished results.
344. Kang, J. H.; Kim, Y.; Won, S. H.; Park, S. K.; Lee, C. W.; Kim, H. M.; Lewin, N. E.; Perry, N. A.; Pearce, L. V.; Lundberg, D. J.; Surawski, R. J.; Blumberg, P. M.; Lee, J. Polar 3-alkylidene-5-pivaloyloxymethyl-5'-hydroxymethyl- $\gamma$ -lactones as protein kinase C ligands and antitumor agents. *Bioorg. Med. Chem. Lett.* **2010**, *20*, 1008-1012.
345. El Kazzouli, S.; Lewin, N. E.; Blumberg, P. M.; Marquez, V. E. Conformationally constrained analogues of diacylglycerol. 30. An investigation of diacylglycerol-lactones containing heteroaryl groups reveals compounds with high selectivity for Ras guanyl nucleotide-releasing proteins. *J. Med. Chem.* **2008**, *51*, 5371-5386.
346. Boije af Gennäs, G.; Yli-Kauhaluoma, J. Unpublished results.
347. Patrick, G. L. 10.5 Drug design - making drugs more resistant to hydrolysis and drug metabolism. In *An Introduction to Medicinal Chemistry*; Oxford University Press Inc.: New York, USA, **2002**; 230-235.
348. Brown, H. C.; Bhat, K. S. Enantiomeric (*Z*)- and (*E*)-crotyldiisopinocampheylboranes. Synthesis in high optical purity of all four possible stereoisomers of  $\beta$ -methylhomoallyl alcohols. *J. Am. Chem. Soc.* **1986**, *108*, 293-294.
349. Hafner, A.; Duthaler, R. O.; Marti, R.; Rihs, G.; Rothe-Streit, P.; Schwarzenbach, F. Enantioselective syntheses with titanium carbohydrate complexes. Part 7. Enantioselective allyltitanation of aldehydes with cyclopentadienyldialkoxyallyltitanium complexes. *J. Am. Chem. Soc.* **1992**, *114*, 2321-2336.
350. Amans, D.; Bellosta, V.; Cossy, J. Total Synthesis of Pseudotrienic Acid B: A Bioactive Metabolite from *Pseudomonas* sp. MF 381-IODS. *Angew. Chem. Int. Ed.* **2006**, *45*, 5870-5874.

351. Pellissier, H. Use of TADDOLs and their derivatives in asymmetric synthesis. *Tetrahedron* **2008**, *64*, 10279-10317.
352. Carlsen, P. H. J.; Katsuki, T.; Martin, V. S.; Sharpless, K. B. A greatly improved procedure for ruthenium tetroxide catalyzed oxidations of organic compounds. *J. Org. Chem.* **1981**, *46*, 3936-3938.
353. Mosmann, T. Rapid colorimetric assay for cellular growth and survival: application to proliferation and cytotoxicity assays. *J. Immunol. Methods* **1983**, *65*, 55-63.
354. Roth, B. L.; Poot, M.; Yue, S. T.; Millard, P. J. Bacterial viability and antibiotic susceptibility testing with SYTOX green nucleic acid stain. *Appl. Environ. Microbiol.* **1997**, *63*, 2421-2431.